NSF/RA-800219

PB81-148436

Geometrically Nonlinear Analysis of Rectangular Glass Plates by the Finite Element Method

Abdul-Hamid J. Al-Tayyib

May 1980

Institute for Disaster Research

TEXAS TECH UNIVERSITY

Lubbock, Texas 79409

EAS INFORMATION RESOURCES
NATIONAL SCIENCE FOUNDATION

GEOMETRICALLY NONLINEAR ANALYSIS OF RECTANGULAR GLASS PLATES BY THE FINITE ELEMENT METHOD

by

Abdul-Hamid J. Al-Tayyib

Institute for Disaster Research
Texas Tech University
Lubbock, Texas 79409

May, 1980

FOREWORD

The work reported herein was conducted as a part of a continuing program of research involving engineered window glass at Texas Tech University. The program is administered through the Institute for Disaster Research in the College of Engineering.

The specific project on the analysis of rectangular glass plates was directed by Dr. C. V. G. Vallabhan. The principal investigator was Dr. Abdul-Hamid J. Al-Tayyib. The project was supported by the National Science Foundation under Award No. PFR 77-24063, the Institute for Disaster Research, and the Department of Civil Engineering at Texas Tech University. This report was adapted for publication by Dr. J. E. Minor and W. L. Beason from Dr. Al-Tayyib's dissertation entitled, "Geometrically Nonlinear Analysis of Rectangular Glass Panels by the Finite Element Method." This editing was performed so that terminology used in this publication will be consistent with other IDR publications in the glass area. Any opinions, findings, and conclusions or recommendations expressed in this publication are those of the author and editors, and do not necessarily reflect the views of the National Science Foundation.

ACKNOWLEDGMENTS

The author is deeply indebted to Dr. C. V. Girija Vallabhan for his valuable assistance, guidance, and constructive criticism given during the course of this investigation. Appreciation is also expressed to Drs. M. M. Ayoub, K. C. Mehta, J. H. Smith, J. E. Minor, and W. P. Vann for their helpful suggestions.

In addition, deep gratitude is expressed by the author to the Saudi Arabian government for supporting his wish to broaden his knowledge in the field of Civil Engineering. Finally, the author wishes to make special mention of the generous amount of computer time provided by the Department of Civil Engineering at Texas Tech University during the development of the computer program which is a part of this work.

ABSTRACT

The primary objective of this study is to develop a finite element model for the stress analysis of geometrically nonlinear, simply supported, uniformly loaded, rectangular plates. Actual framing configurations for glass plates allow the boundary edges to move in the plane of the plate with little restrain. In such a situation, when the loads become large, membrane behavior plays a significant role in changing the overall behavior of the glass plate. In this investigation, the geometric nonlinearity treated is that associated with large lateral elastic displacements which induce stretching of the middle surface of the plate. The formulation is not restricted by the magnitude of the displacements, as is linear plate theory, provided that engineering strains do not exceed the proportional limit and structural instability does not occur.

A finite element program which includes a nonlinear thin plate formulation is developed. The formulation uses a rectangular finite element with displacement fields depicted by shape functions which are products of one-dimensional Hermitian polynomials of order one. These functions are used to represent both membrane and bending behaviors. A 48 degree of freedom element results, with linear and nonlinear stiffness matrices which are derived from a purely geometric standpoint. Thirty-two of the 48 degrees of freedom are allowed to represent the membrane behavior of the plate. This representation of membrane behavior is important in studying stress distributions in glass plates, particularly at the glass plate perimeter. The system equilibrium equations are then formulated and solved using a Langrangian type linear incremental approach.

Example problems, for which published experimental and theoretical results are available in the literature, are solved to demonstrate the validity and versatility of the finite element formulation. In these example problems, theoretical bending and membrane stresses are compared separately to better assess membrane behavior in plates with large displacements. The glass plate problem with boundary edges that are simply supported and free to move in the plane of the plate are analyzed and force-displacement results are compared with independent experimental data. Computer displacements agree well with the experimental data.

Numerical studies conducted on the glass plate problem reveal that convergence differs between bending and membrane stresses, and depends upon the fineness of the finite element discretization, the location within the plate, and the relative magnitude of the loading increment. This observation, in the author's opinion, is valuable for anyone involved in analyzing geometrically nonlinear thin plate problems.

TABLE OF CONTENTS

LIST OF ILLUSTRATIONS

LIST OF TABLES

LIST OF SYMBOLS

A	:	Area of element
a	:	Plate dimension in the x-direction
$[B_0]$	:	A matrix containing the derivatives of the shape functions
$[B_L]$	:	A matrix which is a function of the slopes w_x and w_y, and contains the derivatives of the shape functions
$[\tilde{B}]$	:	The sum of $[B_0]$ and $[B_L]$
b	:	Plate dimension in the y-direction
$[C]$	:	A [3x2] matrix which contains the slopes w_x and w_y
$D = [D^b]$	:	Flexural rigidity of the plate
$[D^m]$	:	A [3x3] matrix containing the plate properties used for plane stress analysis
$[D^*]$	:	A [6x6] matrix containing $[D^m]$ and $[D^b]$
E	:	Young's modulus of elasticity
$\{ f \}$	:	Force vector
G	:	Shear modulus
$[G]$	:	A matrix that contains the derivatives of the shape functions associated with the slopes w_x and w_y
$H^n_{mi}(x)$	:	A Hermitian polynomial of order n in the x-direction
$[K_0]$	:	The linear stiffness matrix
$[K_L]$	:	The "displacment" stiffness matrix
$[K_\sigma]$	:	The "initial stress" stiffness matrix
$[K_T]$	:	The total or "tangential" stiffness matrix
M_x, M_y, M_{xy}	:	Stress moments in plate theory
N_x, N_y, N_{xy}	:	Stress resultants in plate theory

N	:	Assumed shape functions
$\{ q \}$	:	Load vector
$\{ \Delta q \}$	:	Incrmental load vector
t	:	Plate thickness
U	:	Strain energy functional
U_b	:	Bending strain energy functional
U_m	:	Membrane strain energy functional
u	:	Displacement component in the x-direction
V	:	An energy functional
v	:	Displacement component in the y-direction
w	:	Displacement component in the z-direction
x,y,z	:	Coordinates of a point within the plate
$\{ \alpha \}$	:	A vector matrix containing the nodal displacement parameters
$\{ \Delta\alpha \}$	:	A vector matrix containing incremental nodal displacement parameters
γ_{xy}	:	Shear strain
δ_{ij}	:	Kronecker Delta
ε_{ij}	:	Strain tensor
$\{ \varepsilon \}$	:	Vector of components of the strain tensor
$\{ \varepsilon_L \}$	:	Vector of the linear components of the strain
$\{ \varepsilon_{NL} \}$	:	Vector of the non-linear components of the strain
$\varepsilon_x^m, \varepsilon_y^m, \varepsilon_{xy}^m$	:	Components of the membrane strain
$\varepsilon_x^b, \varepsilon_y^b, \varepsilon_{xy}^b$	:	Components of the bending strain
$\{ \Theta \}$	:	A vector matrix containing the slopes w_x and w_y
λ	:	Lame´ parameter

ν	:	Poisson's ratio
σ_{ij}	:	Stress tensor
$\{ \sigma \}$	:	Vector of components of the stress tensor
$\sigma_x^m, \sigma_y^m, \sigma_{xy}^m$	:	Components of the membrane stress
$\sigma_x^b, \sigma_y^b, \sigma_{xy}^b$	:	Components of the bending stress
$\Phi(\alpha)$	:	Potential energy functional

CHAPTER 1

INTRODUCTION

1.1 Initiation of the Problem

The Institute for Disaster Research at Texas Tech University, acting in cooperation with other organized research institutes and researchers in the glass industry, has called attention to the need for a reevaluation of the window glass design process. Included as a part of this reevaluation is a study of the response of window glass to wind loads. Structural modeling of the response of glass plates subjected to lateral loads representative of wind pressures is a principal concern (6)*.

When glass plates are used in windows and exterior walls of modern high rise buildings, they are often secured in the framing system by neoprene gaskets as shown in Fig. 1.1 (2). The response of such glass plates when subjected to moderately high wind loads (which can be assumed for stress analysis purposes to be uniformly distributed static loads) is such that large deflections are experienced. The effects of relatively high loads combined with uncertainties regarding degrees of fixity of the plate edges on the response of the glass plate present to the designer a unique large deflection plate problem.

1.2 Definition of the Problem

The glass plate problem investigated in this research can be modeled structurally as a simply supported rectangular plate** subjected to moderately

---

*References used in this report are listed alphabetically by author.

**The terms "glass plate" and "plate" are used interchangeably to refer to the glass panel problem investigated in this research.

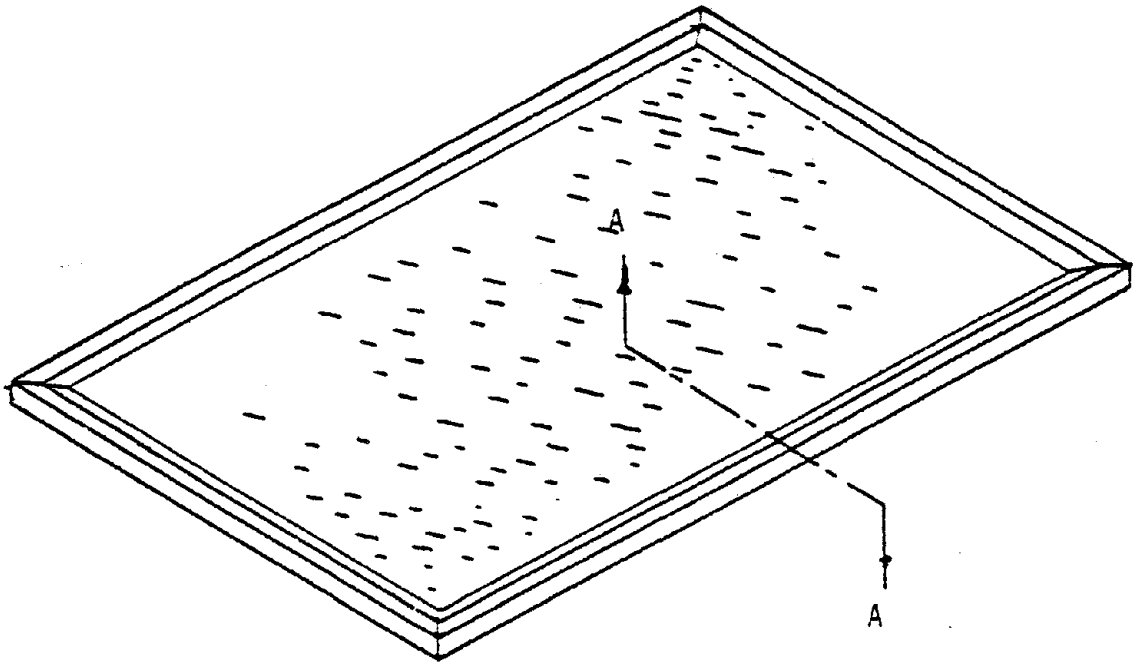

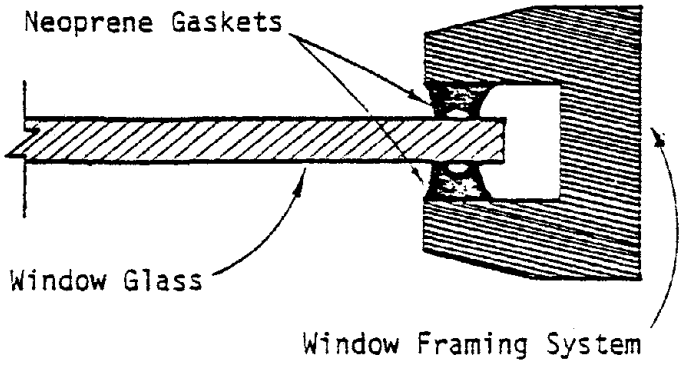

Figure 1.1 Section Through a Window Framing System

high lateral uniform static loads that cause large deflections. The edges of the plate are assumed to be restrained from deflecting out-of-plane but are free to rotate in the lateral direction, while in the transverse direction, the edges are free to translate. The latter assumption means that the plate edges do not necessarily remain straight in the transverse direction, but rather the plate edges are free to deform as shown in Fig. 1.2. The maximum lateral deflection of the plate is assumed to be small when compared with the length of the shorter side of the plate. The material of the plate is assumed to remain elastic during deformation; hence, the structural system is represented as a geometrically nonlinear plate problem in which the geometrical nonlinearity is characterized as large deflection, small strain.

1.3 Previous and Current Work

The large deflection plate problem assumed to model the glass plate problem under investigation was first solved in 1936 by V. R. Kaiser (29). Kaiser determined, theoretically and experimentally, deflections and stresses in a statically loaded, simply supported plate experiencing large deflections. He assumed that the edges of the plate are free to move in the plane of the plate and do not necessarily remain straight as the plate deflects. This assumption is not consistent with the observed response of glass plate edges (2).

Concurrent with theoretical work of Beason (6), who solved the nonlinear plate equations using a Galerkin approach to determine deflections and stresses for the glass plate problem, Anians (2) experimentally determined central and edge displacements of a 96 in. x 48 in. x 0.25 in. aluminum plate subjected to uniform lateral pressures. Anians, in his experimental work, evaluated the response of this plate under several different support conditions.

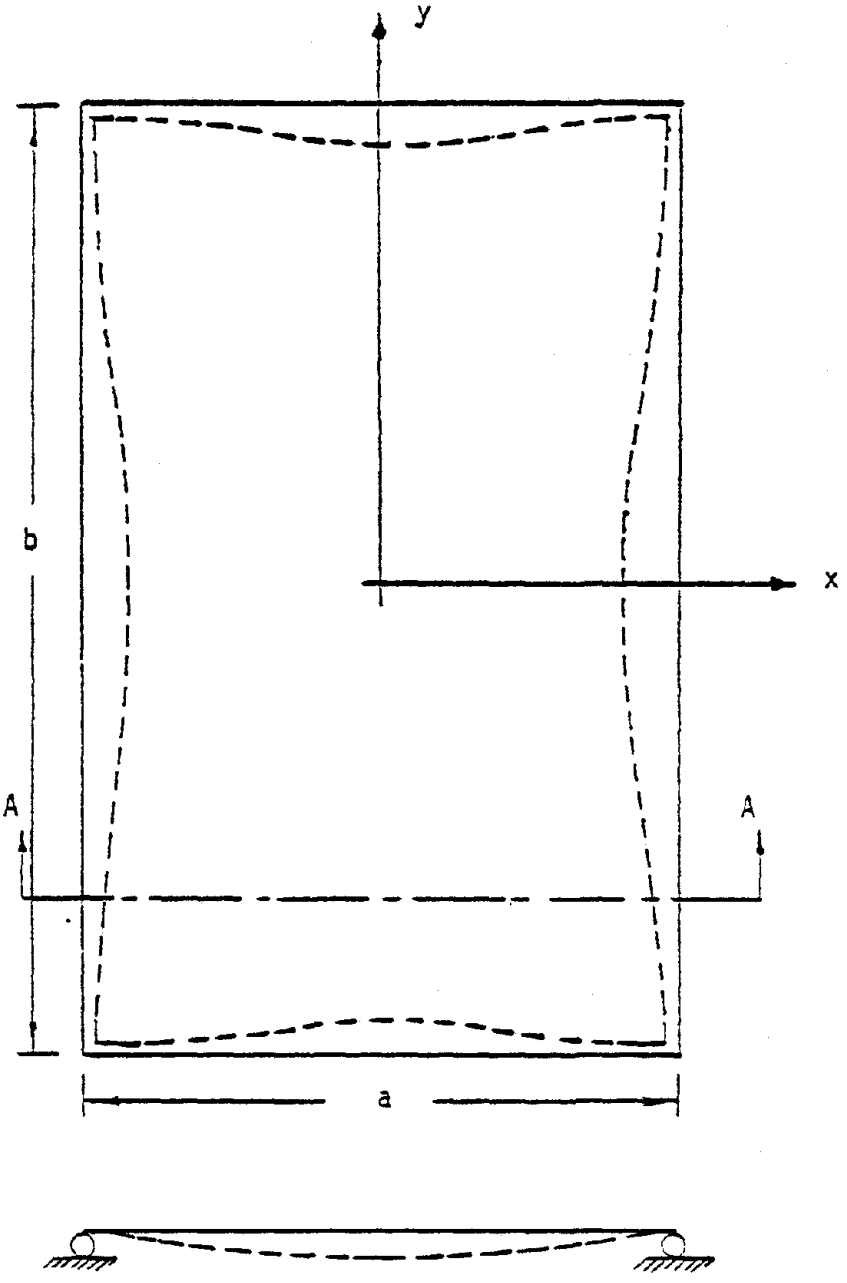

Figure 1.2 Schematic Representation of Assumed In-plane Deformations Along the Edges of the Plate

This work was conducted in the Civil Engineering Laboratories at Texas Tech University, Lubbock, Texas, under the supervision of the Institute for Disaster Reserach, also at Texas Tech University.

Research on the glass plate problem is being continued by researchers at the Institute for Disaster Research to determine experimentally the distribution of stresses in uniformly loaded rectangular plates which experience large displacements.

1.4 Approach

The approach used in this investigation is a finite element method with a displacement formulation which employs rectangular finite elements. Displacement fields within the rectangular finite plate element are depicted by products of one-dimensional Hermitian polynomials of order one. These functions are used to represent both membrane and bending displacement fields. The main advantage of the proposed finite element formulation is that it provides adequate representation of membrane behavior. A linear incremental approach is used to solve the nonlinear equilibrium equations. A computer program was developed to accomplish the analysis of specific glass plates which experience large deflections.

1.5 Objective and Scope of Research

The primary objective of this research is to develop a finite element model to study theoretically the response of glass plates subjected to relatively large uniform static loads that cause large deflections. The scope of this investigation is defined in the following review of the contents of this report.

In Chapter 2, the nonlinear plate problem is defined with specific details given to geometric nonlinearity. Assumptions related to linear theory

of plates are outlined to introduce the concept of nonlinear plate formulation. The nonlinear equilibrium equations are derived in terms of the displacement components of the plate using an energy approach. Equilibrium equations thus obtained are converted to the commonly known von Karman plate equations. Chapter 2 concludes with a brief account of previous attempts made to solve the nonlinear plate equations.

The first section in Chapter 3 describes the concept of the finite element method and the second section introduces the rectangular finite element used to discretize the glass plate. Next, the shape functions assumed to depict the element displacement fields are defined. This step is followed by a section in which procedures for deriving the element linear and nonlinear stiffness matrices are given. Subsequent to the procedure for evaluating the equivalent load vector, a section describing the calculation of bending and membrane stresses and their combined effects closes the chapter.

The solution procedure for solving the system of nonlinear equilibrium equations is presented in Chapter 4 in an incremental form. Also, the algorithm of the incremental approach adopted in the proposed finite element formulation is given.

Chapter 5 is divided into three sections. In sections 5.1 and 5.2, examples of uniformly loaded simply supported plates with different in-plane boundary conditions are solved and results of displacements and stressed are compared with theoretical and experimental results. The bending and the membrane stresses are compared separately so that the membrane behavior in the glass plate can be better assessed. These results are then discussed in section 5.3. In this chapter, numerical studies conducted on the glass plate problem reveal that the convergence of stresses differs between

bending and membrane stresses, and depends upon the fineness of the finite element discretization, the location within the plate and the relative magnitude of the loading increment. This observation, in the author's opinion, is valuable for anyone involved in analyzing geometrically nonlinear plate problems.

In Chapter 6, conclusions are offered and recommendations for further investigation are advanced.

CHAPTER 2

LARGE DEFLECTION THEORY OF THIN PLATES

2.1 Nonlinear Plate Problems

In linear analysis of thin plates by the classical theory, it is assumed that the middle surface of the plate is free from deformation. This assumption is valid only if the plate is bent into a developable surface (63): a developable surface is one that can be made from a flat sheet without causing any in-plane strain of the middle surface: i.e., a cone or an open ended cylinder. However, application of the classical theory to problems in which the middle surface of the plate experiences some straining will still be valid depending upon the kind of restraints imposed at the edges and the magnitude of maximum lateral displacement of the plate. For example, if the lateral displacement of a uniformly loaded clamped plate is small in comparison with its thickness, it is found that the calculated stresses of the middle surface, which in plate theory are called the membrane stresses, are small and of negligible value when compared with the bending stresses (61). The membrane stresses are also found to be small in the case of cylindrical bending of uniformly loaded long rectangular plates with edges that are free to move in the plane of the plate even though maximum displacements in such plates are of the order of the plate thickness. However, if the edges of these plates are restrained from moving, the membrane stresses become significant and, hence, stress distributions obtained by the classical theory will be in error (65). Therefore, wnen the membrane stresses become large and the deflec-

tions are of the order of the plate thickness, the deformation of the middle surface must then be taken into account when formulating the governing differential equations of the plate. This brings forth partial differential equations which are coupled and nonlinear.

Formulation of these plate equations using mechanics of nonlinear continua leads to classifying the nonlinearity involved into two principal classes, namely (41):

1. Geometric nonlinearity which is ascribed to problems in which the strain-displacement relations are nonlinear. Geometric nonlinear problems are of two types. The first type involves problems with large displacements and large strains. The second type involves also problems with large displacements but small strains. Plate bending with large deflections and elastic structural instabilities are examples of geometric nonlinear problems.
2. Material nonlinearity which is ascribed to problems in which the stress-strain relations are nonlinear. In such problems the material constants are updated depending on the stresses and the strains in the medium and new equilibrium equations are developed. Plasticity and creep phenomena are examples of material nonlinearity.

The problem of geometric nonlinearity of glass plate bending with large displacements and small strains has been investigated in this research.

Geometric nonlinearity arises because of large lateral displacements that alter the shape of the structure which in turn causes the

applied loads to change their distribution (41). This nonlinearity can be introduced into the formulation of the system equations either by inclusion of high powers of the derivatives of the displacements or their products in the strain-displacement relations or by coordinate transformations in which the coordinates of the system account for all nonlinear geometric effects (69).

In order to derive the nonlinear thin plate equations, it is worthwhile to examine the assumptions limiting the linear theory of thin plates.

2.2 Assumptions of the Linear Theory of Thin Plates

The classical theory of thin plates assumes that (21, 61):

1. The plate is initially flat and free from stresses,
2. Tractions on planes parallel to the middle surface are small and can be neglected, and strains vary linearly within the plate thickness,
3. The thickness, t, is much smaller than the typical plate dimension, a, where a is the shorter side in the case of a rectangular plate,
4. The maximum deflection of the middle surface of the plate in the lateral direction is small in comparison with the thickness,
5. The middle surface of the plate is free from deformation during bending,
6. The slopes of the deflected middle surface are small compared to unity, and

7. The vertical deflection of a point on the middle surface of the plate is measured on a normal to its initial plane.

These are generally known as Kirchoff's assumptions in plate theory. If these assumptions are considered, all stress components can be calculated in terms of the normal deflection of the middle surface of the plate, w, which is a function of two coordinates in the plane of the plate (68).

2.3 Nonlinear Thin Plate Equations

If assumptions 4 and 5 above are violated, the middle surface of the plate will experience some deformation which must be taken into consideration when deriving the differential plate equations. The equations thus obtained are nonlinear and the solution becomes much more complicated (61). In 1910, Theodore von Karman derived the nonlinear plate equations and suggested that the quadratic terms in w_x and w_y* which are the derivatives of the lateral displacement w, with respect to the x and y directions, respectively, be retained in the strain tensor but that other quadratic terms involving higher powers of the derivatives of the in-plane displacement components u and v be dropped because they have about the same magnitude as the square of the strain components. With this suggestion and in addition to the assumptions used in the classical theory of thin plates, excluding assumption 4, von Karman assumed that (21):

1. The magnitude of the lateral deflection w is of the same order as the plate thickness, but small when compared

*Subscripts on symbols denote derivatives with respect to that subscript unless stated differently.

with the typical plate dimension a, where a is the shorter side in the case of a rectangular plate, i.e., $|w| = O(t)$*, $w \ll a$.

2. The in-plane displacement components u and v are small and hence higher powers of their derivatives and their products are negligible.

For rectangular plates, the use of a Cartesian coordinate system is the most convenient (Fig. 2.1). Consider a flat rectangular thin plate in a right-handed rectangular Cartesian frame of reference with the x-y plane coinciding with the middle surface of the plate in its initial undeformed state, and the z-axis perpendicular to it as shown in Fig. 2.1. Let the displacement components of an arbitrary point (x, y, z) be denoted by $(\bar{u}, \bar{v}, \bar{w})$ and those of the corresponding point (x, y, 0) of the middle surface be denoted by (u, v, w). Using assumptions 5 and 6 introduced in the previous section, and considering the geometry of a section of the plate at y = constant, as shown in Fig. 2.2, and by comparing the section before and after it is deflected, the displacement component $\bar{u}$ can be written as

$$\bar{u} = -z\, w_x \tag{2.1}$$

similarly,

$$\bar{v} = -z\, w_y \tag{2.2}$$

By comparing the rectangular parallelogram abcd shown in Fig. 2.3 which is located at a distance z from the middle surface, with its

*O(t) stands for a function of the order of t.

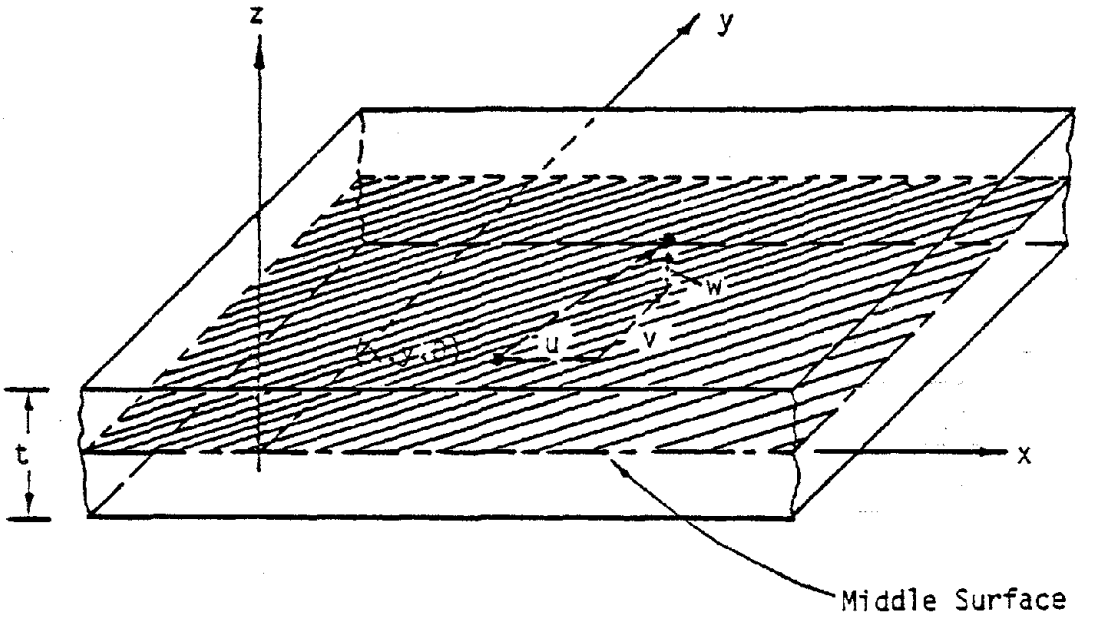

Figure 2.1 Coordinates of Flat Rectangular Plate and Notations of Displacement Components

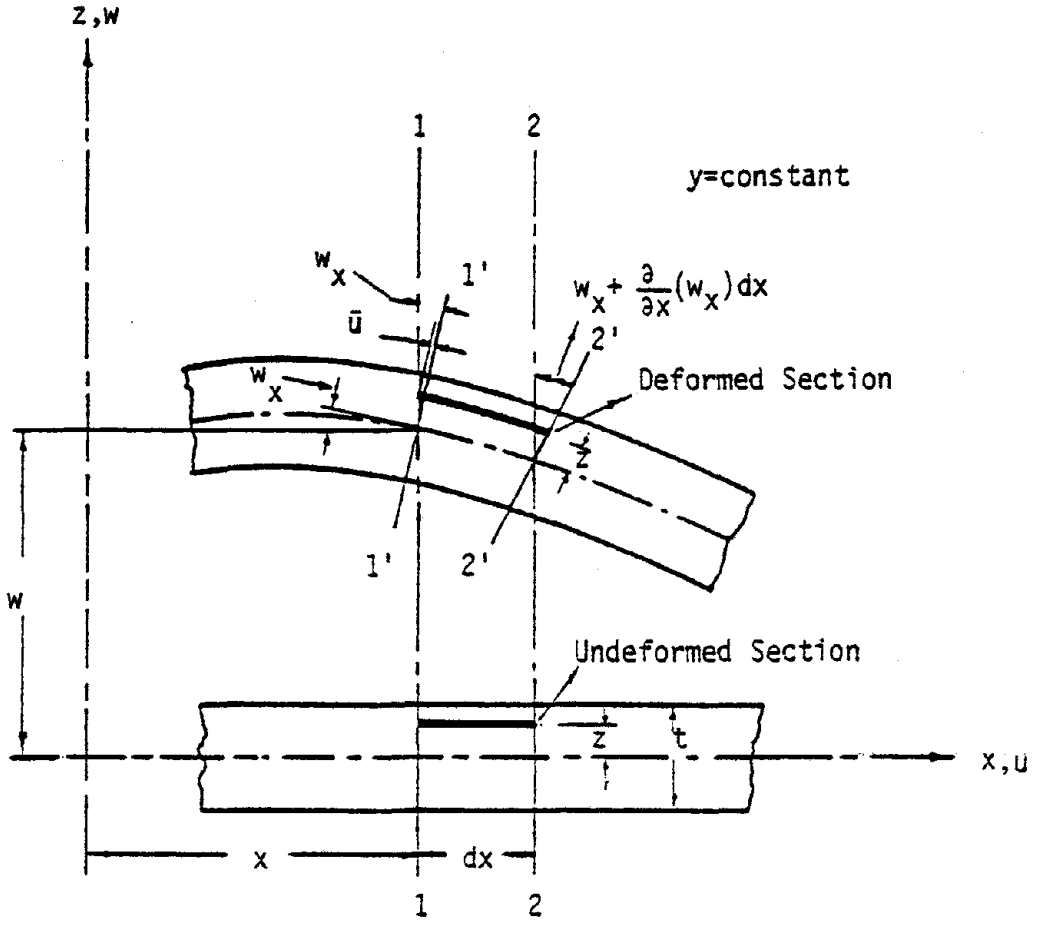

Figure 2.2 Section of a Plate Before and After Deformation

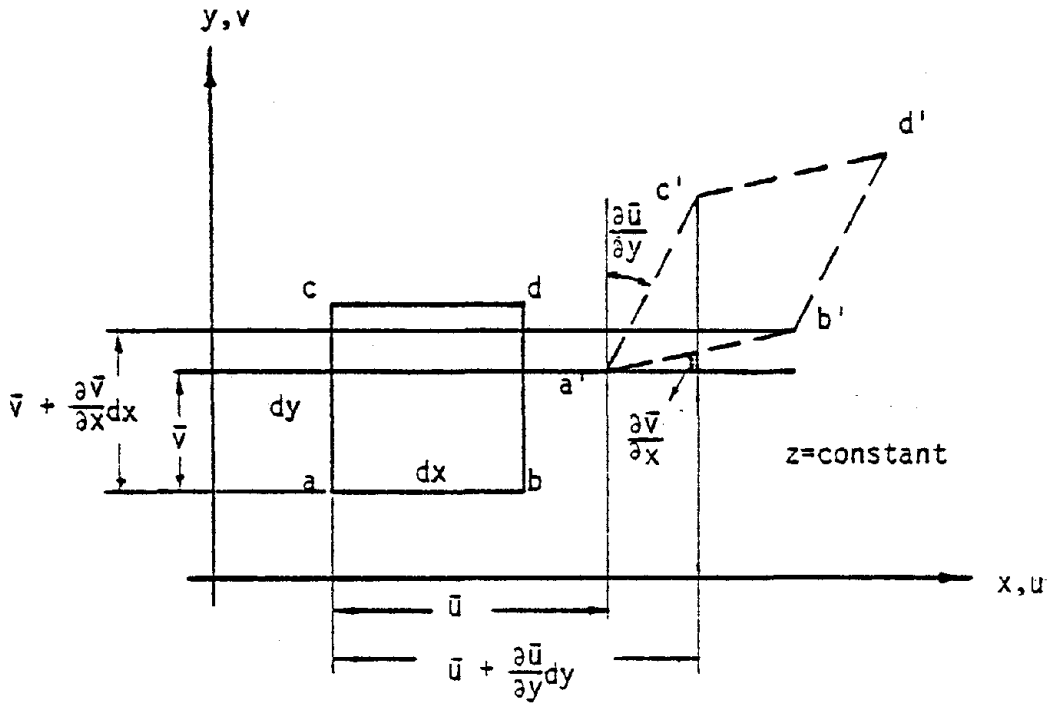

Figure 2.3 Angular Distortion

deformed shape a'b'c'd' on the deflected plate surface, the shear strain γ_{xy} can be determined from the angular distortions $\bar{u}_y$ and $\bar{v}_x$ as

$$\gamma_{xy} = \bar{u}_y + \bar{v}_x \tag{2.3}$$

Using Eq.(2.1) and Eq.(2.2), Eq.(2.3) can be written as

$$\gamma_{xy} = - 2z\, w_{xy} \tag{2.4}$$

If a point (x, y, 0) of the middle surface of the plate undergoes a displacement (u, v, w), then the displacement components of a corresponding point in the plate can be expressed as

$$\begin{aligned} \bar{u} &= u - z\, w_x \\ \bar{v} &= v - z\, w_y \\ \bar{w} &= w \end{aligned} \tag{2.5}$$

For any point in the plate, the nonlinear Lagrangian strain tensor, known as the Green's strain tensor (35), is written in terms of the displacement components in index notation as

$$\bar{\varepsilon}_{ij} = \frac{1}{2} \left\{ \frac{\partial \bar{u}_i}{\partial x_j} + \frac{\partial \bar{u}_j}{\partial x_i} + \left(\frac{\partial \bar{u}_k}{\partial x_i}\right) \left(\frac{\partial \bar{u}_k}{\partial x_j}\right) \right\} \tag{2.6}$$

where the indices i, j, and k correspond to the standard notation used in tensor mechanics. The quantities $\bar{u}_1$, $\bar{u}_2$, and $\bar{u}_3$ indicate the displacement components $\bar{u}$, $\bar{v}$, and $\bar{w}$, respectively, while x_1, x_2, and x_3 refer to the coordinates x, y, and z, respectively. It can be

shown that Eq.(2.6) can be reduced to a simpler form, if assumption 2 introduced in section 2.2 and von Karman's assumption are considered. Assumption 2 implies that $\varepsilon_{zx} = \varepsilon_{yz} = \varepsilon_z = 0$. These relations signify the fact that points on the plate which are initially on a normal to the middle surface before deformation remain on the normal to the middle surface after deformation; this is known as the "Kirchhoff assumption" in the theory of plates. And von Karman's assumption suggests discarding all quadratic terms in Eq.(2.6) except w_x^2, w_y^2, and $w_x w_y$. Hence, Eq.(2.6) can be written as

$$\begin{aligned} \bar{\varepsilon}_x &= \bar{u}_x + \frac{1}{2} w_x^2 \\ \bar{\varepsilon}_y &= \bar{v}_y + \frac{1}{2} w_y^2 \\ \bar{\gamma}_{xy} &= \bar{u}_y + \bar{v}_x + w_x w_y \end{aligned} \tag{2.7}$$

Using Eq.(2.5), Eq.(2.7) can be expressed in terms of the middle surface strains ε_x, ε_y, and γ_{xy} as

$$\begin{aligned} \bar{\varepsilon}_x &= \varepsilon_x - z w_{xx} \\ \bar{\varepsilon}_y &= \varepsilon_y - z w_{yy} \\ \bar{\gamma}_{xy} &= \gamma_{xy} - 2z w_{xy} \end{aligned} \tag{2.8}$$

where

$$\begin{aligned} \varepsilon_x &= u_x + \frac{1}{2} w_x^2 \\ \varepsilon_y &= v_y + \frac{1}{2} w_y^2 \\ \gamma_{xy} &= u_y + v_x + w_x w_y \end{aligned} \tag{2.9}$$

Corresponding to Green's strain tensor, the Kirchhoff's stress tensor in the Lagrangian description is expressed in index notation for an isotropic homogeneous material as (21)

$$\sigma_{ij} = \lambda \varepsilon_{kk} \delta_{ij} + 2G \varepsilon_{ij} \tag{2.10}$$

where

$$\lambda = \frac{2G\nu}{(1-2\nu)}$$

and

$$G = \frac{E}{2(1+\nu)}$$

where λ and G are the well-known Lamé parameters. The indices i, j, and k in Eq.(2.10) correspond to the conventional mechanics notation, and δ_{ij} denotes the Kronecker delta. The Young's modulus of elasticity and the Poisson's ratio of the material are indicated by E and ν, respectively. Based on the Kirchhoff's assumption of plate theory the Kirchhoff's stress tensor can be reduced to

$$\begin{aligned} \bar{\sigma}_x &= \frac{E}{1-\nu^2} (\bar{\varepsilon}_x + \nu \bar{\varepsilon}_y) \\ \bar{\sigma}_y &= \frac{E}{1-\nu^2} (\bar{\varepsilon}_y + \nu \bar{\varepsilon}_x) \\ \bar{\sigma}_{xy} &= \frac{E}{2(1+\nu)} \bar{\gamma}_{xy} \end{aligned} \tag{2.11}$$

where $\bar{\sigma}_x$, $\bar{\sigma}_y$, and $\bar{\sigma}_{xy}$ are the stress components at any point in the plate. Inversion of Eq.(2.11) yields

$$\bar{\varepsilon}_x = \frac{1}{E}(\bar{\sigma}_x - \nu\,\bar{\sigma}_y)$$

$$\bar{\varepsilon}_y = \frac{1}{E}(\bar{\sigma}_y - \nu\,\bar{\sigma}_x) \qquad (2.12)$$

$$\bar{\gamma}_{xy} = \frac{2(1+\nu)}{E}\,\bar{\sigma}_{xy}$$

Eq.(2.11) expresses a state of plane stress for which the strain energy density is written as

$$U_0 = \frac{E}{2(1-\nu^2)}(\bar{\varepsilon}_x^2 + \bar{\varepsilon}_y^2 + 2\nu\,\bar{\varepsilon}_x\,\bar{\varepsilon}_y + \frac{1}{2}(1-\nu)\bar{\gamma}_{xy}) \qquad (2.13)$$

The strain energy of the entire plate is the volume integral of Eq. (2.13) which can be written as

$$U = \iiint U_0\, dV \qquad (2.14)$$

or

$$U = \iint \{ \int_{-t/2}^{+t/2} U_0\, dz \}dx\, dy \qquad (2.15)$$

Substituting Eq.(2.8) into Eq.(2.13) and then substituting the resulting expression in Eq.(2.15), the strain energy U, when integrated over the thickness t of the plate, separates into a sum $U = U_m + U_b$, where U_m is the membrane strain energy which is linear in t, and U_b is the bending strain energy which is cubic in t. If the material properties E and ν are considered constant, U_m and U_b can be written as

$$U_m = \frac{Et}{2(1-\nu^2)} \iint [\varepsilon_x^2 + \varepsilon_y^2 + 2\nu\,\varepsilon_x\,\varepsilon_y + \frac{1}{2}(1-\nu)\,\gamma_{xy}^2]\,dx\,dy \qquad (2.16)$$

and

$$U_b = \frac{Et^3}{24(1-\nu^2)} \iint [w_{xx}^2 + w_{yy}^2 + 2\nu\,w_{xx}w_{yy} + \frac{1}{2}(1-\nu)\,w_{xy}^2]\,dx\,dy \qquad (2.17)$$

The potential energy function of a uniformly distributed load q (x, y) applied to the plate is defined as

$$V = -\iint w\,q(x,y)\,dx\,dy \qquad (2.18)$$

The total potential energy Φ of the plate is the sum of the strain energy U and the potential energy function V, that is

$$\Phi = U_m + U_b + V \qquad (2.19)$$

Using Euler's equation of the calculus of variations (32), it can be demonstrated that the differential equations of equilibrium in terms of the middle surface displacement components (u, v, w) in the x, y, and z directions are obtained from the total energy expression of Eq. (2.19) and they are written as

$$\frac{\partial}{\partial x}[u_x + \nu\,v_y + \frac{1}{2}w_x^2 + \frac{\nu}{2}w_y^2] + \frac{1-\nu}{2}\frac{\partial}{\partial y}[u_y + v_x + w_x w_y] = 0 \qquad (2.20)$$

$$\frac{\partial}{\partial y}[v_y + \nu\,u_x + \frac{1}{2}w_y^2 + \frac{\nu}{2}w_x^2] + \frac{1-\nu}{2}\frac{\partial}{\partial x}[u_y + v_x + w_x w_y] = 0 \qquad (2.21)$$

$$w_{xxxx} + 2w_{xxyy} + w_{yyyy} = \frac{q}{D} + \frac{12}{t^2}\left[\{(u_x + \frac{1}{2}w_x^2) + \right.$$

$$\nu(v_y + \frac{1}{2}w_y^2)\}\, w_{xx} + \{(v_y + \frac{1}{2}w_y^2) + \nu(u_x + \frac{1}{2}w_x^2)\}$$

$$\left. w_{yy} + 1-\nu\,(u_y + v_x + w_x w_y)\, w_{xy}\right] \qquad (2.22)$$

where

$$D = \frac{Et^3}{12(1-\nu^2)}$$

The quantity D is called the "flexural rigidity" of the plate.

Eq.(2.20) through (2.22) are the basic equilibrium equations for the geometric nonlinear problem in a displacement formulation. Alternatively, these equations can be converted to the well-known von Karman plate equations if the membrane stress resultants defined in plate theory by the statical relations (21)

$$N_x = \int_{-t/2}^{+t/2} \sigma_x \, dz$$

$$N_y = \int_{-t/2}^{+t/2} \sigma_y \, dz \qquad (2.23)$$

$$N_{xy} = \int_{-t/2}^{+t/2} \sigma_{xy} \, dz$$

are expressed in terms of a stress function F(x, y) such that

$$N_x = \frac{\partial^2 F(x,y)}{\partial y^2}$$

$$N_y = \frac{\partial^2 F(x,y)}{\partial x^2} \tag{2.24}$$

$$N_{xy} = -\frac{\partial^2 F(x,y)}{\partial x \partial y}$$

Using Eqs.(2.9) and (2.11), it can be demonstrated that

$$N_x = \frac{Et}{1-\nu^2}(\varepsilon_x + \nu\,\varepsilon_y)$$

$$N_y = \frac{Et}{1-\nu^2}(\varepsilon_y + \nu\,\varepsilon_x) \tag{2.25}$$

$$N_{xy} = N_{yx} = \frac{Et}{2(1+\nu)}\gamma_{xy}$$

From Eqs.(2.24) and (2.25),we can write

$$\frac{\partial^2 F(x,y)}{\partial x^2} = F_{xx} = \frac{Et}{1-\nu^2}(\varepsilon_y + \nu\,\varepsilon_x)$$

$$\frac{\partial^2 F(x,y)}{\partial y^2} = F_{yy} = \frac{Et}{1-\nu^2}(\varepsilon_x + \nu\,\varepsilon_y) \tag{2.26}$$

$$\frac{\partial^2 F(x,y)}{\partial x \partial y} = F_{xy} = -\frac{Et}{2(1+\nu)}\gamma_{xy}$$

From Eqs.(2.20), (2.21), (2.22), and (2.25), we get

$$\frac{\partial N_x}{\partial x} + \frac{\partial N_{xy}}{\partial y} = 0 \tag{2.27}$$

$$\frac{\partial N_{xy}}{\partial x} + \frac{\partial N_y}{\partial y} = 0 \tag{2.28}$$

$$D\,[w_{xxxx} + 2w_{xxyy} + w_{yyyy}] = q + N_x\, w_{xx} + 2N_{xy}\, w_{xy} + N_y\, w_{yy} \tag{2.29}$$

Substituting Eq.(2.25) in Eq.(2.29), we get

$$D\,[w_{xxxx} + 2w_{xxyy} + w_{yyyy}] = q + F_{yy}\, w_{xx} - 2F_{xy}\, w_{xy} + F_{xx}\, w_{yy} \tag{2.30}$$

A second relation between the functions F(x, y) and w(x, y) can be obtained by deriving the strain compatibility equation. If Eq. (2.25) is inverted, it yields

$$\begin{aligned} \varepsilon_x &= \frac{1}{Et}\,(F_{yy} - \nu\, F_{xx}) \\ \varepsilon_y &= \frac{1}{Et}\,(F_{xx} - \nu\, F_{yy}) \\ \gamma_{xy} &= -\frac{2(1+\nu)}{Et}\, F_{xy} \end{aligned} \tag{2.31}$$

Using Eq.(2.9), it can be shown that the compatibility condition can be obtained as

$$\frac{\partial^2 \varepsilon_x}{\partial y^2} - \frac{\partial^2 \gamma_{xy}}{\partial x \partial y} + \frac{\partial^2 \varepsilon_y}{\partial x^2} = w_{xy}^2 - w_{xx}\, w_{yy} \tag{2.32}$$

Substituting Eq.(2.31) in Eq.(2.32), we get

$$F_{xxxx} + 2F_{xxyy} + F_{yyyy} = Et\,[w_{xy}^2 - w_{xx}\, w_{yy}] \tag{2.33}$$

Eq.(2.30) and Eq.(2.33) are the well-known von Karman equations. This form of the nonlinear plate equations is most known to investigators dealing with nonlinear plate equations. The von Karman equations are mixed equations which involve a stress function and a displacement function. Such equations are not treated by the displacement approach in the finite element method which is used in this report.

For more understanding of the formulation of the nonlinear plate equations, the interested reader is advised to consult the following references (21, 32, 35, 50, 60, 61, 62, 63, 64, 65).

2.4 Brief Review of Previous Work on Solution of Nonlinear Plate Equations

To the best of the writer's knowledge, there is only one original closed form solution of the von Karman nonlinear thin plate equations. This solution is attributed to Samuel Levy (33, 34) who represented the nonlinear differential equations in terms of trigonometric series and solved for the deflections and the stresses in clamped and simply supported uniformly loaded rectangular plates. Levy solved two types of simply supported uniformly loaded rectangular plates: one, the boundaries of which remained straight and were immovable (he called that type of boundaries "Edge Displacement = 0"), and two, the boundaries of which are assumed to remain straight and free to move in the in-plane direction of the plate (he called that type of boundaries "Edge Compression = 0") (33, 34).

Because of the difficulties involved in solving the von Karman nonlinear thin plate equations, researchers directed their efforts to the development of alternative approaches to the problem which are based on either simplified physical theories or approximate

numerical methods such as the variational methods, the finite difference method, and the finite element method (60).

Marguerre, K., Bengston, H. W., Timoshenko, S., Cox, H. L., and von Karman are some of the early pioneers who formulated approximate solutions based on simplified physical theories to solve the nonlinear thin plate equations. According to Timoshenko, numerical results obtained by these approximate methods give satisfactory accuracy for technical purposes. However, he cautioned that a good understanding of the hypothesis providing the basis of the method is essential in the application of these approximate methods (7, 8, 13, 63, 65).

In 1936, Kaiser, R., solved the nonlinear thin plate equations using finite difference formulations. In his solution, Kaiser assumed that the boundaries of the plate were free to move in the in-plane direction of the plate and that the edges did not necessarily remain straight. Kaiser supported his theoretical work with experimental results that he obtained from a 60cm x 60cm x 0.315cm uniformly loaded simply supported square plate and showed very good agreement of his theoretical and experimental works (29). Also, in 1948, Wang, C. T., used the finite difference method to solve nonlinear problems of uniformly loaded simply supported rectangular plates with boundary conditions that approximate plates with riveted edges. Wang used the successive approximation and the relaxation methods to solve his finite difference equations. The numerical results Wang obtained by his formulation do not agree with those obtained by Levy (70, 71).

With the fast and advanced development of computers the finite element method placed in the hands of researchers an alternative ver-

satile tool for tackling the large deflection plate problem. The finite element method does not directly deal with partial differential equations of equilibrium or compatibility; rather, it converts the problem into one requiring the solution of simultaneous equations. Advancement of this field in solving the nonlinear plate equations is briefly outlined in the next chapter.

CHAPTER 3

THE FINITE ELEMENT METHOD

3.1 Concept

Very often, the structural engineer is confronted with the problem of determining stresses and displacements in continuous structural systems which have complicated configurations and which cannot be handled by available classical methods of stress analysis. A numerical discretization technique, so called "finite element method," enabled the structural engineer to tackle such problems using electronic computers. The concept of this method is simple: if the behavior of a subregion or a finite part, which is known as "finite element," of the whole structural system can be modeled, then the behavior of the entire structural system can be modeled as well. In this case, the entire structural system is considered to be made-up of an assemblage of finite elements which are interconnected at joints called "nodes" or "nodal points." Based on this concept, users of the finite element method are able to divide a structure into several substructures which are made of rather simple geometric shapes such as bars, beams, triangles, rectangles, tetrahedra, and prisms. These different shape elements or a combination of them make it possible to model any structure of any arbitrary shape. Since 1960, the finite element method has gained increasing popularity among structural engineers. This is attributed to the fact that the method handles easily not only problems having complex geometry and mixed boundary conditions, but also problems having nonlinear characteristics.

Formulation of the equations of the finite element model is based upon energy principles. Either of the two well-known methods of structural analysis, namely the force or displacement method, can be used to derive the equations necessary for the finite element analysis. In finite element applications, the displacement model has been employed most commonly. This is because a displacement model can be expressed in various simple forms such as polynomials and trigonometric functions, whereas such functions in the force model are relatively difficult to formulate. Also, the displacement model has better computational schemes for most problems in solid mechanics (19).

The finite element method can be viewed as an extension of the Ritz method, in which the displacement of a continuum are approximated by a set of assumed functions. The unknown constants in these functions are determined using the well-known minimum potential energy theorem which states that (17):

> "Among all displacement configurations that satisfy internal compatibility and kinematic boundary conditions, those that also satisfy the equations of equilibrium make the potential energy a stationary value. If the stationary value is a minimum, the equilibrium is stable."

While in the classical Ritz method, the assumed displacement function describes the total displacement field of the entire continuum; in the finite element, displacement functions are assumed for each element and the entire displacement field of the continuum is approximately expressed in terms of their nodal point values. The total potential energy of individual elements has a stationary value when the whole system is in equilibrium. This condition leads to the minimi-

zation of the total potential energy function of the whole assemblage of elements, which in turn yields the necessary equations corresponding to its equilibrium state (17). The resulting set of equations is called the "stiffness matrix" equation.

The basis for the formulation of the stiffness matrix equations is fully explained in numerous publications by authors such as Argyris (3), Martin (40, 41), Gallagher (22), Zienkiewicz (73), Cook (17), Desai (19), and many others. Hence, only the essential features of the displacement approach of the finite element method pertinent to the problem under investigation are described in this report.

For accomplishing a finite element displacement analysis, the following steps must be considered:

1. Discretization of the structure into some convenient geometrical shapes to model the overall geometry of an actual structure.
2. Selection of a displacement field that belongs to a finite class or space of functions continuous in the domain of the selected element and satisfies requirements of rigid body motion, constant strain, and a minimum number of conditions of displacement continuity along its boundaries.
3. Derivation of the element stiffness matrix which is a function of the geometric and constitutive properties of the element by relating generalized displacements and their associated generalized forces.
4. Formation of the global stiffness matrix by assembling the individual element stiffness matrices to a common system of

reference called the global system. The resulting global matrix equation expresses the equilibrium state of the entire structure.

5. Solution for nodal displacements after prescribing the boundary conditions on the structure.
6. Determination of the strains which are related to the displacements. The stresses are then calculated using Hooke's law.

3.2 Rectangular Finite Element

To represent the complex geometric nonlinear behavior of the glass plate problem under investigation, it was decided to provide adequate representation of the membrane behavior of the structure that is comparable to the bending. This is accomplished by using displacement shape functions suggested by Bogner, Fox, and Schmit (9) which are limited to elements with boundaries parallel to an orthogonal coordinate system. A rectangular plate element due to Schmit, Bogner, and Fox (56) is used in this work as a discretizing unit. The action of the four corner nodes of this geometrically nonlinear bending membrane rectangular plate element is represented by twelve degrees of freedom: four degrees of freedom w, w_x, w_y, and w_{xy} to represent the bending action and eight degrees of freedom u, u_x, u_y, u_{xy}, v, v_x, v_y, and v_{xy} to represent the membrane action. These degrees of freedom will be defined in a later section of this chapter. Twelve degrees of freedom per node result in a 48 degrees of freedom rectangular finite element. The geometry, the nodal

numbering scheme, and local coordinate system for this element are shown in Fig. 3.1.

The displacement shape functions assumed to represent the displacement components u, v, and w of the middle surface of the plate element are formulated using products of one-dimensional Hermitian polynomials of order one. It is noted by Schmit, Bogner, and Fox (56) that although the use of these interpolation polynomials to represent the membrane behavior increases the number of degrees of freedom, it adequately represents the six-rigid body modes and describes the membrane stress state more accurately.

3.3 Hermitian Polynomials

A Hermitian polynomial of order n is a polynomial of degree 2n+1 and can be written as

$$H^n_{mi}(x) \tag{3.1}$$

which gives, when $x = x_i$

$$\frac{d^k H}{dx^k} = 1, \qquad k = m \qquad \text{for } m = 0 \text{ to } n$$

and

$$\frac{d^k H}{dx^k} = 0, \qquad k \neq m \qquad \text{or when } x = x_j$$

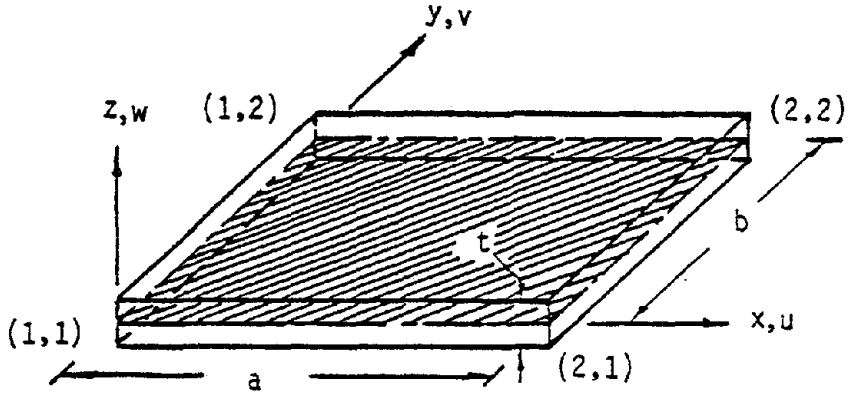

Figure 3.1 Geometric Shape, Nodal Numbering Scheme, and Coordinate System of a Flat Rectangular Finite Element Plate

By setting $n = 1$ and $m = 0$ and 1, a set of Hermitian polynomials of order one is obtained. The set is a set of cubics giving shape functions for a line element ij at the ends of which slopes and values of the function are used as variables. Such a set of polynomials can be written for the rectangular finite element as

$$\left.\begin{aligned} H_{01}^{(1)}(x) &= \frac{1}{a^3}(2x^3 - 3ax^2 + a^3) \\ H_{02}^{(1)}(x) &= \frac{1}{a^3}(2x^3 - 3ax^2) \\ H_{11}^{(1)}(x) &= \frac{1}{a^2}(x^3 - 2ax^2 + a^2x) \\ H_{12}^{(1)}(x) &= \frac{1}{a^2}(x^3 - ax^2) \end{aligned}\right\} \quad \text{For all } x \ 0 \le x \le a \qquad (3.2)$$

These are known as the "osculatory polynomials" and are plotted in Fig. 3.2. Similar expressions for the y-direction are obtained by replacing x by y and a by b.

Using these Hermitian interpolation formulas, the middle surface displacement components u, v, and w of a typical discrete element can be approximated by a sum of their products and undetermined parameters. For example, the displacement component u, in a rectangular plate element can be expressed as

$$u(x,y) = \sum_{i=1}^{2}\sum_{j=1}^{2}\Big[H_{0i}^{(1)}(x)H_{0j}^{(1)}(y)u_{ij} + H_{1i}^{(1)}(x)H_{0j}^{(1)}(y)u_{xij} + H_{0i}^{(1)}(x)H_{1j}^{(1)}(y)u_{yij} + H_{1i}^{(1)}(x)H_{1j}^{(1)}(y)u_{xyij}\Big] \qquad (3.3)$$

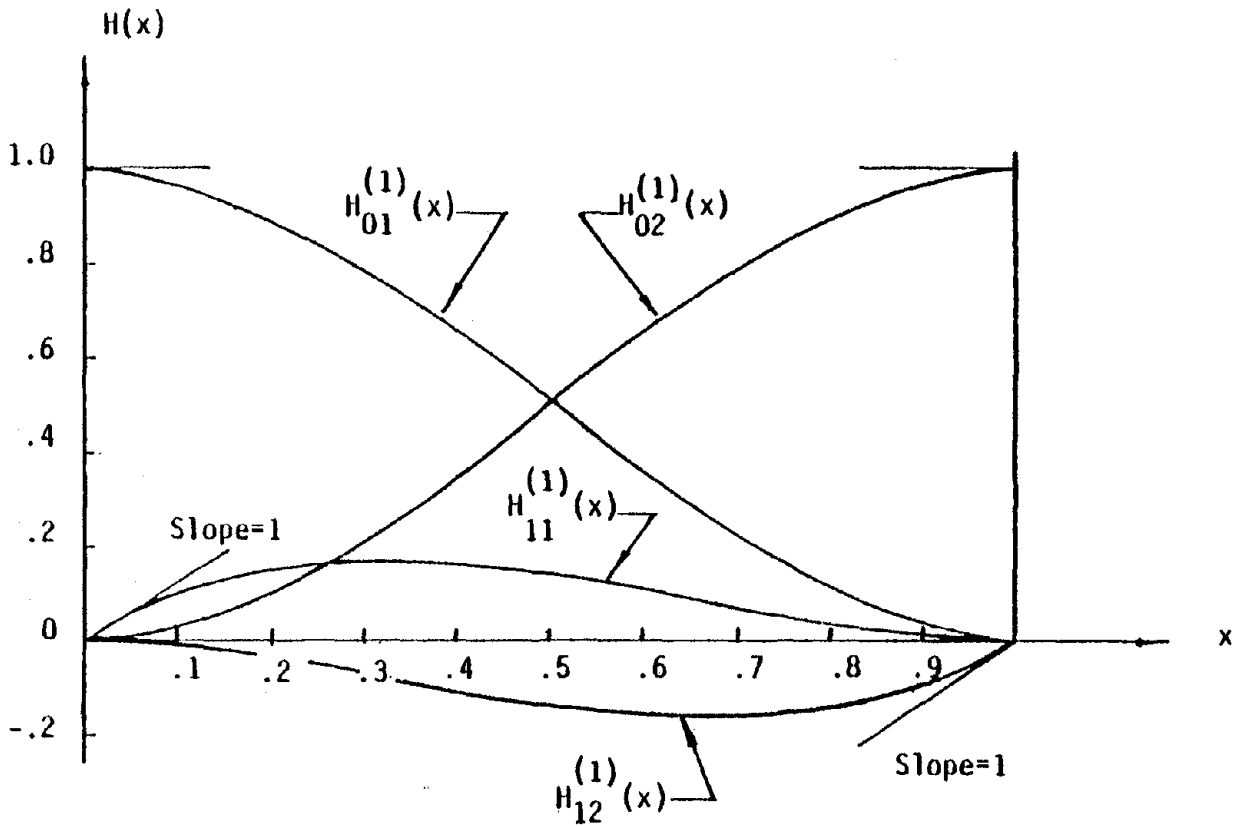

Figure 3.2 Hermitian Polynomials of Order One

where the indicies (i, j) refer to a node of the element as shown in Fig.3.1, and the displacement parameters are defined as

u_{ij} = u displacement at node (i, j)

u_{xij} = $(\frac{\partial u}{\partial x})$ at node (i, j)

u_{yij} = $(\frac{\partial u}{\partial y})$ at node (i, j)

u_{xyij} = $(\frac{\partial^2 u}{\partial x \partial y})$ at node (i, j)

Expressions for the displacement components v and w can be written in similar form as in Eq.(3.3) in which the displacement parameters for each component are interpreted as shown above.

The displacement components can be written more conveniently in matrix form as

$$\{\hat{u}\} = \begin{Bmatrix} u \\ v \\ w \end{Bmatrix} = [N]\{\alpha\} \qquad (3.4)$$

where $\{\hat{u}\}$ is a vector matrix representing the displacement components, [N] is a matrix containing the assumed shape functions which are dependent on the Cartesian coordinates x and y, and $\{\alpha\}$ is a vector containing the nodal displacement parameters.

There are certain requirements and limitations imposed on the assumed shape functions to guarantee a successful finite element formulation. Basically, a shape function assumed over the region of an element is supposed to represent the pattern of displacements in that element. Therefore, a primary consideration in choosing a

shape function is that the function must maintain some minimum continuity requirements between adjacent elements as they deform. The function must also satisfy certain other requirements to minimize the discretization errors in the analysis. These requirements, outlined below, are satisfied for both bending and membrane behavior in this study. The requirements are (16):

1. The functions must include all rigid body displacement states. That is, they must be independent of the external reference system so that the solution to a problem will be invariant with respect to the position of that external reference system and hence prevent self-straining of the elements.
2. The functions must include uniform strain states to assure the convergence of the finite element analysis to the actual strain field as the element size is reduced.
3. The functions and their normal slopes are uniquely specified along any element interface by nodal values selected on that interface. In other words, the displacements and their normal derivatives on an interface of an element are dependent only upon the nodal values occurring at the nodes associated with that interface. This requirement assures compatibility and continuity of the assumed shape function.
4. The shape functions must be linear functions of the nodal parameters so that the resulting system equations are a set of simultaneous, linear algebraic equations in terms of these parameters (44).

3.4 Nonlinear Element Stiffness Matrix

The strains in terms of the middle surface displacements indicated by Eq.(2.7) and Eq.(2.8) in Chapter 2 can be written more conveniently as membrane and bending strains in matrix notation as

$$\{\varepsilon\} = \begin{Bmatrix} (\frac{\partial u}{\partial x}) \\ (\frac{\partial v}{\partial y}) \\ (\frac{\partial u}{\partial y}) + (\frac{\partial v}{\partial x}) \\ -(\frac{\partial^2 w}{\partial x^2}) \\ -(\frac{\partial^2 w}{\partial y^2}) \\ 2(\frac{\partial^2 w}{\partial x \partial y}) \end{Bmatrix} + \begin{Bmatrix} \frac{1}{2}(\frac{\partial w}{\partial x})^2 \\ \frac{1}{2}(\frac{\partial w}{\partial y})^2 \\ (\frac{\partial w}{\partial x})(\frac{\partial w}{\partial y}) \\ 0 \\ 0 \\ 0 \end{Bmatrix} \tag{3.5}$$

where the first vector on the right side of the equation expresses the linear membrane and bending strain components and the second gives the nonlinear membrane strain components. Alternatively, Eq. (3.5) can be written as

$$\begin{aligned} \{\varepsilon\} &= \left[[B_0] + [B_L] \right] \{\alpha\} \\ &= [\bar{B}] \{\alpha\} \end{aligned} \tag{3.6}$$

where $\{\alpha\}$ is a vector containing the nodal displacement parameters and $[B_0]$, $[B_L]$, and $[\bar{B}]$ are matrices containing the derivatives of the shape functions. Details of these matrices will be outlined in later

sections of this chapter.

The corresponding "stresses" are in fact the membrane tractions per unit length in the x and y directions as defined in Eq.(2.23) in Chapter 2, and the bending and twisting moments per unit length in the x and y directions as defined in plate theory.

$$\{\sigma\} = \begin{Bmatrix} N_x \\ N_y \\ N_{xy} \\ M_x \\ M_y \\ M_{xy} \end{Bmatrix} \tag{3.7}$$

Because the membrane strains and stresses are assumed to have constant variations across the thickness of the plate, the membrane stresses are obtained from the following expressions

$$\begin{aligned} \sigma_x^m &= \frac{N_x}{t} \\ \sigma_y^m &= \frac{N_y}{t} \\ \sigma_{xy}^m &= \frac{N_{xy}}{t} \end{aligned} \tag{3.8}$$

where σ_x^m and σ_y^m refer to the membrane stresses in the x and y direction, respectively, σ_{xy}^m indicates the membrane shear stress, and t is the thickness of the plate.

The bending strains and stresses are assumed to vary linearly across the thickness of the plate and they can be found anywhere

along the thickness from the following expressions

$$\sigma_x^b = \frac{12}{t^3} M_x z$$

$$\sigma_y^b = \frac{12}{t^3} M_y z \qquad (3.9)$$

$$\sigma_{xy}^b = \frac{12}{t^3} M_{xy} z$$

where σ_x^b and σ_y^b are the true bending stresses in the x and y directions, σ_{xy}^b is the true bending shear stress, and z is the vertical distance measured from the middle surface of the plate.

Assuming linear, isotropic, homogeneous material within the element, the stress-strain relations are expressed as

$$\{\sigma\} = [D^*] \{\varepsilon\} \qquad (3.10)$$

where $[D^*]$ is a matrix defined in terms of the elastic constants of the material as

$$[D^*] = \frac{E}{1-\nu^2} \begin{bmatrix} 1 & \nu & 0 & 0 & 0 & 0 \\ \nu & 1 & 0 & 0 & 0 & 0 \\ 0 & 0 & \frac{1-\nu}{2} & 0 & 0 & 0 \\ 0 & 0 & 0 & \frac{t^3}{12} & \frac{\nu t^3}{12} & 0 \\ 0 & 0 & 0 & \frac{\nu t^3}{12} & \frac{t^3}{12} & 0 \\ 0 & 0 & 0 & 0 & 0 & \frac{t^3(1-\nu)}{24} \end{bmatrix} \qquad (3.11)$$

where E is Young's modulus of elasticity, ν is the Poisson's ratio, and t is the thickness of the plate.

Using the virtual displacement principle and Eq.(3.4), a virtual

displacement of a point within an element can be expressed in terms of the nodal virtual displacement parameters as

$$\{\delta\tilde{u}\} = [N]\ \{\delta\alpha\} \tag{3.12}$$

Consequently, the virtual strain at that point can be written in terms of the virtual displacement parameters as

$$\{\delta\varepsilon\} = [\bar{B}]\ \{\delta\alpha\} \tag{3.13}$$

The virtual strain energy is equal to the virtual work done by forces in an element, that is,

$$\int_V \{\delta\varepsilon\}^T\ \{\sigma\} dV = \{\delta\tilde{u}\}^T\ \{q_z\} \tag{3.14}$$

where $\{q_z\}$ represents the distributed forces per unit volume acting on the element.

Substituting Eq.(3.12) and (3.13) in (3.14) and integrating over the volume of the element, it can be shown that

$$\int_V [\bar{B}]^T\ \{\sigma\} dV = \{f\} \tag{3.15}$$

where

$$\{f\} = \int_A [N]^T\ \{q_n\}\ dA \tag{3.16}$$

Eq.(3.15) can be rewritten as

$$\{\Phi(\alpha)\} = \int_V [\bar{B}]^T\ \{\sigma\}\ dV - \{f\} = 0 \tag{3.17}$$

where $\{\Phi(\alpha)\}$ is a function of the nodal displacement parameters α.

Taking the appropriate variations of the function $\{\Phi(\alpha)\}$ in Eq.(3.17) with respect to α, we get

$$\{\delta\Phi(\alpha)\} = \int_V [\bar{B}]^T \{\delta\sigma\}\, dV + \int_V [\delta\bar{B}]^T \{\sigma\}\, dV \tag{3.18}$$

Taking the appropriate variations of Eq.(3.10) yields

$$\{\delta\sigma\} = [D^*]\,\{\delta\varepsilon\} \tag{3.19}$$

Substituting Eq.(3.13) into Eq.(3.19), we get

$$\{\delta\sigma\} = [D^*]\,[\bar{B}]\,\{\delta\varepsilon\} \tag{3.20}$$

In Eq.(3.6), $[\bar{B}] = [B_0] + [B_L]$, where $[B_L]$ is a function of the displacement parameters α, hence by taking the variations of $[\bar{B}]$, we obtain

$$[\delta\bar{B}] = [\delta B_L] \tag{3.21}$$

Substituting Eq.(3.20) and (3.21) into Eq.(3.18), one gets

$$\{\delta\Phi(\alpha)\} = \int_V [\bar{B}]^T [D^*][\bar{B}]\, dV\, \{\delta\alpha\} + \int_V [\delta B_L]^T \{\sigma\}\, dV \tag{3.22}$$

Expanding the first term in Eq.(3.22) by substituting the value of $[\bar{B}]$ given in Eq.(3.6) we get

$$\int_V [\bar{B}]^T [D^*][\bar{B}]\, dV\, \{\delta\alpha\} = \Big[\int_V [B_0]^T [D^*][B_0]\, dV + \int_V [B_0]^T [D^*][B_L]\, dV + \int_V [B_L]^T [D^*][B_L]\, dV + \int_V [B_L]^T [D^*][B_0]\, dV \Big] \{\delta\alpha\} \tag{3.23}$$

The first term on the right side of Eq.(3.23) is the usual linear stiffness matrix which can be expressed as

$$[K_0] = \int_V [B_0]^T [D^*][B_0]\, dV \tag{3.24}$$

The rest of the terms in Eq.(3.23) signify the effects of large displacements on the stiffness of the structural system. This may be expressed as

$$[K_L] = \int_V [B_0]^T [D^*][B_L]\, dV + \int_V [B_L]^T [D^*][B_L]\, dV + \int_V [B_L]^T [D^*][B_0]\, dV \tag{3.25}$$

where $[K_L]$ is called the "large displacement" stiffness matrix (73).

In Eq.(3.22), the second term can be written as equal to $[k_\sigma]$ times $\{\delta\alpha\}$, where $[K_\sigma]$ is called the "initial stress" or the "geometric" stiffness matrix (73) which depends on the stress level in the element and which can be shown to be symmetric. That is

$$\int_V [\delta B_L]^T \{\sigma\}\, dV = [K_\sigma]\{\delta\alpha\} \tag{3.26}$$

Alternatively, Eq.(3.18) is written as

$$\{\delta\Phi(\alpha)\} = \Big[[K_0] + [K_L] + [K_\sigma]\Big]\{\delta\alpha\} \tag{3.27}$$

The stiffness matrices $[K_0]$ and $[K_L]$ are calculated by integrating the expressions given by (3.24) and (3.25) over the volume of the element after the matrices $[B_0]$ and $[B_L]$ are evaluated. Evalua-

tion of these matrices is outlined in the following two sections which are followed by a section outlining the procedures involved in calculating the stiffness matrix $[K_\sigma]$.

For convenience and clarity in evaluating these matrices, let the following equations previously stated be rewritten in such a manner that the membrane and the bending quantities are separated as

$$\{\tilde{u}\} = \begin{bmatrix} [N^m] & [0] \\ [0] & [N^b] \end{bmatrix} \begin{Bmatrix} \{\alpha^m\} \\ \{\alpha^b\} \end{Bmatrix} \tag{3.4.1}$$

where $[N^m]$ and $[N^b]$ are matrices containing the shape functions of membrane and bending, respectively. Similarily, $\{\alpha^m\}$ and $\{\alpha^b\}$ represent the displacement parameters for membrane and bending, respectively.

Also, Eq.(3.5), can be redefined as

$$\{\varepsilon\} = \{\varepsilon_L\} + \{\varepsilon_{NL}\}$$

$$= \begin{Bmatrix} \{\varepsilon^m_L\} \\ \{\varepsilon^b_L\} \end{Bmatrix} + \begin{Bmatrix} \{\varepsilon^m_{NL}\} \\ \{0\} \end{Bmatrix} \tag{3.5.1}$$

where $\{\varepsilon^m_L\}$ and $\{\varepsilon^b_L\}$ indicate the linear membrane and bending strain components, while $\{\varepsilon^m_{NL}\}$ and $\{0\}$ represent the nonlinear strain components of membrane and bending, respectively.

The quantities in Eq.(3.5.1) are expressed in terms of the derivatives of the shape functions as

$$\begin{Bmatrix} \{\varepsilon_L^m\} \\ \{\varepsilon_L^b\} \end{Bmatrix} = \begin{bmatrix} [B_0^m] & [0] \\ [0] & [B_0^b] \end{bmatrix} \begin{Bmatrix} \{\alpha^m\} \\ \{\alpha^b\} \end{Bmatrix} \tag{3.5.2}$$

where $[B_0^m]$ and $[B_0^b]$ represent the membrane and the bending quantities in matrix $[B_0]$ defined in Eq.(3.6), and

$$\begin{Bmatrix} \{\varepsilon_{NL}^m\} \\ \{0\} \end{Bmatrix} = \begin{bmatrix} [0] & [B_L^b] \\ [0] & [0] \end{bmatrix} \begin{Bmatrix} \{\alpha^m\} \\ \{\alpha^b\} \end{Bmatrix} \tag{3.5.3}$$

or

$$\{\varepsilon_{NL}^m\} = [B_L^b]\{\alpha^b\} \tag{3.5.4}$$

where $[B_L^b]$ represent the induced membrane effects due to large displacements (in this case w_x and w_y) and it contains the derivatives of the shape functions and the slopes w_x and w_y.

The corresponding "stresses" are also divided into membrane and bending components, thus Eq.(3.7) becomes

$$\{\sigma\} = \begin{Bmatrix} \{\sigma^m\} \\ \{\sigma^b\} \end{Bmatrix} \tag{3.7.1}$$

The matrix [D*] defined by Eq.(3.11) is written as

$$[D^*] = \begin{bmatrix} [D^m] & [0] \\ [0] & [D^b] \end{bmatrix} \tag{3.11.1}$$

where

$$[D^m] = \frac{E}{1-\nu^2} \begin{bmatrix} 1 & \nu & 0 \\ \nu & 1 & 0 \\ 0 & 0 & \frac{1-\nu}{2} \end{bmatrix} \tag{3.11.2}$$

and

$$[D^b] = \frac{Et^3}{12(1-\nu^2)} \begin{bmatrix} 1 & \nu & 0 \\ \nu & 1 & 0 \\ 0 & 0 & \frac{1-\nu}{2} \end{bmatrix} \tag{3.11.3}$$

These definitions enable us to proceed with evaluating the matrices $[B_0]$, $[B_L]$, and $[K_\sigma]$ as illustrated in the following sections.

3.4-A Evaluation of $[B_0]$

If the nodal numbering scheme for the flat rectangular bending membrane element shown in Fig. 3.1 is followed, the displacement component u(x, y) given by Eq.(3.3) can be written as

$$u(x,y) = \Big[H^{(1)}_{01}(x)H^{(1)}_{01}(y),\ H^{(1)}_{11}(x)H^{(1)}_{01}(y),\ H^{(1)}_{01}(x)H^{(1)}_{11}(y),\ H^{(1)}_{11}(x)H^{(1)}_{11}(y),\ H^{(1)}_{01}(x)H^{(1)}_{02}(y),\ H^{(1)}_{11}(x)H^{(1)}_{02}(y),\ H^{(1)}_{01}(x)H^{(1)}_{12}(y),\ H^{(1)}_{11}(x)H^{(1)}_{12}(y),\ H^{(1)}_{02}(x)H^{(1)}_{02}(y),\ H^{(1)}_{12}(x)H^{(1)}_{02}(y),\ H^{(1)}_{02}(x)H^{(1)}_{12}(y),\ H^{(1)}_{12}(x)H^{(1)}_{12}(y),\ H^{(1)}_{02}(x)H^{(1)}_{01}(y),\ H^{(1)}_{12}(x)H^{(1)}_{01}(y),\ H^{(1)}_{02}(x)H^{(1)}_{11}(y),\ H^{(1)}_{12}(x)H^{(1)}_{11}(y),\Big] \{ u_{11},\ u_{x11},\ u_{y11},\ u_{xy11},\ u_{12},\ u_{x12},\ u_{y12},\ u_{xy12},\ u_{22},\ u_{x22},\ u_{y22},\ u_{xy22},\ u_{21},\ u_{x21},\ u_{y21},u_{xy21} \} \quad (3.28)$$

Similar expressions can be written for the displacement components v and w. This makes it possible to write the linear strain components in terms of the derivatives of the shape functions and the nodal displacement parameters as

$$\{\varepsilon_L\} = [B_0]\ \{\alpha\} \quad (3.29)$$

where $[B_0]$ is a [6 x 48] matrix which has the general partitioned form

$$[B_0] = \begin{bmatrix} \cdots\cdots\cdots & \cdots\cdots\cdots \\ [B_0^m\ (3x32)] & [\bigcirc] \\ \cdots\cdots\cdots & \cdots\cdots\cdots \\ [\bigcirc] & [B_0^b\ (3x16)] \end{bmatrix} \quad (3.30)$$

Forms of the matrix $[B_0]$ evaluated for the computer program are shown in Appendix A.

3.4-B Evaluation of $[B_L]$

From Eqs.(3.5) and (3.5.4), we can write

$$\{\varepsilon_{NL}^m\} = [B_L^b]\{\alpha^b\} = \begin{Bmatrix} \frac{1}{2}\left(\frac{\partial w}{\partial x}\right)^2 \\ \frac{1}{2}\left(\frac{\partial w}{\partial y}\right)^2 \\ \left(\frac{\partial w}{\partial x}\right)\left(\frac{\partial w}{\partial y}\right) \end{Bmatrix} \tag{3.31}$$

the right side of Eq.(3.31) can be conveniently written as

$$\begin{Bmatrix} \frac{1}{2}\left(\frac{\partial w}{\partial x}\right)^2 \\ \frac{1}{2}\left(\frac{\partial w}{\partial y}\right)^2 \\ \left(\frac{\partial w}{\partial x}\right)\left(\frac{\partial w}{\partial y}\right) \end{Bmatrix} = \frac{1}{2}\begin{bmatrix} \left(\frac{\partial w}{\partial x}\right) & 0 \\ 0 & \left(\frac{\partial w}{\partial y}\right) \\ \left(\frac{\partial w}{\partial y}\right) & \left(\frac{\partial w}{\partial x}\right) \end{bmatrix} \begin{Bmatrix} \left(\frac{\partial w}{\partial x}\right) \\ \left(\frac{\partial w}{\partial y}\right) \end{Bmatrix} = \frac{1}{2}[C]\{\Theta\} \tag{3.32}$$

where

$$[C] = \begin{bmatrix} \left(\frac{\partial w}{\partial x}\right) & 0 \\ 0 & \left(\frac{\partial w}{\partial y}\right) \\ \left(\frac{\partial w}{\partial y}\right) & \left(\frac{\partial w}{\partial x}\right) \end{bmatrix} \tag{3.33}$$

and

$$\{\Theta\} = \begin{Bmatrix} \left(\frac{\partial w}{\partial x}\right) \\ \left(\frac{\partial w}{\partial y}\right) \end{Bmatrix} \tag{3.34}$$

The quantity $\{\Theta\}$ is defined by expressing the slopes w_x and w_y in terms of the derivatives of the shape functions as

$$\{\Theta\} = [G]\ \{\alpha^b\} \tag{3.35}$$

or

$$\{\delta\Theta\} = [G]\ \{\delta\alpha^b\} \tag{3.36}$$

where [G] is a [2 x 16] matrix which is a pure function of the element coordinates.

From Eqs.(3.31) and (3.32), we can write

$$\{\varepsilon_{NL}^m\} = \frac{1}{2}\ [C]\{\Theta\} \tag{3.37}$$

Taking the variations on both sides of Eq.(3.37)

$$\{\delta\varepsilon_{NL}^m\} = \frac{1}{2}\ [\delta C]\{\Theta\} + \frac{1}{2}\ [C]\{\delta\Theta\} \tag{3.38}$$

But, it can be shown that

$$[\delta C]\{\Theta\} = [C]\{\delta\Theta\} \tag{3.39}$$

Because of a special property* of the matrices [C] and $\{\Theta\}$ using Eqs. (3.36) and (3.39), Eq.(3.38) can be written as

$$\{\delta\varepsilon_{NL}^m\} = [C]\{\delta\Theta\} = [C][G]\{\delta\alpha^b\} = [B_L^b]\ \{\delta\alpha\} \tag{3.40}$$

where

$$[B_L^b] = [C][G] \tag{3.41}$$

---

*See Ref. (73) page 510 for the special property of the matrices [C] and $\{\Theta\}$.

Eqs.(3.6) or (3.5.3) imply that

$$[B_L] = \begin{bmatrix} [0] & [C][G] \\ [0] & [0] \end{bmatrix} \tag{3.42}$$

where $[B_L]$ is a [6 x 48] matrix which is a function of the derivatives of the shape functions and the slopes w_x and w_y. Forms of the $[B_L]$ matrix as evaluated for the computer program are shown in Appendix A.

3.4-C "Initial Stress" Stiffness Matrix $[K_\sigma]$

The "initial stress" stiffness matrix is defined by Eq.(3.26) and rewritten here for convenience as

$$[K_\sigma]\{\delta\alpha\} = t \int_A [\delta B_L]^T \{\sigma\}\, dA \tag{3.43}$$

where A is the area of the element and dA indicates integration over that area.

Using Eq.(3.7.1) and taking the variations on both sides of Eq. (3.42), Eq.(3.43) becomes

$$[K_\sigma]\{\delta\alpha\} = t \int_A \begin{bmatrix} [0] & [0] \\ [G]^T[\delta C]^T & [0] \end{bmatrix} \begin{Bmatrix} \{\sigma^m\} \\ \{\sigma^b\} \end{Bmatrix} dA$$

$$= t \int_A \begin{bmatrix} [0] + [0] \\ [G]^T[\delta C]^T\{\sigma^m\} + [0] \end{bmatrix} dA \tag{3.44}$$

From Eq.(3.7) and Eq.(3.7.1), we can write

$$\{\sigma^m\} = \begin{Bmatrix} N_x \\ N_y \\ N_{xy} \end{Bmatrix} \tag{3.45}$$

Again, using the special property of the matrices [C] and {Θ}, we can write

$$[\delta C]^T\{\sigma^m\} = [\delta C]^T \begin{Bmatrix} N_x \\ N_y \\ N_{xy} \end{Bmatrix} = \begin{bmatrix} N_x & N_{xy} \\ N_{xy} & N_y \end{bmatrix} \{\delta\Theta\}$$

$$= \begin{bmatrix} N_x & N_{xy} \\ N_{xy} & N_y \end{bmatrix} [G]\{\delta\alpha^b\} \tag{3.46}$$

substituting Eq.(3.46) into Eq.(3.44), we get

$$[K_\sigma] = \begin{bmatrix} [0] & [0] \\ [0] & [K_\sigma^b] \end{bmatrix} \tag{3.47}$$

where

$$[K_\sigma^b] = t \int_A [G]^T \begin{bmatrix} N_x & N_{xy} \\ N_{xy} & N_y \end{bmatrix} [G]\, dA \tag{3.48}$$

Adding the linear stiffness matrix $[K_0]$, the "displacement" stiffness matrix $[K_L]$, and the "initial stress" stiffness matrix $[K_\sigma]$, the total element stiffness matrix is obtained as

$$[K_T] = [K_0] + [K_L] + [K_\sigma] \tag{3.49}$$

where $[K_T]$ is the total or "tangential" stiffness matrix. Expressions for portions of the matrices $[K_0]$, $[K_L]$, and $[K_\sigma]$, as calculated in the computer program, are shown in Appendices B, C, and D, respectively.

It should be noted that the approach used to derive the stiffness matrices just shown is attributed to Zienkiewicz (73).

3.5 Equivalent Load Vectors

The concept used in determining the load vector for a structural system subjected to some loading is that the total work done by the equivalent loads must be equal to the work done by the actual loads. In the computer program prepared for this investigation, membrane load vectors q_m for concentrated nodal loads, distributed edge shear loads, and uniformly distributed in-plane loadings on each of the four edges of the element are formulated. Similar expressions are also formulated for the bending load vectors due to concentrated nodal loads, distributed edge moments, distributed edge shears, and uniformly distributed lateral loads.

As an illustration, the calculation of the bending load vector q_b due to a uniformly distributed lateral load q will be demonstrated here. A displacement, say w in this case, may be expressed in terms of products of one-dimensional Hermitian interpolation polynomials as

$$w(x,y) = \sum_{i=1}^{2} \sum_{j=1}^{2} \left[H_{0i}^{(1)}(x) H_{0j}^{(1)}(y) w_{ij} + H_{1i}^{(1)}(x) H_{0j}^{(1)}(y) w_{xij} \right.$$

$$\left. + H_{0i}^{(1)}(x) H_{1j}^{(1)}(y) w_{yij} + H_{1i}^{(1)}(x) H_{1j}^{(1)}(y) w_{xyij} \right] \qquad (3.50)$$

For a rectangular flat plate element with dimensions a and b along the x and y axes, respectively, the components of the bending load vector are calculated from

$$V = -\int_0^b \int_0^a q\, w(x,y)\, dx\, dy \qquad (3.51)$$

For example, the component of the bending load vector corresponding to the nodal parameter w_{x11} at node (1,1) is obtained as

$$(q_b)_{w_{x11}} = \int_0^b \int_0^a H_{11}^{(1)}(x)' H_{01}^{(1)}(y)\, q\, dx\, dy \qquad (3.52)$$

Substituting the expressions for $H_{11}^{(1)}(x)'$* and $H_{01}^{(1)}(y)$ and carrying out the indicated integration, we obtain

$$(q_b)_{w_{x11}} = \frac{qa^2b}{24} \qquad (3.53)$$

All components of the membrane and the bending load vectors are obtained in exactly the same manner (9). Table 3.1 shows the bending load vector components for a rectangular element due to a uniformly distributed lateral load.

With all components necessary for computing the large deflection

*The prime on $H_{11}^{(1)}(x)$ indicates derivatives.

Table 3.1 Equivalent Loads of Uniformly Distributed Lateral Load for a Rectangular Plate Element

Node	Displacement Parameter	Uniform Lateral Load q
(1,1)	w_{11}	$qab/4$
	w_{x11}	$qa^2b/24$
	w_{y11}	$qab^2/24$
	w_{xy11}	$qa^2b^2/144$
(1,2)	w_{12}	$qab/4$
	w_{x12}	$qa^2b/24$
	w_{y12}	$-qab^2/24$
	w_{xy12}	$-qa^2b^2/144$
(2,2)	w_{22}	$qab/4$
	w_{x22}	$-qa^2b/24$
	w_{y22}	$-qab^2/24$
	w_{xy22}	$qa^2b^2/144$
(2,1)	w_{21}	$qab/4$
	w_{x21}	$-qa^2b/24$
	w_{y21}	$qab^2/24$
	w_{xy21}	$-qa^2b^2/144$

problem available, the solution of the assembly of all the elements is accomplished in the usual manner as if the stiffness of each element were simply the sum of $[K_0]$, $[K_L]$, $[K_\sigma]$ stiffness matrices. Thus the solution of the nonlinear problem becomes a sequence of solutions of linear problems in which calculated displacements and stresses are added to the previous values to give an up-to-date account of the geometric state of the structure as the applied load is increased. An outline of the solution technique used in this work is presented in the next chapter.

3.6 Combined Bending and Membrane Stresses

The stresses at the middle and outer planes of a plate element due to the applied external loads are the ones of interest in this investigation. Figure 3.3 shows that in the x-direction a bending stress attains its extreme levels at the outer surfaces of the element and it is zero at the middle surface, while the membrane stress is uniform throughout the plate thickness. If this is assumed to hold true for all stress components, the bending and membrane stresses can be superimposed to obtain the total stresses acting on the plate.

For each of the four nodes of the rectangular element the membrane and the bending "stresses" are obtained from the stress-strain relations indicated by Eq.(3.10) which may be written in matrix form as

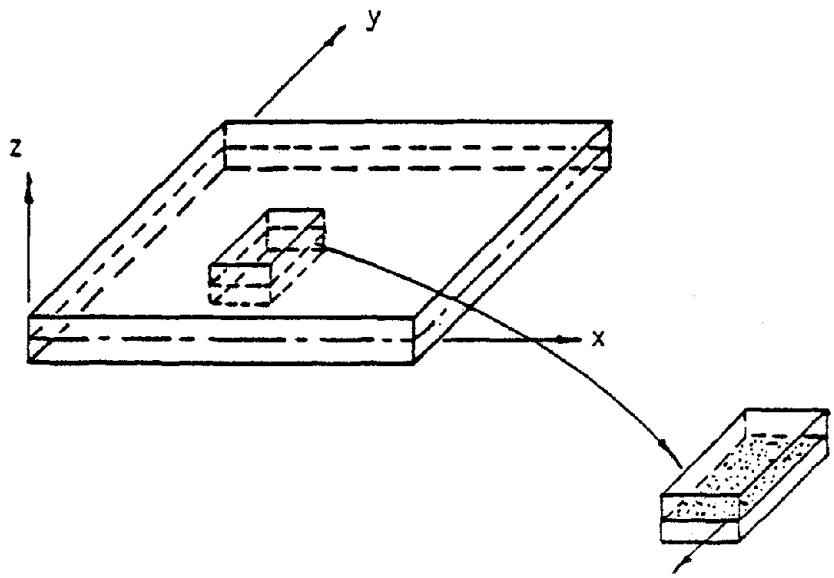

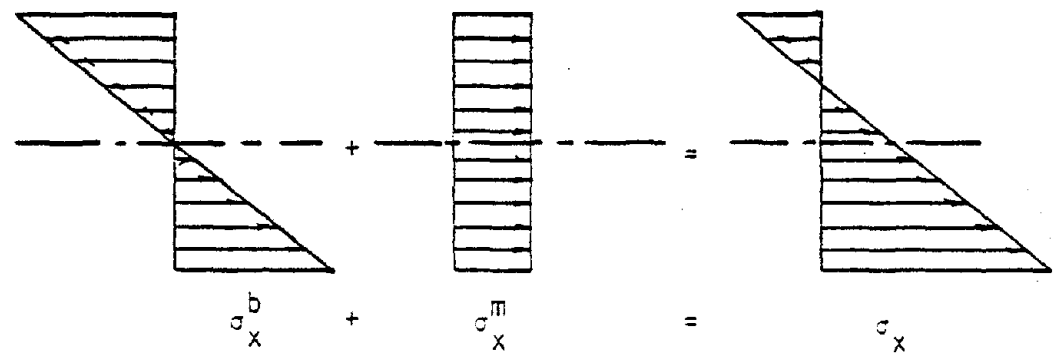

Figure 3.3 Combined Bending and Membrane Stresses

$$\begin{Bmatrix} N_x \\ N_y \\ N_{xy} \\ M_x \\ M_y \\ M_{xy} \end{Bmatrix} = \frac{E}{(1-\nu^2)} \begin{bmatrix} 1 & \nu & 0 & 0 & 0 & 0 \\ \nu & 1 & 0 & 0 & 0 & 0 \\ 0 & 0 & \frac{1-\nu}{2} & 0 & 0 & 0 \\ 0 & 0 & 0 & \frac{t^3}{12} & \frac{\nu t^3}{12} & 0 \\ 0 & 0 & 0 & \frac{\nu t^3}{12} & \frac{t^3}{12} & 0 \\ 0 & 0 & 0 & 0 & 0 & \frac{t^3(1-\nu)}{24} \end{bmatrix} \begin{Bmatrix} \varepsilon_x^m \\ \varepsilon_x^m \\ \varepsilon_{xy}^m \\ \varepsilon_x^b \\ \varepsilon_y^b \\ \varepsilon_{xy}^b \end{Bmatrix} \tag{3.54}$$

where ε_x^m, ε_y^m, and ε_{xy}^m denote the membrane strain components while ε_x^b, ε_y^b, and ε_{xy}^b indicate the bending components, all of which can be calculated from Eq.(3.6).

The true membrane and bending stresses can then be calculated using Eq.(3.8) and (3.9). The combined stress components due to membrane and bending action are obtained at the extreme surfaces of the plate by simply adding the respective components as

$$\begin{aligned} \sigma_x &= \sigma_x^m \mp \{\sigma_x^b\} \\ \sigma_y &= \sigma_y^m \mp \{\sigma_y^b\} \\ \sigma_{xy} &= \sigma_{xy}^m \mp \{\sigma_{xy}^b\} \end{aligned} \tag{3.55}$$

The stress components σ_x, σ_y, and σ_{xy} calculated at each of the four nodes of the rectangular element are then used to calculate the principal stresses at the plate surfaces. The principal stress equations being the standard ones for two-dimensional stress will not be shown here.

These stresses are averaged at nodes that are common to more than one element. This averaging tends to reduce the error inherent in the displacement approach in which equilibrium condition of the forces is not completely satisfied.

3.7 A Brief Review of the Development of the Finite Element Method in Nonlinear Problems

In 1960, Turner, Dill, Martin, and Melosh (68) introduced the finite element method to geometrically nonlinear problems in a paper in which they analyzed the effects of initial in-plane stress on the stiffness of stringers (i.e., beam-columns with zero bending stiffness) and of plane stress triangle elements. The approach was to develop the initial stiffness matrices for use in the incremental force-displacement relation. Gallagher, et al. (22), substituted a complete cubic function into the strain energy expression to derive the stiffness matrices. Martin (39) reviewed several papers on the derivation of nonlinear stiffness matrices and concluded that the same functions need not be used to represent both linear and nonlinear effects. Kapur and Hartz (30) derived "stability-coefficient" matrices for nine independent states of in-plane stress which represented an extension beyond previous derivations that were based on only three stress states. Clough and Felippa (16) made comparison studies of several finite element formulations in plate buckling in which both consistent and inconsistent approaches were used and found that the inconsistent approach gave good results. Murray and Wilson (48) used constant stiffness matrices and accounted for all geometric nonlinearities by coordinate

rotations. They noted that their approach was equivalent to using the Kirchhoff's assumptions for each individual element, rather than the nonlinear von Karman theory. Mallett and Marcal (36) presented a unifying basis for formulating the large deflection problems. They derived the total strain energy as a function of nodal displacements, using functions and including strain energy terms which previously had been neglected. Stricklin, et al. (59) applied the matrix displacement method in which they employed linear and nonlinear equilibrium equations by separating the linear and nonlinear portions of the strain energy and then applying the nonlinear terms as additional generalized forces.

Recent papers on finite element methods in nonlinear plate analysis have focused on the method of solution. Kawi and Yoshimura (31) gave an iterative procedure for solving large deflection plate problems. Their approach was similar to the unbalanced-force iteration, but their formulation included all stiffness terms. Schmit, Bogner, and Fox (56) used a direct minimization technique for solving large deflection problems of plates and cylindrical shells. To compute strain energy, rectangular coefficient matrices were summed with linear and quadratic displacement vectors. Haisler and Stricklin (23) developed and evaluated several solution procedures for geometrically nonlinear problems and concluded that the selection of solution procedure depends highly on the degree of nonlinearity the problem possesses.

The interested reader is advised to consult the following references for more understanding of the various finite element

formulations of geometrically nonlinear problems (1, 3, 7, 11, 14, 17, 40, 42, 43, 44, 45, 49, 51, and 62).

At this point, it should be noted that the present finite element formulation is not the only attempt to solve the geometrically nonlinear rectangular glass plate problem. Tsai and Stewart (67) used a finite element program developed by Melliere (43) to study the stress distributions in glass plates. Moore (46) used the ARGUS nonlinear finite element structural analysis program to analyze rectangular glass solar panels subjected to uniform normal pressure loads. The formulation of both above mentioned computer programs include only constant strains to represent the membrane behavior of the plate whereas, the present finite element program includes not only constant strains but also linear strains to represent the membrane behavior of the plate. Representation of the membrane behavior as such is important in better assessing the overall stress distribution within the glass plate, particularly at the perimeters of the plate.

CHAPTER 4

SOLUTION OF THE NONLINEAR SYSTEM EQUATIONS

4.1 Incremental Approach

The method of solution of the nonlinear system equations adopted in this investigation falls under what Haisler (23) classified as "Class-I incremental methods without equilibrium checks." The concept of this method is to assume a linear response of the structure at each loading increment when the total load is applied in a sequence of sufficiently small increments. These incremental quantities are added to corresponding displacements, strains and stresses to give an up-to-date account of the geometry of the plate. These up-dated quantities are then used in a following loading increment to compute the stiffness matrices which include the nonlinear effects of the deformed geometry of the plate. The process is repeated by applying subsequent increments of the load until the total load is applied. The resulting effect is to solve a sequence of linear problems in which the stiffness matrices are recalculated based on the prevailing geometry of the structure prior to each loading increment. The procedure of the method can be mathematically written as

$$\left[[\bar{K}_0] + [\bar{K}^{NL}(\alpha)]\right]_{i-1} \{\Delta\bar{\alpha}\}_i = \{\Delta\bar{q}\}_i \qquad (4.1)$$

where $[\bar{K}_0]$ is the linear part of the stiffness matrix and $[\bar{K}^{NL}(\alpha)]$ is the nonlinear part. The nonlinear part of the stiffness matrix is a function of α, the displacement components representing the deformed geometry of the structure prior to applying the loading increment,

and $\{\Delta\bar{\alpha}\}$ is the increment of displacements resulting from applying the ith loading increment $\{\Delta\bar{q}\}$. After applying the ith loading increment the total displacements are obtained by

$$\{\bar{\alpha}\}_i = \sum_{j=1}^{i} \{\Delta\bar{\alpha}\}_j \tag{4.2}$$

Incremental solution procedures for geometrically nonlinear problems are presented in the literature in several different forms. Incorporation of a particular form of an incremental procedure in the formulation of a geometrically nonlinear problem depends on several factors such as the degree of accuracy desired, the degree of nonlinearity in the problem, the complexity of the problem formulation, the availability of computer dollars, etc. Haisler (23) and Stricklin, Haisler, and von Rieseman (58, 59) have made intensive studies of several solution procedures for geometrically nonlinear problems and the interested reader is referred to their work.

4.2 Algorithm of the Incremental Approach

To solve the geometric nonlinear problem under investigation using the proposed finite element formulation, the following algorithm is used for the incremental approach.

During the ith step, an incremental load vector $\{\Delta q\}_i$ is applied to the assembled elements of the plate to yield an incremental displacement vector $\{\Delta\alpha\}_i$. For each element of the structure at the end of the ith step:

1. Determine current deformed geometry of the element by adding the resulting incremental displacement vector to the total displacement vector

$$\{\alpha\}_i = \{\alpha\}_{i-1} + \{\Delta\alpha\}_i \tag{4.3}$$

2. Calculate corresponding strain components by formulating the $[\bar{B}]$ matrix which is a function of the derivatives of the shape functions and only w_x and w_y of the displacement vector $\{\alpha\}_i$

$$\{\varepsilon\}_i = [\bar{B}]_i\{\alpha\}_i \tag{4.4}$$

3. Calculate corresponding stress components using the relation

$$\{\sigma\}_i = [D^*]\{\varepsilon\}_i \tag{4.5}$$

4. Calculate $[K_0]$ and $[K_L]$ using

$$[K_0] + [K_L] = \int_V [\bar{B}]^T[D^*][\bar{B}]\, dV \tag{4.6}$$

5. Calculate $[K_\sigma^b]$ using

$$[K_\sigma^b] = \int_V [G]^T \begin{bmatrix} N_x & N_{xy} \\ N_{xy} & N_y \end{bmatrix} [G]\, dV \tag{4.7}$$

6. Repeat algorithm 1 through 5 for all elements and assemble the global stiffness matrix for the entire structure.
7. Apply the next loading increment $\{\Delta q\}_{i+1}$ to the assembled structure and calculate $\{\Delta\alpha\}_{i+1}$ by solving the simultaneous equations of equilibrium.

$$[K_T]_i\{\Delta\alpha\}_{i+1} = \{\Delta q\}_{i+1} \tag{4.8}$$

8. Repeat algorithm 1 through 7 until the entire load is applied.

The incremental approach outlined above is schematically outlined in Fig. 4.1.

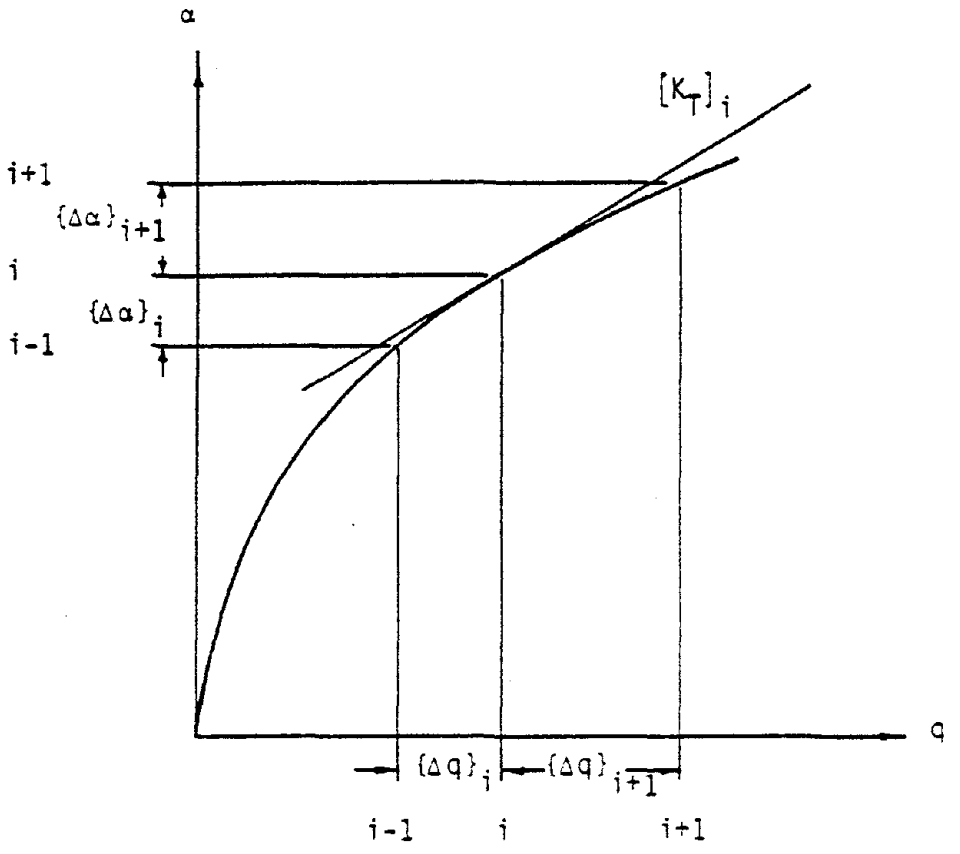

Figure 4.1 Incremental Approach

CHAPTER 5

NUMERICAL EXAMPLES

Four examples of simply supported uniformly loaded large deflection rectangular thin plates are analyzed in this chapter to demonstrate the validity and versatility of the finite element formulation presented in this investigation. Results are then compared with theoretical solutions and experimental data available in the literature. Although the program formulation is capable of analyzing various types of boundary conditions such as clamped or free edges, and different combinations of loading such as concentrated and uniformly distributed static loads, only problems pertinent to this investigation are presented here.

In the example problems treated, results of two classes of simply supported rectangular thin plates with uniform static loads are shown. These results show the difference which is mainly due to the prescribed boundary conditions in the plane of the plate. This difference is described in more detail in appropriate sections of this chapter. The uniform static loads are replaced by equivalent concentrated loads at the nodes as described in Chapter 3. Uniform and non-uniform discretization schemes of the plate structure are employed in this dissertation to assess the effects of the boundary conditions.

Due to limited research funds and the lengthy CPU time consumed by each run of the computer program, the discretization of one quarter of the plate is limited to a grid size of 16 elements. Also, the

number of loading increments is limited to 100 when the grid size of one quarter of the plate is 9 elements.

5.1 Simply Supported Rectangular Plates: Edge Displacement = 0

Levy (34) called the boundary conditions of this class of problems "Edge Displacement = 0," while Timoshenko (65) named them "immovable" edges. In this class of problems, the boundary edges of the plate are assumed to be laterally supported and free to rotate along the edges in the lateral direction. In the transverse direction, they remain completely restrained from having any displacement along these edges in the plane of the plate. These boundary conditions were mathematically formulated and shown in Chapter 2. Two examples of this class of problems are shown in the following sections. The first example problem exhibits results of a simply supported square thin plate with a uniform static load and the second illustrates results of a simply supported rectangular plate with an aspect ratio of 1.6 and a uniform static load.

5.1-A Example I. Simply Supported Uniformly Loaded Square Plate: Edge Displacement = 0

In this example, a 10-inch simply supported square plate which has a constant thickness of 0.04 inch is subjected to a monotonically increasing static lateral load of 1.837 psi. The elastic constants of the material of the plate are assumed to be 27.6 x 10^6 psi for the Young's modulus of elasticity and 0.316* for the

*The value of 0.316 is used to agree with that in Levy's (34) solution.

Poisson's ratio. Because of the double symmetry, the problem is modeled by discretizing only one quarter of the plate. In this example, a grid size of 2 x 2 elements of equal areas is used. The total load is applied in 40 equal increments and the results agree reasonably well with Levy's solution (34).

Fig. 5.1 shows a non-dimensional plot* of the deflection of the center of the plate vs. the applied load. A maximum deflection of nearly twice the thickness of the plate is attained as shown in the curve of Fig. 5.1. The curve clearly indicates the nonlinear load-displacement relationship involved in this problem, where the displacement does not increase proportionally as the load is increased. This effect is due to the increased stiffness of the plate which in turn is a result of the membrane effect induced by large lateral displacements.

Membrane and bending stresses are also plotted against the load and are shown separately. Stresses at different points on the plate are drawn so that direct comparison with Levy's solution is possible. In Fig. 5.2, Curve A shows the bending stresses σ_x^b or σ_y^b of the extreme fibers at the center of the plate while Curve B indicates the shearing stress due to bending σ_{xy}^b of the extreme fibers of the upper right corner of the plate. It should be noted that the difference in the two solutions as revealed in Curve B, is believed to be due in part to the coarse discretization since

---

*Unless otherwise stated, non-dimensional plots are used throughout this investigation so that arbitrary dimensions of square and rectangular plates with arbitrary material constants may be used for comparison.

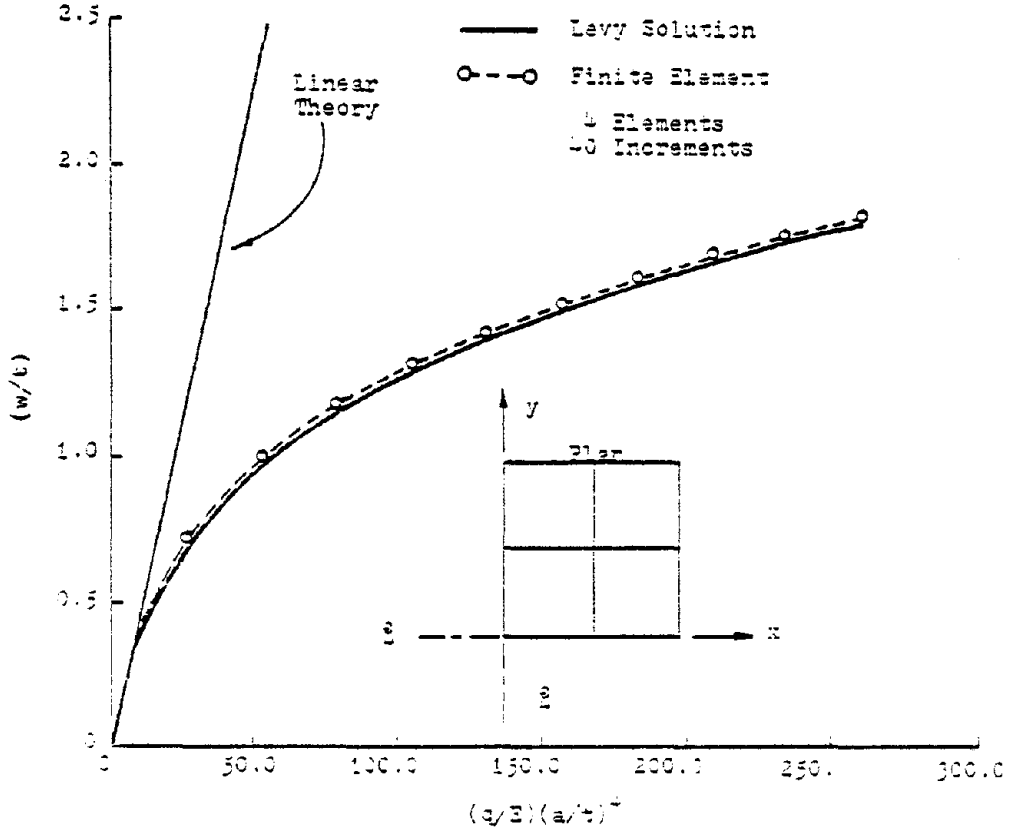

Figure 5.1 Load-Deflection of Simply Supported Square Plate: Edge Displacement = 0

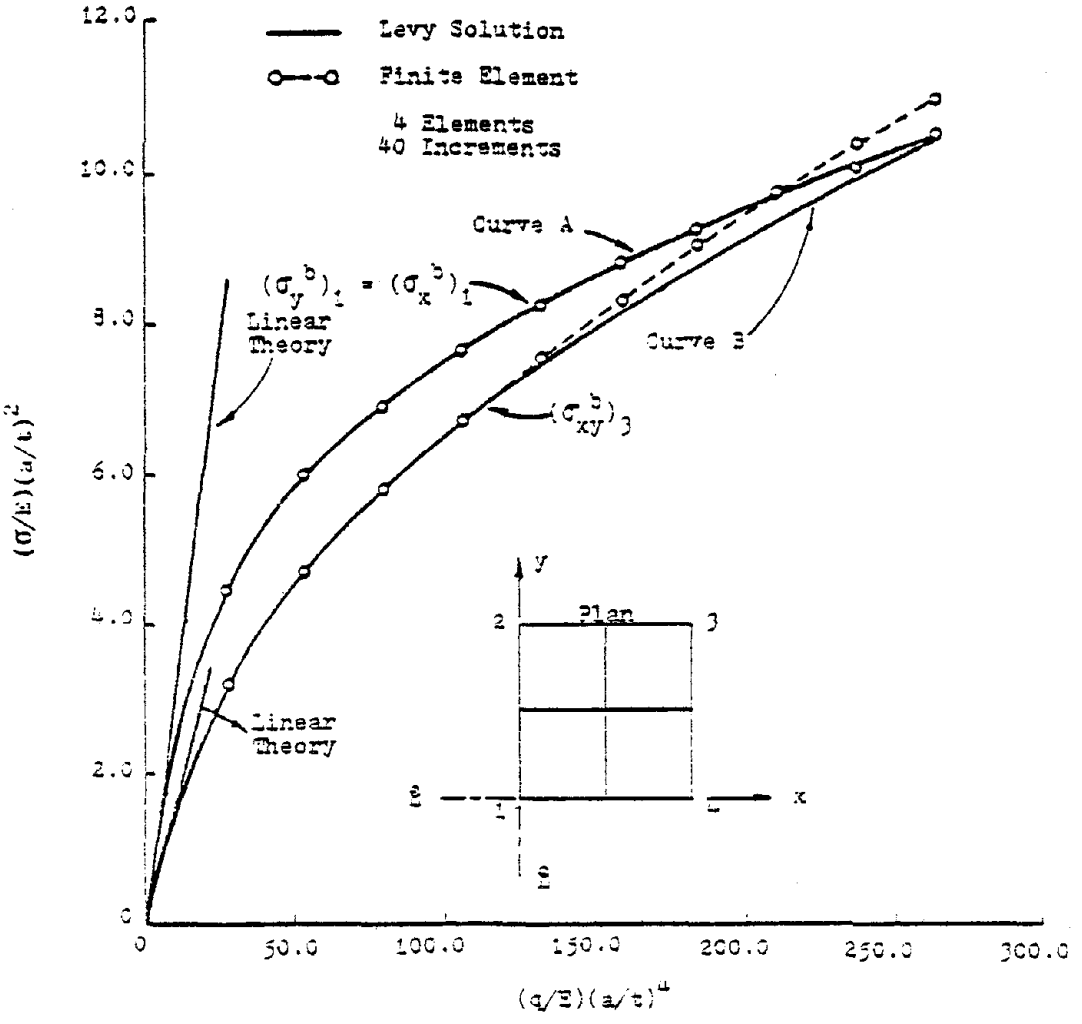

Figure 5.2 Bending Stresses at Center and Corner of Simply Supported Square Plate: Edge Displacement = 0

only 4 elements are used to model the problem. It should also be noted that the boundary condition of the bending moment being equal to zero at the edges of the plate is not completely satisfied by this finite element formulation. Non-dimensional membrane stresses vs. non-demensional applied loads are shown in Fig. 5.3 for different points on the plate. Curves A and C in Fig. 5.3 illustrate the variation of the membrane stresses σ_x^m and σ_y^m, respectively, at the center edge of the right side of the plate. Curves B refer to either of the variations of the membrane stresses σ_x^m or σ_y^m at the center of the plate, and Curves D reveal either of the variations of the membrane stresses σ_x^m or σ_y^m at the corner of the plate. It should be noted that despite the coarseness of the discretization used to model this plate problem, good agreement with Levy's results for displacements and bending and membrane stresses are achieved as exhibited in Fig. 5.1 through Fig. 5.3. This is attributed to the fact that the assumed shape functions used in this investigation do, in fact, depict the displacement fields of this plate structure extremely well.

Since the difference between the present finite element solution and Levy's solution is small as shown by the curves in Fig. 5.1 through 5.3, it seemed unnecessary to carry out the analysis any further by refining the grid size or increasing the number of loading increments to obtain results that would match Levy's solution point-by-point. The size of the loading increment and the fineness of the discretization, no doubt, have major effects on the accuracy of the results obtained by the finite element formulation. In the second class of problems treated in this investigation, these two factors become more important in achieving good accuracy as is demonstrated in a later problem.

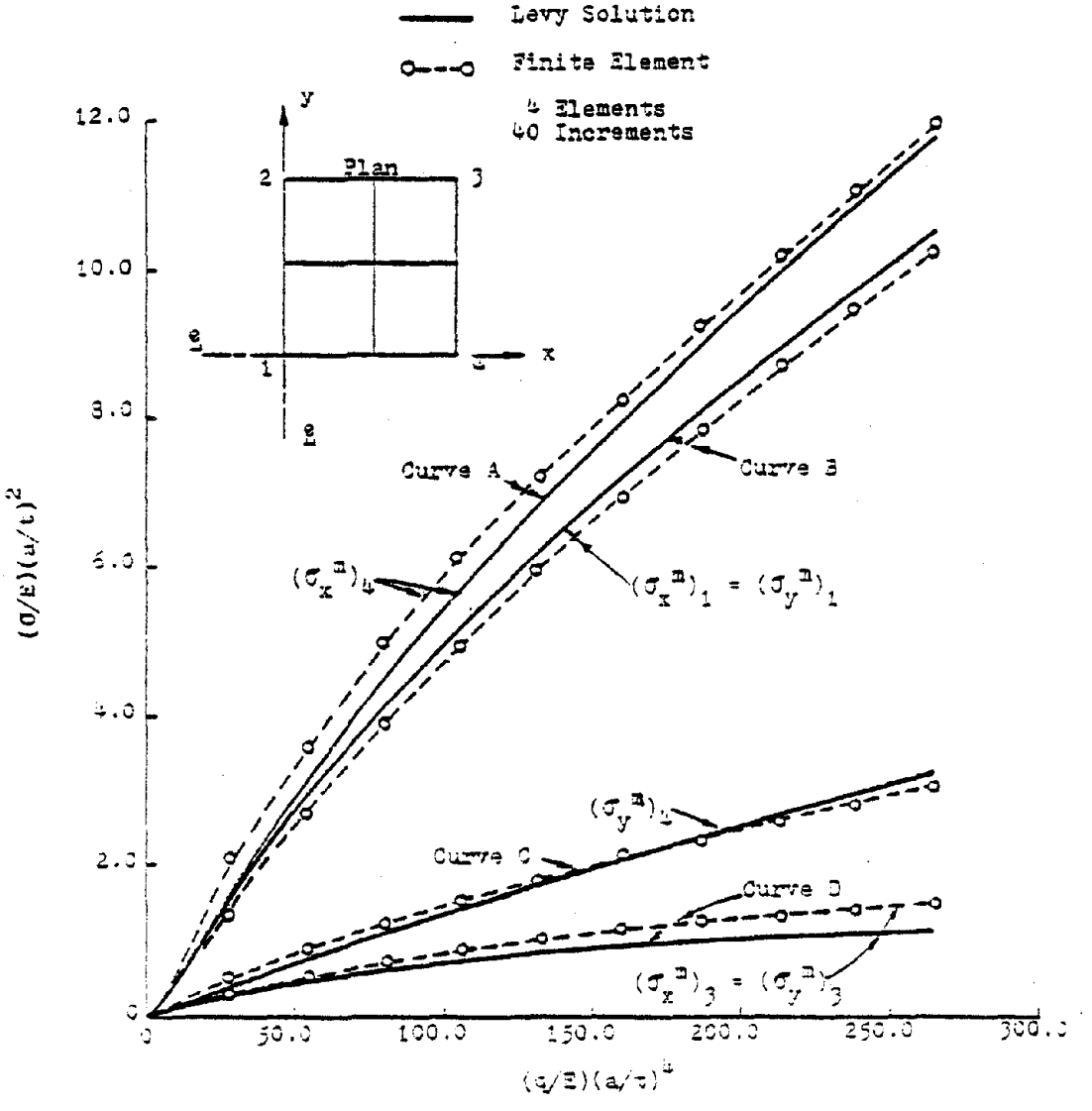

Figure 5.3 Membrane Stresses at Center, Center Edge, and Corner of Simply Supported Square Plate: Edge Displacement = 0

5.1-B Example II. Simply Supported Uniformly Loaded Rectangular Plate: Edge Displacement = 0

A 96.0-inch long, 60.0-inch wide and 0.25-inch thick aluminum plate subjected to static lateral uniform load of 0.70 psi is used in this example. The Young's modulus of elasticity and Poisson's ratio for aluminum are 10.6×10^6 psi and 0.33, respectively. One quarter of the plate is discretized into nine rectangular elements of different areas. The elements with smaller areas are placed along the edges of the plate as shown in Fig. 5.4. The total load is applied in 50 equal increments in order to obtain the load-deflection relationship exhibited by the dashed curve in Fig. 5.4. The solid line shown in the figure represents an approximate solution attributed to Timoshenko (65); calculations for this curve are reported by Anians (2).

As was demonstrated in the example of the previous section, bending and membrane stresses are plotted separately for different points on the plate. Variations in bending stresses are shown in Fig. 5.5 at the center and at the corner of the plate. Bending stresses σ_x^b and σ_y^b are indicated by Curve B and Curve C, respectively. As expected, the bending stress parallel to the shorter side of the plate, in this case σ_y^b, is larger than the bending stress parallel to the other side. However, the general behavior of the center bending stresses, particularly parallel to the shorter side of the plate, is similar to that of a square plate. It can be noted by examining Fig. 5.5 that σ_x^b varies almost linearly after the load $(q/E)\ (b/t)^4$ reaches a magnitude of about 48.0. The shear stress due to bending σ_{xy}^b at the corner of the plate is indicated by Curve A. It should be noted that this shear stress has a comparable or larger magnitude than the center stress in this plate. The opposite was the case for the

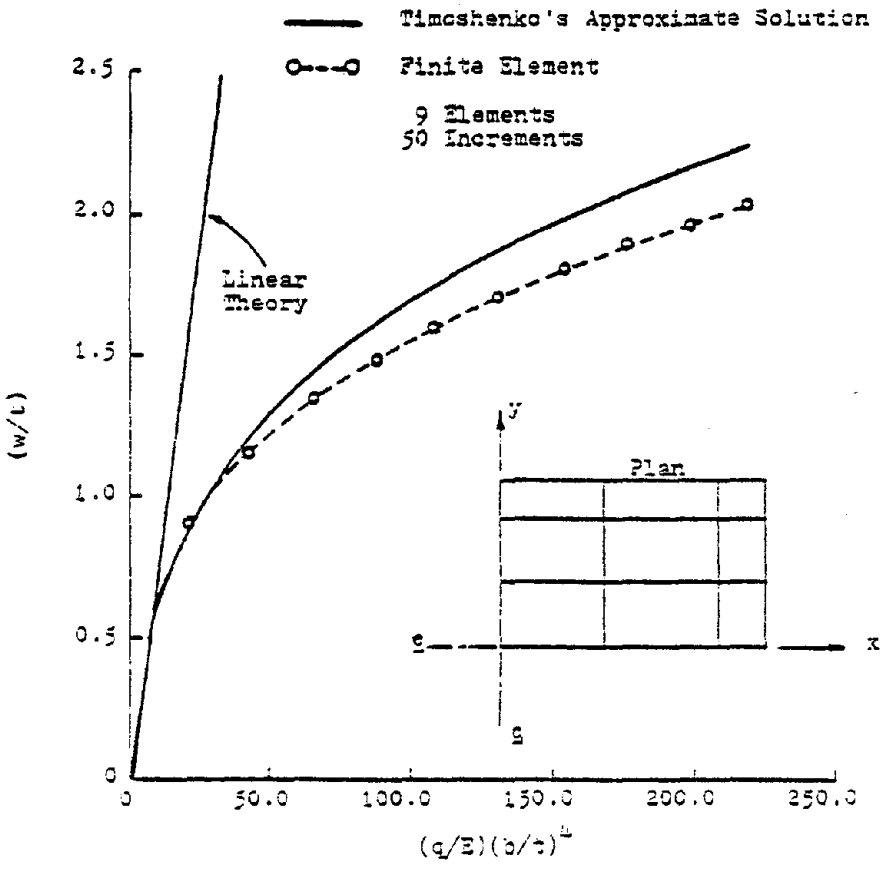

Figure 5.4 Load-Deflection of Simply Supported Rectangular Plate: Edge Displacement = 0

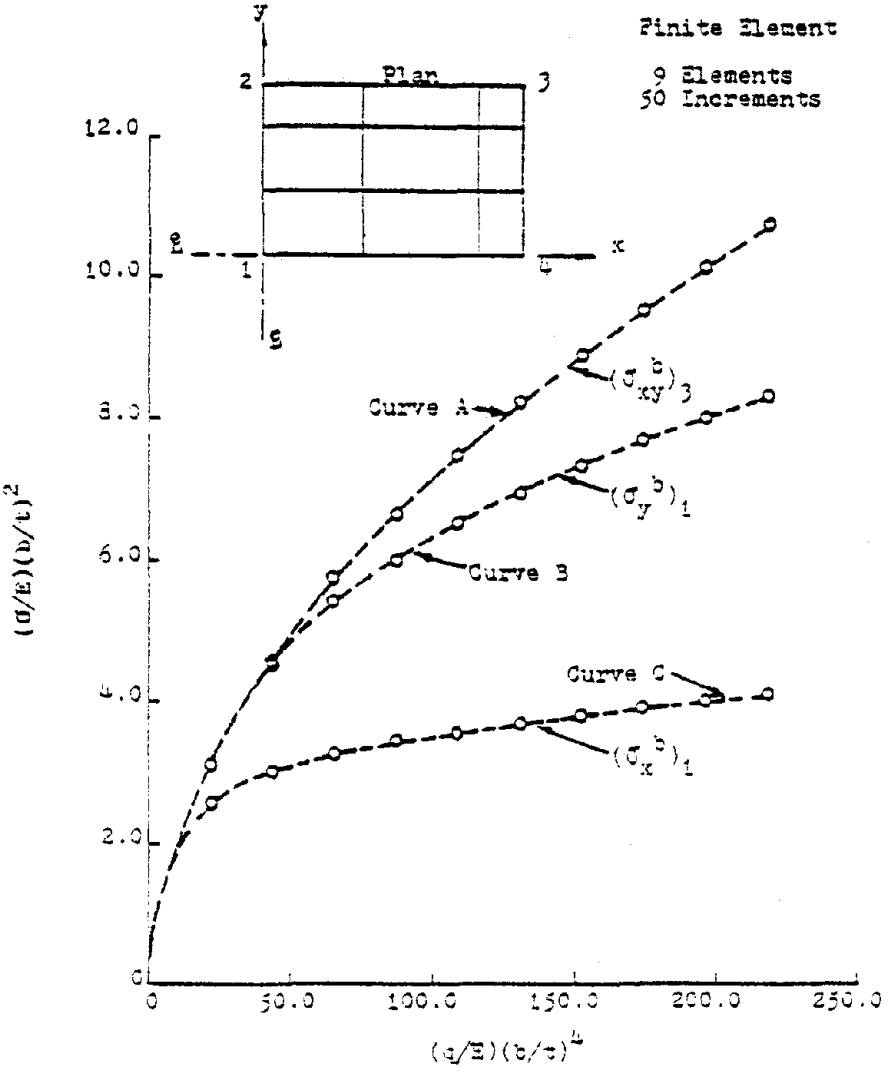

Figure 5.5 Bending Stresses at Center and Corner of Simply Supported Rectangular Plate: Edge Displacement = 0

corresponding stresses in the square plate (see Fig. 5.2). In Fig. 5.6, membrane stress variations in the x and y directions are shown for the center, the center of the short edge, and the corner of the plate, and are indicated by Curves A, B, C, D, and E. It should be noted that the magnitudes of σ_x^m and σ_y^m at the corner of the plate differ slightly but the difference is so small that it cannot be shown in the figure.

5.2 Simply Supported Rectangular Plates: Edge Displacement ≠ 0

In this class of problems, the boundaries are also assumed to be laterally supported and free to rotate in the lateral direction. But, it is also assumed that the plate edges can move in the plane of the plate. Levy (34) presented a plate solution of this type in which he assumed that the plate edges could move in-plane, but were constrained to remain straight. Levy termed this set of boundary conditions "Edge Compression = 0." These boundary conditions assumed by Levy do not define the actual edge conditions of the thin glass plates under investigation. The edges of typically installed glass plates can translate in the plane of the plate, and do not necessarily remain straight. This fact was confirmed experimentally by Anians (2) who measured the in-plane edge displacements of a laterally loaded window glass plate installed in an actual framing system. Kaiser (29) presented a solution for a uniformly loaded, simply supported square plate with edges that are both free to move and distort in-plane. He used a finite difference formulation to solve the nonlinear plate equations and compared his results with data obtained from an experiment which he conducted on a square plate. Results obtained from the present finite element formulation are compared with Kaiser's solution.

Differences in the in-plane boundary conditions of simply supported plates, as defined by Levy and Kaiser, result in a substantial difference

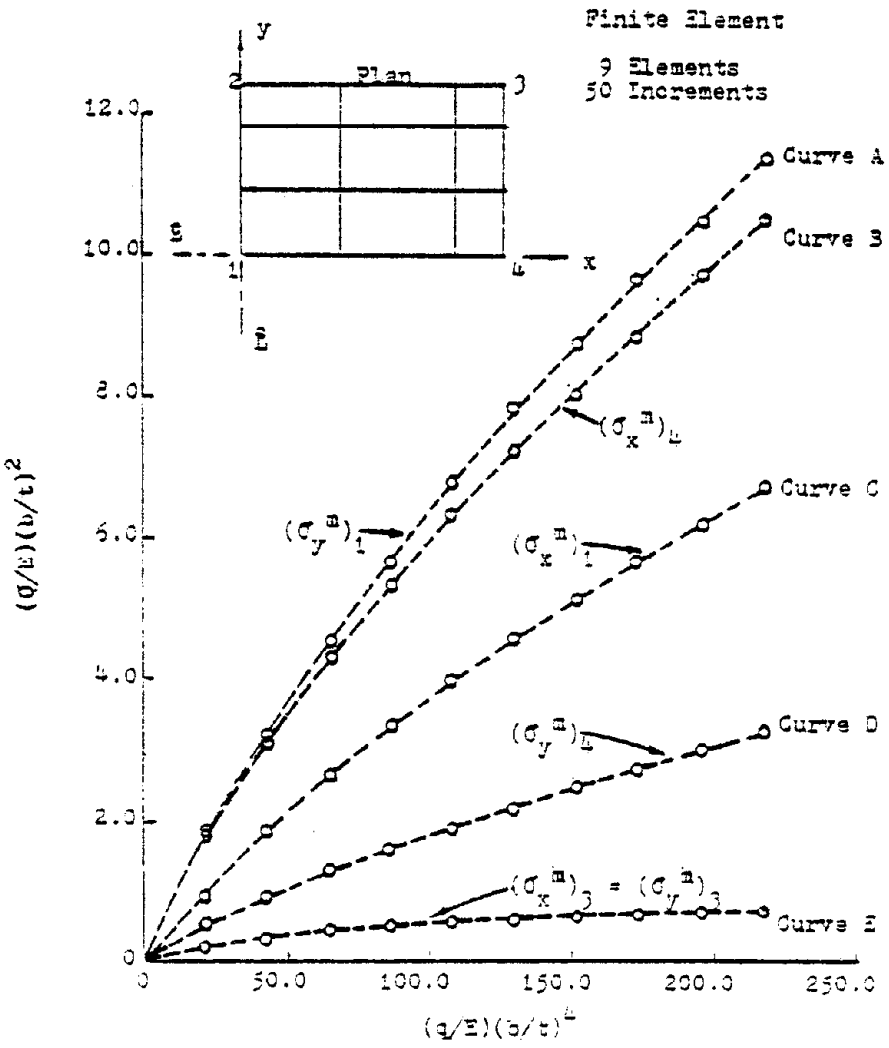

Figure 5.6 Membrane Stresses at Center, Center Edge, and Corner of Simply Supported Rectangular Plate: Edge Displacement = 0

in the center deflection results obtained in each case as shown in Fig. 5.7. For example, when Levy (34) compared his results for "Edge Compression = 0" with Kaiser's solution he found that a load of $(q/E)(a/t)^4 = 118.8$, the center deflection obtained by his method was about 25 percent lower than the center deflection obtained by Kaiser.

Two examples in this class of simply supported rectangular plate problems are demonstrated using the same plate dimensions used in Example I and Example II in Section 5.2. In the first example, center deflections and bending and membrane stresses are plotted against applied loads. Effects of the size of the loading increment and the fineness of the discretization on the stresses are illustrated. Center deflections of a rectangular plate calculated in the second example are compared with experimental results obtained by Anians (2). Finally, membrane and bending stresses at the center of the plate are plotted against the applied loads.

5.2-A Example I. Simply Supported Uniformly Loaded Square Plate: Edge Displacement $\neq 0$

The square plate problem analyzed in Example I of Section 5.1-A is analyzed again in this section. In this analysis, it is assumed that the edges of the plate are free to move in the plane of the plate and do not necessarily remain straight. In order to compare results with Kaiser's solution (29), the lateral load is changed to 0.83 psi and is applied to the plate structure in 100 equal increments. Also, one quarter of the plate is idealized by nine rectangular elements of different dimensions. This scheme is adopted for this problem so that discretization errors at the edges of the plate are minimized.

The center deflection obtained by the finite element solution is compared with Kaiser's solution in Fig. 5.8. A center deflection larger

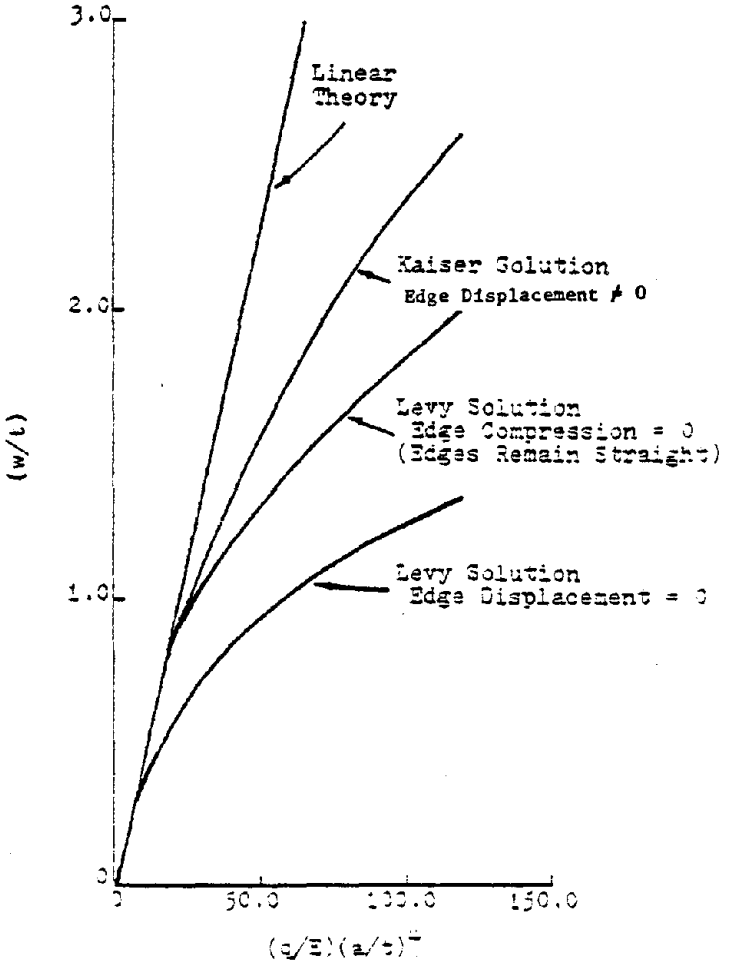

Figure 5.7 Effect of Boundary Edge Condition on Center Deflection of Simply Supported Square Plate

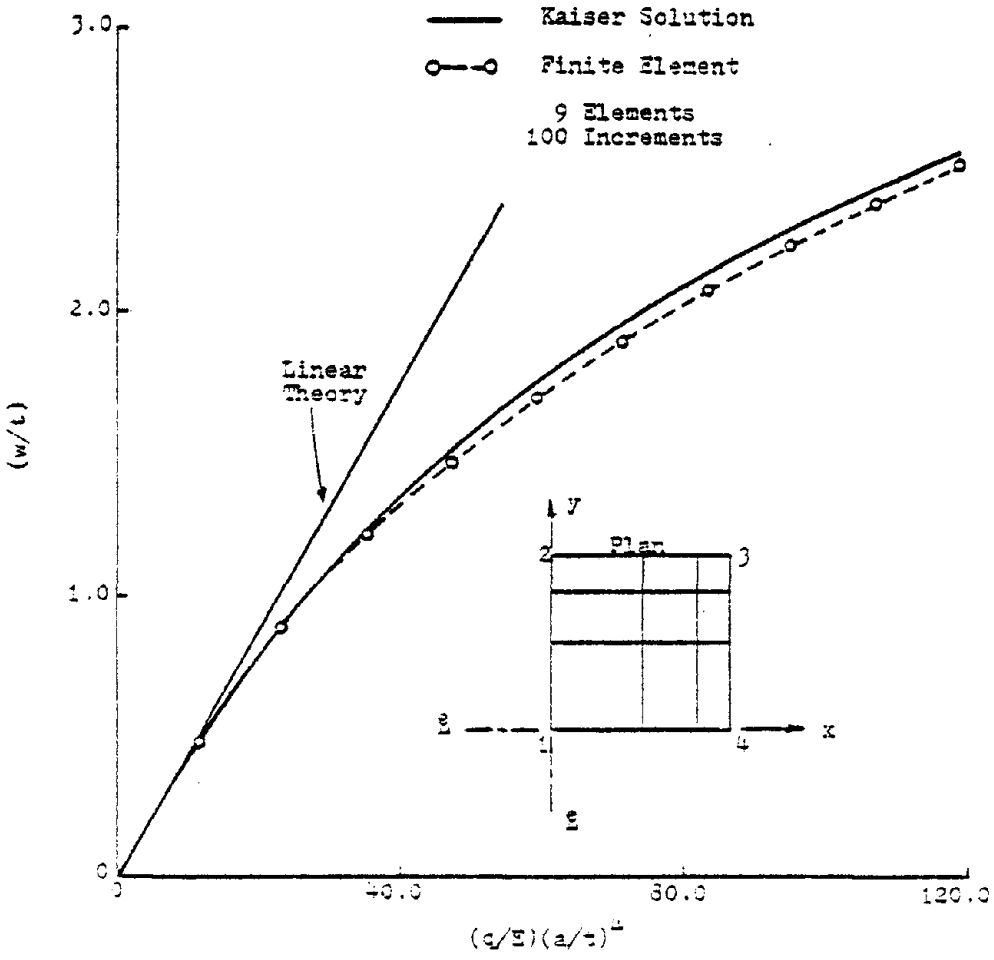

Figure 5.8 Load-Deflection of Simply Supported Square Plate: Edge Displacement ≠ 0

than twice the thickness of the plate was attained. Obviously, this is well within the nonlinear range. The stiffening of the plate with increasing deflection is again indicated by the decreasing slope of the curve. It should be noticed that the center deflections obtained by the finite element method are slightly lower than those obtained by Kaiser, but uniformly so throughout the application of the load. This difference is partially attributed to the coarse finite element discretization, particularly at the center of the plate (see diagram in Fig. 5.8).

Membrane, bending, and total stresses are plotted against the load in Fig. 5.9. Agreement of bending stresses with Kaiser's solution is not as good as the agreement between membrane stresses. However, both the finite element solution and Kaiser's solution are subject to numerical errors. Differences are also apparent in comparisons of total stresses which are simply the sum of the bending and membrane stresses. It should be noted that, for clarity, results of only every 10th loading increment are indicated on the curves of Fig. 5.8 and Fig. 5.9.

The effects of the size of the loading increment on the accuracy of the center deflection, bending, and membrane stresses are studied in this example. The above plate problem is solved using the same dimensions, elastic constants, and discretization scheme with the loading applied in 20, 50, and 100 equal increments. The effect of the size of the loading increment on the center deflection is revealed in Fig. 5.10. The convergence of the deflection improves as the number of loading increments is increased. The center deflections obtained when applying the load in 20, 50 and 100 increments are slightly lower than those obtained by Kaiser's solution, but uniformly so throughout the load. These comparisons indicate that the deflections of

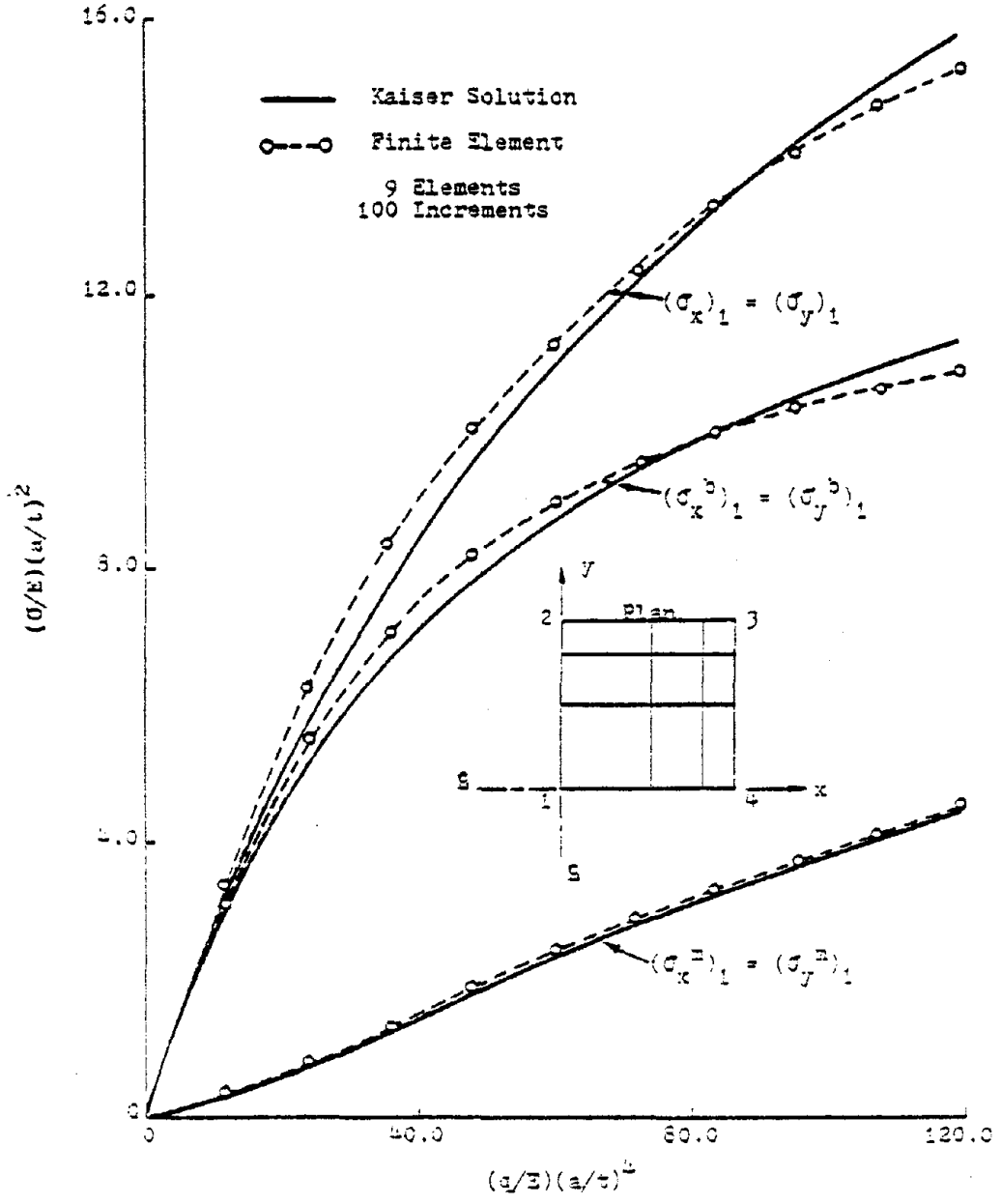

Figure 5.9 Bending, Membrane, and Total Stresses at Center of Simply Supported Square Plate: Edge Displacement $\neq 0$

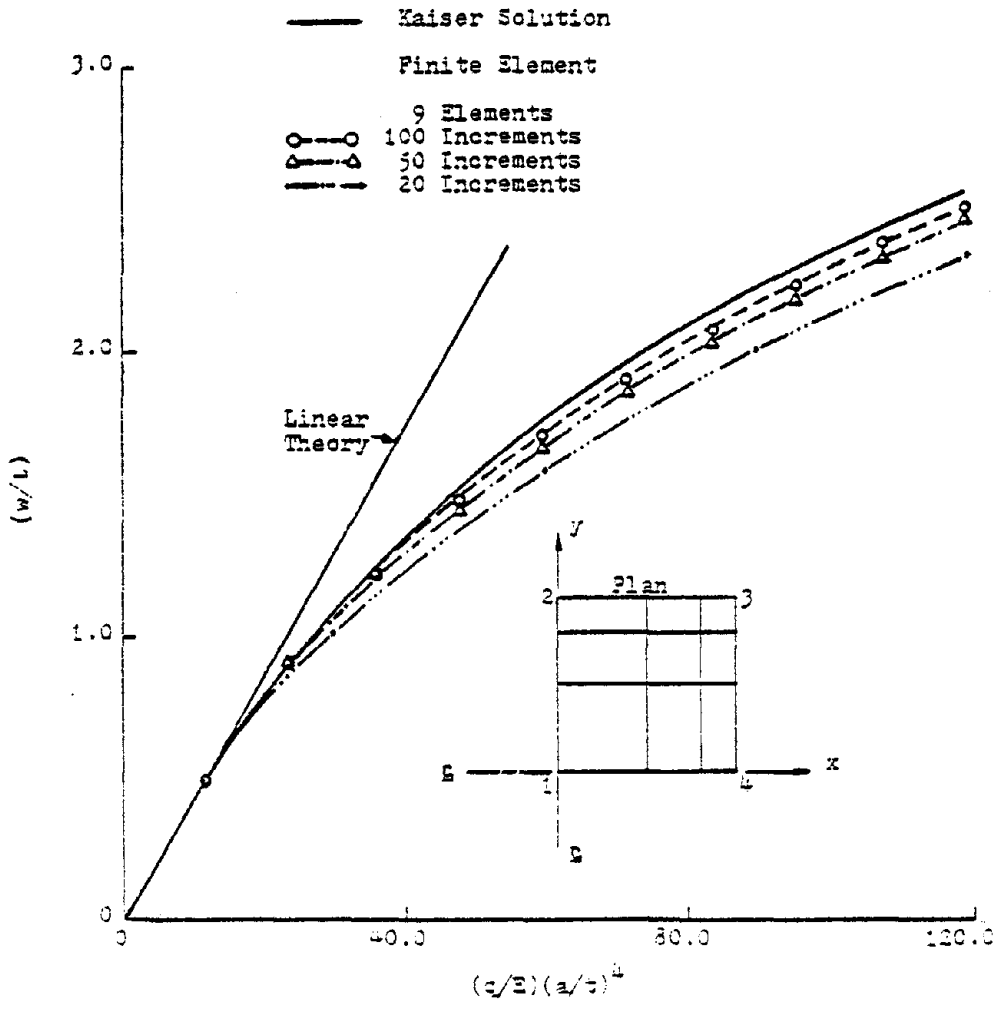

Figure 5.10 Effect of Increment Size on Center Deflection of Simply Supported Square Plate: Edge Displacement ≠ 0

the plate are well represented by the finite element formulation when 100 load increments are used.

Parallel to the comparison of results made in Section 5.1-A, the bending stresses at the center and the corner of the plate are shown in Fig. 5.11. Central stresses are also compared with those obtained by Kaiser (29). In Fig. 5.11, it is indicated that as the number of loading increments is increased, the magnitude of the bending stress at the center of the plate decreases while the corner shear stress increases.

Figure 5.12 illustrates effects of the number of loading increments on the membrane stresses at the center and the corner of the plate. The stresses at both locations appear to converge as the number of loading increments increases. Confidence is further increased by the reasonably good agreement of the center membrane stress with that obtained from Kaiser's solution. It should also be noted that the stress at the edge center of the plate is a compressive stress, indicating distortion of the edges of the plate.

When studying the effect of discretization on the accuracy of the finite element plate model one quarter of the square plate used above is idealized with 1, 4, and 9 elements and the load is applied in 50 equal increments. (Fifty increments are used to solve the problem; once for one element discretization and again for four element discretization. Results of displacements and stresses are already available for the 9 element discretization.)

The effect of the discretization on the bending stresses at the center and the corner of the plate is shown in Fig. 5.13. These stresses converge as the discretization is refined. Convergence also occurs for membrane stresses at the center and the edge center of the plate, as indicated in Fig. 5.14.

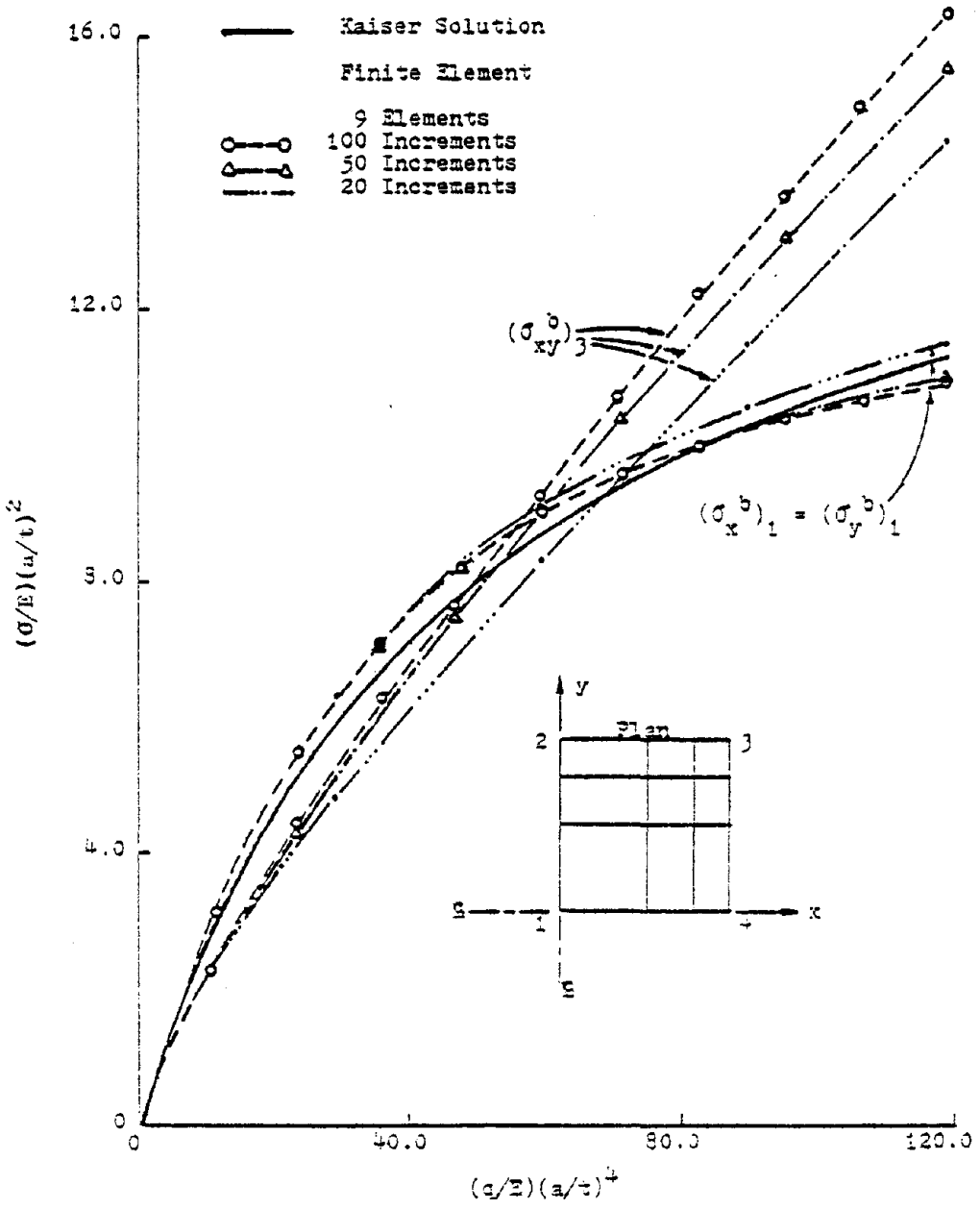

Figure 5.11 Effect of Increment Size on Bending Stresses at Center and Corner of Simply Supported Square Plate: Edge Displacement ≠ 0

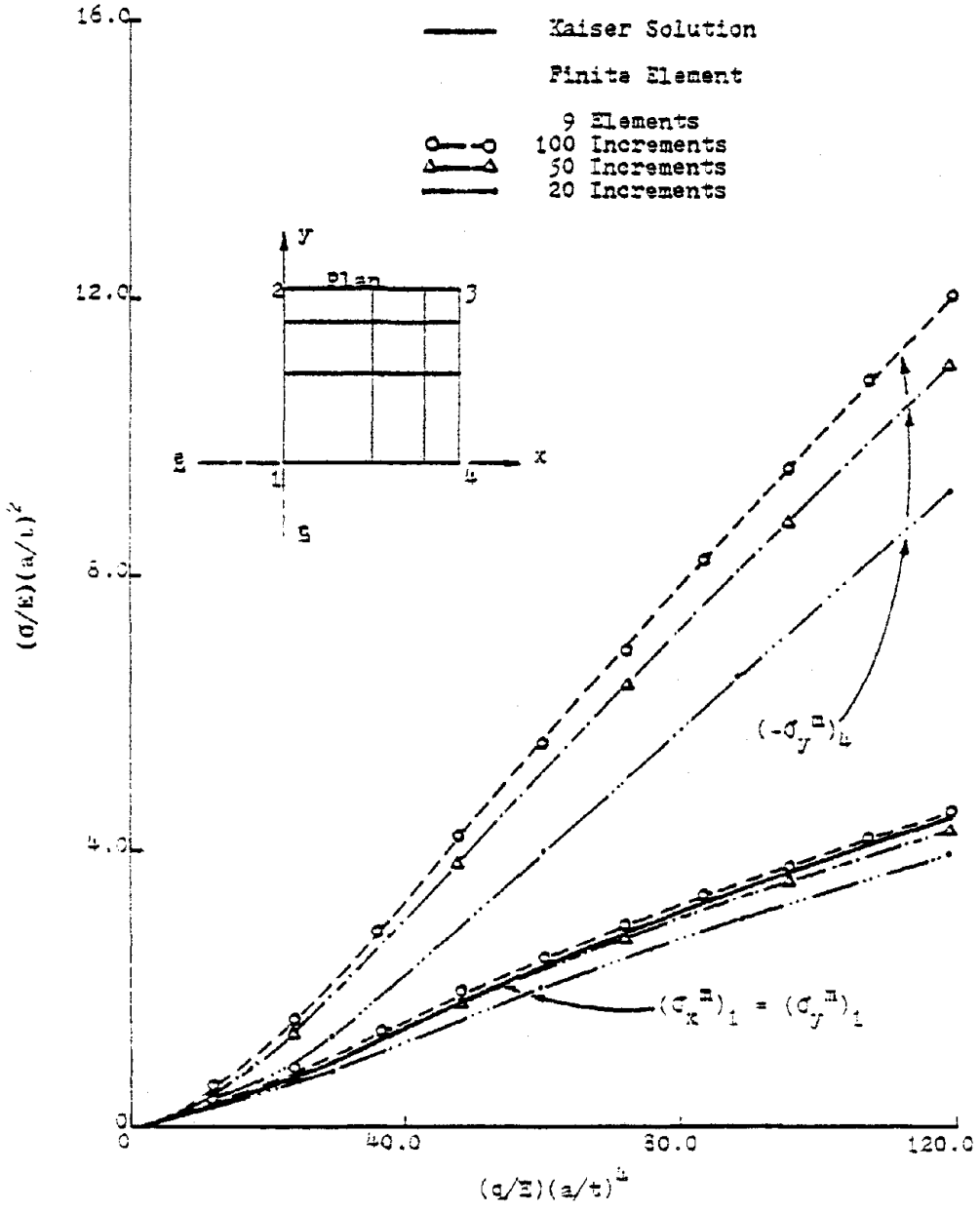

Figure 5.12 Effect of Increment Size on Membrane Stresses at Center and Center Edge of Simply Supported Square Plate: Edge Displacement ≠ 0

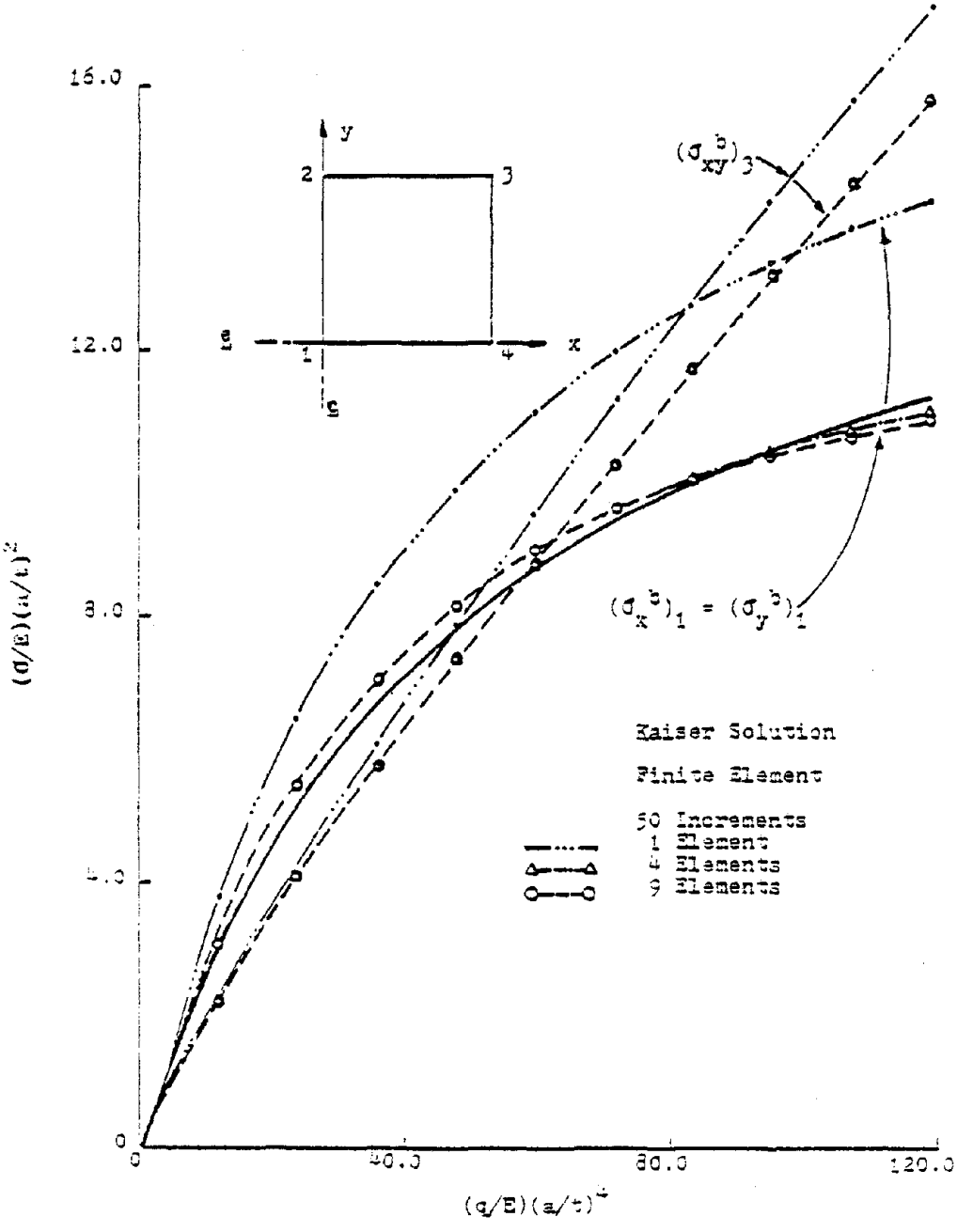

Figure 5.13 Effect of Discretization on Bending Stresses at Center and Corner of Simply Supported Square Plate: Edge Displacement ≠ 0

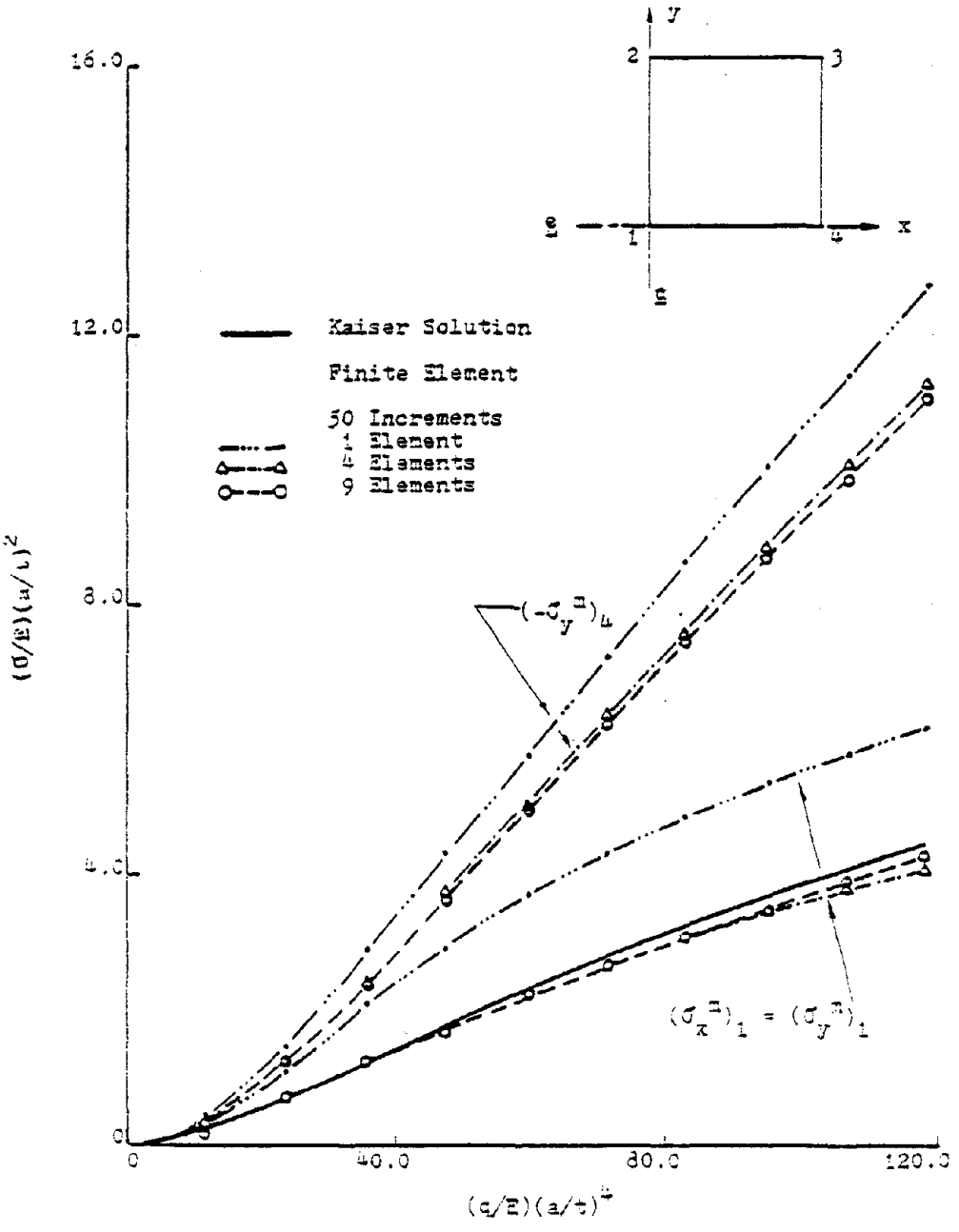

Figure 5.14 Effect of Discretization on Membrane Stresses at Center and Center Edge of Simply Supported Square Plate: Edge Displacement ≠ 0

Effects of the number of loading increments and the discretization on the accuracy of the finite element solution are discussed later in more detail.

5.2-B Example II. Simply Supported Uniformly Loaded Rectangular Plate: Edge Displacement $\neq 0$

The aluminum rectangular plate problem analyzed in Example II of Section 5.1-B is solved in this example assuming simply supported edges that are free to move in the plane of the plate and are not constrained to remain straight. The load is applied in 100 equal increments to obtain the variation of the center deflection of the plate shown in Fig. 5.15. It should be observed that the axes of the load-deflection curve are expressed in terms of loads and deflections expressed in units of psi and in., respectively. The curve is plotted in this manner in order that a point-by-point comparison of the finite element solution can be made with experimental data presented by Anians (2).

Anians (2) studied the center displacements of an aluminum plate mounted in an actual window glass framing system similar to that presented in Fig. 1.1. To assure that the aluminum plate was free to slip in-plane, the interface between the aluminum plate and the neoprene gaskets was lubricated prior to testing. To further assure that the plate edges were free to slip in-plane, the outer neoprene gaskets were installed only near the plate corners to resist localized corner uplift. Center deflection results measured by Anians are compared to theoretical results generated with the finite element analysis in Fig. 5.15.

As is the case in all deflection curves presented previously in this investigation, the deflection curve obtained by the present finite element formulation reveals the stiffening of the plate with increasing deflection. This effect is indicated by the decreasing slope of the curve. It should

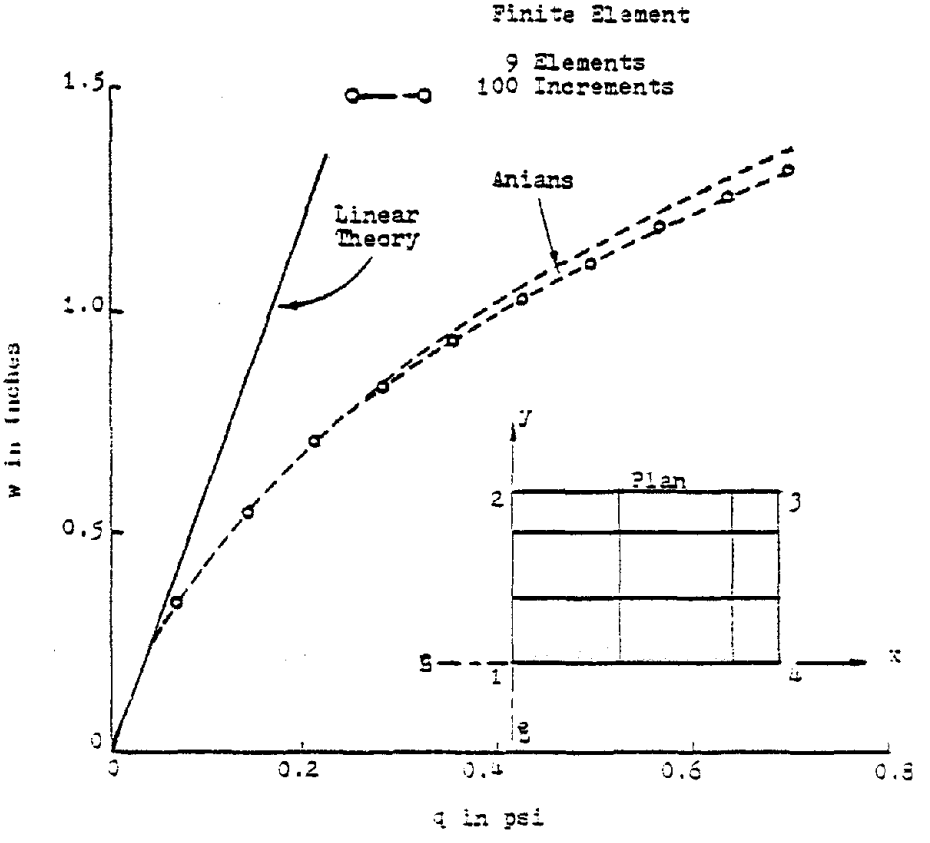

Figure 5.15 Load-Deflection of Simply Supported Rectangular Plate: Edge Displacement ≠ 0

be noticed that there is an excellent agreement between the displacement results obtained by Anians and theoretical results up to a central deflection of three times the plate thickness as illustrated in Fig. 5.15. At that point, the theortical deflections tend to be less than the measured deflections. This condition is attributed to the fact that the lateral displacement along the perimeter of the plate is assumed to be zero in the present finite element formulation, while in Anian's experimental work the neoprene gaskets along the plate perimeter allowed the edges to move a small amount in the lateral direction.

In Fig. 5.16, bending and membrane stresses at the center of the plate are shown. The effect of the boundary edge conditions is clearly evident if the value of the membrane stress in the y-direction is compared with that presented previously in Fig. 5.6.

5.3 General Remarks and Discussion of Results

The preceding sections of this chapter included example problems involving large displacement-small strain, simply supported, uniformly loaded, square and rectangular plates with two different in-plane boundary conditions: Edge Displacement = 0 (Examples I and II in Sections 5.1-A and 5.1-B), and Edge Displacement $\neq$ 0 , where the edges do not necessarily remain straight as the plate is deflected (Examples I and II in Sections 5.2-A and 5.2-B, respectively). The validity of the proposed finite element formulation has been demonstrated for specific large displacement square and rectangular plate problems by comparison with closed form solutions. The finite element technique also can be applied to plates of rectangular shape with boundary edge conditions for which no closed-form solution exists.

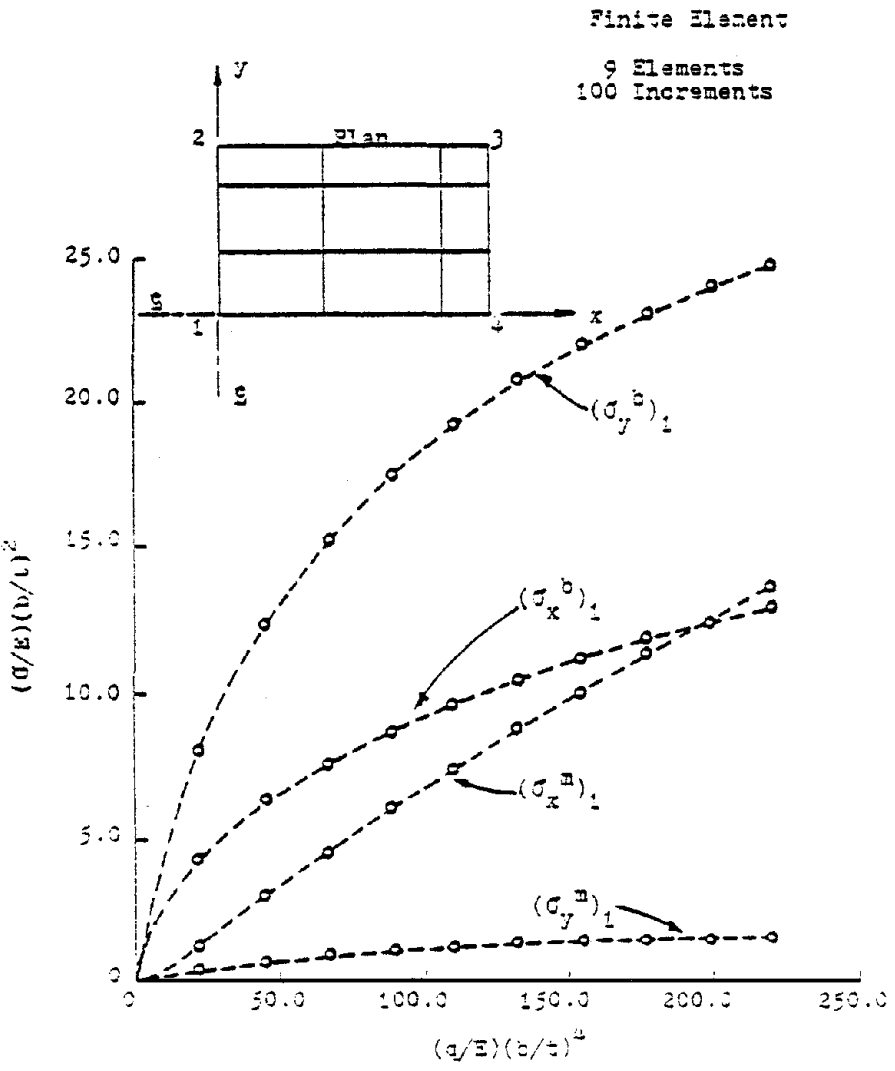

Figure 5.16 Bending and Membrane Stresses at Center of Simply Supported Rectangular Plate: Edge Displacement ≠ 0

It was noted from the numerical studies conducted on the problem in Example I of section 5.2-A that the convergence of stresses to exact values differs between bending and membrane stresses, and depends on the fineness of the finite element discretization, the location within the plate, and the relative magnitude of the loading increment. This difference can be outlined as follows:

1. As the number of loading increments is increased the convergence of the bending
    a) Stress at the center of the plate approaches the exact value from an upper bound,
    b) Stress at the corner of the plate approaches the exact value from a lower bound,

    and the convergence of the membrane
    a) Stress at the center of the plate approaches the exact value from a lower bound,
    b) Stress at the center edge of the plate approaches the exact solution from a lower bound.
2. As the size of the discretized element is reduced the convergence of the bending
    a) Stress at the center of the plate approaches the exact solution from an upper bound,
    b) Stress at the corner of the plate approaches the exact value from an upper bound,

    and the convergence of the membrane
    a) Stress at the center of the plate approaches the exact value from an upper bound,

b) Stress at the center edge of the plate approaches the exact value from an upper bound.

CHAPTER 6

CONCLUSIONS AND RECOMMENDATIONS

In this investigation, a finite element displacement approach formulation has been presented for obtaining numerical solutions to geometrically nonlinear large displacement-small strain problems of rectangular thin elastic plates. It has been demonstrated that the method is capable of solving rectangular plate problems in which membrane and bending behaviors are coupled and that displacements and stresses, particularly membrane stresses, are sufficiently accurate for engineering purposes.

It should be noted that in most finite element research dealing with geometrically nonlinear plate problems, the membrane behavior of the plate is represented by simple shape functions which include only constant strains. In this research, the membrane behavior is modeled by products of one-dimensional Hermitian polynomials of order one. Thus, the resulting shape functions are polynomials capable of representing not only constant strains but also strains which vary linearly within the element. Representation of the membrane behavior as such is important in studying the stress distributions in the glass plate, particularly at the perimeters of that plate. This approach furnished results that are in very good agreement with available theoretical and experimental data. Based on the results obtained from this research, the following conclusions have been made.

1. The proposed finite element formulation fulfills the objective of the investigation.
2. The glass plate which has edges that are free to move in-plane experiences larger central stresses and displacement than plates with "immovable" edges.
3. Appreciable compressive membrane stresses which have maximum values at the center edges develop along the perimeters of the plate.
4. Convergence of stresses differs between bending and membrane stresses and depends upon the fineness of the finite element discretization, the location within the plate, and the relative magnitude of the loading increment.

The present research has given a means by which the stress distribution in rectangular plates can be studied. However, as with any research, this investigation must be continued. Therefore, it is recommended that certain improvements be made on the computational scheme of the proposed approach and that certain topics be pursued

1. Improve the computational scheme by checking the equilibrium at each loading increment and using a geometric progression type incremental approach.
2. Conduct more studies of edge stresses of the glass plate problem by using a finer mesh size along the boundaries and plotting separately the variations of bending and membrane stresses at critical points in the plate.

3. Compare stresses at critical points of the plate that develop when the edges are free to move in the plane of the plate with those developed when the edges are restrained.
4. Conduct corner stress studies when the corners of the glass plate are allowed to lift.
5. Model the perimeters of the glass plate as plates on elastic foundations and impose rotational elastic springs along those perimeters to include the effects of the partial restraint placed by the window framing system on the plate.
6. Compare total stresses with available experimental data on glass.

LIST OF REFERENCES

1. Allman, D. J., "Some Fundamental Aspects of the Finite Element Analysis of Nonlinear Elastic Plates," Finite Element Analysis in Nonlinear Mechanics, 1st Conf. on Finite Element in Nonlinear Solid and Structural Mechanics held at Geilo, Norway, in August, 1977, pp. 345-371.

2. Anians, D. C., "Experimental Study of Edge Displacements of Laterally Loaded Window Glass Plates," Master Thesis, Texas Tech University, 1979.

3. Argyris, J. H., Recent Advances in Matrix Methods of Structural Analysis, Pergamon Press, London, 1964.

4. Bauer, F., Bauer, L., Becker, W., and Reiss, E. L., "Bending of Rectangular Plates with Finite Deflections," Journal of Applied Mechanics, Trans. of the ASCE, December, 1965, pp. 821-825.

5. Bazeley, G. P., Cheung, Y. K., Irons, B. M., and Zienkiewicz, O. C., "Triangular Elements in Plate Bending--Conforming and Non-Conforming Solutions," Conf. on Matrix Methods in Struc. Mech., Wright-Patterson Air Force Base, Dayton, Ohio, 1965.

6. Beason, W. L., "A Failure Prediction Model for Window Glass," Ph.D. Dissertation, Texas Tech University, 1980.

7. Bergan, P. G., and Clough, R. W., "Large Deflection Analysis of Plates and Shallow Shells Using the Finite Element Method," Int. Journal for Numerical Methods in Engineering, Vol. 5, 1973, pp. 543-556.

8. Berger, H. M., "A New Approach to the Analysis of Large Deflections of Plates," Journal of Applied Mechanics, Trans. of the ASCE, December, 1955, pp. 465-472.

9. Bogner, H. M., Fox, R. L., and Schmit, L. A., "The Generation of Interelement, Compatible Stiffness for Mass Matrices by the Use of Interpolation Formulas," Proc. 1st Conf. Matrix Meth. Struct. Mech., AFFDL-TR-66-80, 1965, pp. 397-444.

10. Bogner, F. K., Fox, R. L., and Schmit, L. A., "A Cylindrical Shell Discrete Element," AIAA Journal, Vol. 5, April, 1967.

11. Bowes, W. H., and Tussell, L. T., Stress Analysis by the Finite-Element Method for Practicing Engineers, Lexington Book, D. C. Heath Company, Lexington, Massachusetts, 1975.

12. Brebbia, C., and Conner, J., "Geometrically Nonlinear Finite-Element Analysis," Journal of the Engr. Mech. Div., Proc. of the ASCE, Vol. 95, No. EM 2, April, 1969.

13. Chang, C. C., and Conway, H. D., "The Marcus Method Applied to Solution of Uniformly Loaded and Clamped Rectangular Plate Subjected to Forces in Its Plane," Journal of Applied Mechanics, Trans. of the ASCE, June, 1952, pp. 179-184.

14. Cheung, S. T., "Analysis of Geometrically Nonlinear Structures Using a Lagrangian Strain Representation and a Convected Coordinate System," Master Thesis, Texas A&M University, College Station, Texas, 1974.

15. Conway, H. D., "Bending of Rectangular Plates Subjected to a Uniform Distributed Lateral Load and Tensile or Compressive Forces in the Plane of the Plate," Journal of Applied Mechanics, Trans. of the ASCE, September, 1949, pp. 301-309.

16. Clough, R. W., and Felippa, C. A., "A Refined Quadrilateral Element for the Analysis of Plate Bending," Proc. 2nd Conf. Matrix Meth. Struct. Mech., AFFDL-TR-68-150, pp. 399-440, 1969.

17. Cook, R. D., Concepts and Applications of Finite Element Analysis, John Wiley & Sons, Inc., 1974.

18. Crandall, S. H., Engineering Analysis--A Survey of Numerical Procedures, McGraw-Hill Book Company, New York, 1956.

19. Desai, C. S., and Abel, J. F., Introduction to the Finite Element Method--A Numerical Method for Engineering Analysis, Van Nostrand-Reinhold Company, New York, NY, 1972.

20. Dunne, P. C., "Complete Polynomial Displacement Fields for Finite Element Method," The Aeronautical Journal of the Royal Aeronautic Society, Vol. 72, pp. 245-246.

21. Fung, Y. C., Foundations of Solid Mechanics, Prentice-Hall, Inc. Englewood Cliffs, New Jersey, 1965, pp. 456-470.

22. Gallagher, R. H., Gellatly, R. A., Padlog, J., and Mallett, R. H., "A Discrete Element Procedure for Thin Shell Instability Analysis," AIAA Journal, Vol. 5., January, 1967.

23. Haisler, W. E., "Development and Evaluation of Solution Procedures for Nonlinear Structural Analysis," Ph.D. Dissertation, Texas A&M University, College Station, Texas, 1970.

24. Hibbit, H. D., Marcal, P. V., and Rice, J. R., "A Finite Element Formulation for Problems of Large Strain and Large Displacement," Int. Journal Solids and Struc., Vol. 6, 1970, pp. 1069-1086.

25. Jennings, A., "Frame Analysis Including Change of Geometry," Journal Struc. Div., Proc. of Geometry, Journal Struc. Div., Proc. of ASCE, Vol. 94, No. ST 3, March, 1968, pp. 627-644.

26. Jennings, A., "The Elastic Stability of the Rigidly Jointed Frames," Int. Journal Mech. Sci., Vol. 5, 1962, pp. 99-113.

27. Jobson, D. A., "The Determination of Stresses at Nodal Points from Finite Element Solutions to Elastic Problems," The Aeronautical Journal of the Royal Aeronautic Society, Vol. 75, 1971, pp. 194-196.

28. Jones, R., "Shell and Plate Analysis by Finite Elements," Journal Struc. Div., Proc. of ASCE, Vol. 99, No. ST 5, May, 1973, pp. 889-902.

29. Kaiser, R., "Rechnerische und Experimentelle Ermittlung der Durchbiegungen und Spannungen von Quadratischen Platten bei freier Auflagerung an den Randern, Gleichmassig Verteilter Last und Grossen Ausbiegungen," Z.F.A.M.M., Bd. 16, Heft 2, April, 1936, pp. 73-98.

30. Kapur, K. K., and Hartz, B. J., "Stability of Plates Using the Finite Element Method," Journal Engr. Mech. Div., Proc. of the ASCE, Vol. 92, No. EM 2, April, 1966, pp. 175-195.

31. Kawai, T., and Yoshimura, N., "Analysis of Large Deflection of Plates by the Finite Element Method," Int. Journal for Numerical Methods in Engineering, Vol. 1, 1969, pp. 123-133.

32. Langhaar, H. L., Energy Methods in Applied Mechanics, John Wiley & Sons, Inc., New York, NY, 1962.

33. Levy, S., "Square Plate with Clamped Edges Under Normal Pressure Producing Large Deflections," NACA, Report No. 740, 1942.

34. Levy, S., "Bending of Rectangular Plates with Large Deflections," NACA, TN No. 846, 1942.

35. Malvern, L. E., Introduction to the Mechanics of a Continuum, Prentice-Hall, Inc., Englewood Cliffs, New Jersey, 1969.

36. Mallett, R. H., and Marcal, P. V., "Finite Element Analysis of Nonlinear Structures," Journal of the Struc. Div., Proc. of the ASCE, Vol. 96, No. ST 9, September, 1968. pp. 879-893.

37. Mansfield, E. H., The Bending and Stretching of Plates, The Macmillan Company, New York, NY, 1964.

38. Mansfield, E. H., and Kleeman, P. W., "A Large Deflection Theory for Thin Plates," Aircraft Engineering XXVII, April, 1955, pp. 102-108.

39. Martin, H. C., "Finite Elements and the Analysis of Geometrically Nonlinear Problems," Recent Advances in Matrix Methods of Structural Analysis and Design, The University of Alabama Press, Alabama, 1971, pp. 343-381.

40. Martin, H. C., and Carey, G. F., Introduction to Finite Element Analysis Theory and Application, McGraw-Hill Book Company, New York, NY, 1973, pp. 151-183.

41. Martin, H. C., "On the Derivation of Stiffness Matrices for the Analysis of Large Deflection and Stability Problems," Proc. 1st Conf. Matrix Meth. Struc. Mech., AFFDL-TR-66-80, 1965, pp. 697-715.

42. Meek, J. L., Matrix Structural Analysis, McGraw-Hill Book Company, New York, NY, 1971.

43. Melliere, R. A., "A Finite Element Method for Geometrically Nonlinear Large Displacement Problems in Thin, Elastic Plates and Shells," Ph.D. Dissertation, University of Missouri, Rolla, 1969.

44. Melosh, R. J., "Basis for the Derivation of Matrices for the Direct Stiffness Method," AIAA Journal, Vol. 1, July, 1963.

45. Melosh, R. J., and Bamford, R. J., "Efficient Solution of Load-Deflection Equations," Journal of the Struc. Div., Proc. of the ASCE, Vol. 95, No. ST 4, April, 1969, pp. 661-676.

46. Moore, D., "Design Curves for Non-Linear Analysis of Simply-Supported, Uniformly-Loaded Rectangular Plates," Preprint of Paper Presented at AIAA/ASME/ASCE/AHS 20th Structure, Structural Dynamics and Materials Conference, St. Louis, Missouri, Apr. 4-6, 1979.

47. Morse, R. F., and Conway, H. D., "The Rectangular Plate Subjected to Hydrostatic Tension and to Uniformly Distributed Lateral Load," J. Appl. Mech., June, 1967, pp. 209-210.

48. Murray, D. W., and Wilson, E. L., "Finite-Element Large Deflection Analysis of Plates," Journal of the Engr. Mech. Div., Proc. of the ASCE, Vol. 95, No. EM 1, February, 1969, pp. 143-165.

49. Murray, D. W., and Wilson, E. L., "An Approximate Nonlinear Analysis of Thin Plates," Proc. 2nd Conf. Matrix Methods Struc. Mech., AFFDL-TR-68-150, 1969, pp. 1207-1230.

50. Novozhilov, V. V., Foundations of Nonlinear Theory of Elasticity, Graylock Press, Rochester, New York, 1953.

51. Oden, J. T., Finite Element of Nonlinear Continua, McGraw-Hill Book Company, Inc., 1972.

52. Oliveira, A. R., "Theoretical Foundations of the Finite Element Method," Int. Journal Solids and Struc., Vol. 4, 1968, pp. 929-952.

53. Powell, G. H., "Theory of Nonlinear Elastic Structures," Journal of the Struc. Div., Proc. of the ASCE, Vol. 95, No. ST 12, December, 1969, pp. 198-216.

54. Reissner, E., "The Effect of Transverse Shear Deformation on the Bending of Elastic Plates," Journal of Applied Mechanics, Trans. of the ASCE, June, 1945, pp. 69-77.

55. Saafan, A., "Nonlinear Behavior of Structural Plane Frames," Journal of the Struc. Div., Proc. of the ASCE, Vol. 89, No. ST 4, August, 1963.

56. Schmit, L. A., Bogner, F. K., and Fox, R. L., "Finite Deflection Structural Analysis Using Plate and Shell Discrete Elements," AIAA Journal, Vol. 6, No. 5, May, 1968.

57. Smith, I. M., and Duncan, W., "The Effectiveness of Excessive Nodal Continuities in the Finite Element Analysis of Thin Rectangular and Skew Plates in Bending," Int. Journal Num. Mech. Engr., Vol. 2, 1979, pp. 253-257.

58. Stricklin, J. A., Haisler, W. E., and Riesemann, W. V., "Formulation, Computation, and Solution Procedures for Material and/or Geometric Nonlinear Structural Analysis by the Finite Element Method," Sandia Lab SC-CR-72 3102, 1972.

59. Stricklin, J. A., Haisler, W. E., and Riesemann, W. V., "Geometrically Nonlinear Structural Analysis by Direct Stiffness Method," Journal of the Struc. Div., Proc. of the ASCE, Vol. 97, No. 25 9, September, 1971, pp. 2299-2314.

60. Stoker, J. J., Nonlinear Elasticity, Gordon and Breach, Science Publisher, Inc., New York, NY, 1978.

61 Szilard, R., Theory and Analysis of Plates - Classical and Numerical Methods, Prentice-Hall, Inc., Englewood Cliffs, New Jersey, 1974.

62. Thomas, G. R., and Gallagher, R. H., "A Triangular Thin Shell Finite Element: Nonlinear Analysis," NACA, CR 2483, July, 1975.

63. Timoshenko, S., Theory of Plates and Shells, McGraw-Hill Book Company, Inc., New York, NY, 1940.

64. Timoshenko, S., Theory of Elasticity, McGraw-Hill Book Company, Inc., New York, NY, 1934.

65. Timoshenko, S., and Woinowsky-Krieger, S., Theory of Plates and Shells, McGraw-Hill Book Company, Inc., New York, NY, 1965.

66. Tong, P., and Rossetos, J. N., Finite Element Method--Basic Technique and Implementation, The MIT Press, Cambridge, Mass., 1977.

67. Tsai, C. R., and Stewart, R. A., "Stress Analysis of Large Deflection of Glass Plates by the Finite-Element Method," Journal of American Ceramic Society, Vol. 59, No. 9-10, May 11, 1976.

68. Turner, M. J., Dill, E. H., Martin, H. C., and Melosh, R. J., "Large Deflections of Structures Subjected to Heating and External Loads," Journal of Aero/Space Sciences, Vol. 27, February, 1969, pp. 97-107.

69. Vos, R. G., "Finite-Element Analysis of Plate Buckling and Postbuckling," Ph.D. Dissertation, Rice University, 1970.

70. Wang, C. T., "Bending of Rectangular Plates with Large Deflections," NACA, TN, No. 1462, 1948.

71. Wang, C. T., "Nonlinear Large-Deflection Boundary-Value Problems of Rectangular Plates," NACA, TN, No. 1425, 1948.

72. Yang, T. Y., "A Finite Element Procedure for Large Deflection Analysis of Plates with Initial Deflections," AIAA Journal, Vol. 9, 1971, pp. 1468-1471.

73. Zienkiewicz, O. C., The Finite Element Method - Third Edition, McGraw-Hill Book Company, London, 1977.

APPENDICES

A. The $[B_0]$, $[G]$, and $[B_L]$, and $\{\alpha\}$ Matrices

B. The $[K_0]$ and $[K_L]$ Stiffness Matrices

C. The $[K_\sigma]$ Stiffness Matrix

Appendix A. The $[B_0]$, $[G]$, and $[B_L]$, and $\{\alpha\}$ Matrices

APPENDIX A

THE $[B_0]$, $[G]$, $[B_L]$, AND $\{\alpha\}$ MATRICES

A.1 Hermitian Polynomials and Their Derivatives

The expressions used to construct the matrices $[B_0]$, $[G]$, and $[B_L]$ and consequently the stiffness matrices $[K_0]$, $[K_L]$, and $[K_\sigma]$ are the one-dimensional Hermitian polynomials of order one and their derivatives. A set of Hermitian polynomials is defined in Chapter 3 by Eq. (3-2) and is rewritten here for convenience as

$$\left.\begin{aligned} H_{01}^{(1)}(x) &= \frac{1}{a^3}(2x^3 - 3ax^2 + a^3) \\ H_{02}^{(1)}(x) &= \frac{-1}{a^3}(2x^3 - 3ax^2) \\ H_{11}^{(1)}(x) &= \frac{1}{a^2}(x^3 - 2ax^2 + a^2x) \\ H_{12}^{(1)}(x) &= \frac{1}{a^2}(x^3 - ax^2) \end{aligned}\right\} \quad \text{for all } x \text{ where } 0 \leq x \leq a \qquad \text{(A-1)}$$

The first derivatives of these Hermitian polynomials with respect to the x-coordinate are written as

$$\left.\begin{aligned} H_{01}^{(1)}(x)' &= \frac{6x}{a^3}(x - a) \\ H_{02}^{(1)}(x)' &= \frac{-6x}{a^3}(x - a) \\ H_{11}^{(1)}(x)' &= \frac{1}{a^2}(3x^2 - 4ax + a^2) \\ H_{12}^{(1)}(x)' &= \frac{x}{a^2}(3x - 2a) \end{aligned}\right\} \quad \text{for all } x \text{ where } 0 \leq x \leq a \qquad \text{(A-2)}$$

and the second derivatives with respect to the x-coordinate are expressed as

$$\left.\begin{aligned} H_{01}^{(1)}(x)'' &= \frac{6}{a^3}(2x - a) \\ H_{02}^{(1)}(x)'' &= \frac{-6}{a^3}(2x - a) \\ H_{11}^{(1)}(x)'' &= \frac{1}{a^2}(6x - 4a) \\ H_{12}^{(1)}(x)'' &= \frac{1}{a^2}(6x - 2a) \end{aligned}\right\} \quad \text{for all } x \text{ where } 0 \leqslant x \leqslant a \qquad \text{(A-3)}$$

A.2 Formulation of the $[B_0]$, $[G]$, $[B_L]$ and $\{\alpha\}$ Matrices for the Computer Program

To formulate the stiffness matrices of the flat rectangular bending membrane plate element shown in Fig. 3.1 for coding in the computer program, the nodal displacements at each node of the element are arranged in the sequence u, u_x, u_y, u_{xy}, v, v_x, v_y, v_{xy}, w, w_x, w_y, and w_{xy}. This leads to rearranging the elements of the $[B_0]$, $[G]$, $[B_L]$, and $\{\alpha\}$ matrices such that the membrane and bending components are separated at each node. Thus those matrices are written in a partitioned form for each element as follows:

Eq. (3-29) is written in a partitioned form as

$$\{\varepsilon_L\} = \left[\, [B_{011}] \vdots [B_{012}] \vdots [B_{022}] \vdots [B_{021}] \,\right] \begin{Bmatrix} \{\alpha_{11}\} \\ \cdots\cdots \\ \{\alpha_{12}\} \\ \cdots\cdots \\ \{\alpha_{22}\} \\ \cdots\cdots \\ \{\alpha_{21}\} \end{Bmatrix} \qquad \text{(A-4)}$$

where $[B_{011}]$, $[B_{012}]$, $[B_{022}]$, and $[B_{021}]$ are [6x12] submatrices expressing the derivatives of the shape functions associated with nodes (1,1), (1,2), (2,2), and (2,1) respectively. Naturally, $\{\alpha_{11}\}$, $\{\alpha_{12}\}$, $\{\alpha_{22}\}$,

and $\{\alpha_{21}\}$ are the vector matrices expressing the corresponding displacement parameters. Forms of these matrices are shown in Tables A.1 through A.4.

Similarly, the [G] and [B_L] matrices are partitioned as

$$[\,G\,] = \left[\begin{array}{c:c:c:c} [G_{11}] & [G_{12}] & [G_{22}] & [G_{21}] \end{array}\right] \qquad \text{(A-5)}$$

and

$$[\,B_L\,] = \left[\begin{array}{c:c:c:c} [B_{L11}] & [B_{L12}] & [B_{L22}] & [B_{L21}] \end{array}\right] \qquad \text{(A-6)}$$

respectively. Forms of the matrices $[G_{11}]$, $[G_{12}]$, $[G_{22}]$, and $[G_{21}]$ are shown in Tables A.5 through A.8 while forms of the matrices $[B_{L11}]$, $[B_{L12}]$, $[B_{L22}]$, and $[B_{L21}]$ are shown in Tables A.9 through A.12.

Pages 108-111 have been removed.

Due to legibility problems, the following has been omitted:

- Table A.1 - Portion of the (6x48) Matrix (B_0) Represented by the (6x12) Matrix (B_{011}) and Associated Modal Displacement Parameters (p. 108)
- Table A.2 - Portion of the (6x48) Matrix (B_0) Represented by the (6x12) Matrix (B_{012}) and Associated Modal Displacement Parameters (p. 109)
- Table A.3 - Portion of the (6x48) Matrix (B_0) Represented by the (6x12) Matrix (B_{022}) and Associated Modal Displacement Parameters (p. 110)
- Table A.4 - Portion of the (6x48) Matrix (B_0) Represented by the (6x12) Matrix (B_{021}) and Associated Modal Displacement Parameters (p. 111)*

*For further information regarding these tables, you may contact:

Institute for Disaster Research
Texas Tech University
Lubbock, TX 79409

Table A.5 Portion of the [2x48] Matrix [G] Represented by the [2x12] Matrix $[G_{11}]$

0	0	0	0	0	0	0	0	$H_{01}^{(1)}(x)'H_{01}^{(1)}(y)$	$H_{11}^{(1)}(x)'H_{01}^{(1)}(y)$	$H_{01}^{(1)}(x)'H_{11}^{(1)}(y)$	$H_{11}^{(1)}(x)'H_{11}^{(1)}(y)$
0	0	0	0	0	0	0	0	$H_{01}^{(1)}(x)H_{01}^{(1)}(y)'$	$H_{11}^{(1)}(x)H_{01}^{(1)}(y)'$	$H_{01}^{(1)}(x)H_{11}^{(1)}(y)'$	$H_{11}^{(1)}(x)H_{11}^{(1)}(y)'$

Table A.6 Portion of the [2x48] Matrix [G] Represented by the [2x12] Matrix $[G_{12}]$

0	0	0	0	0	0	0	0	$H_{01}^{(1)}(x)'H_{02}^{(1)}(y)$	$H_{11}^{(1)}(x)'H_{02}^{(1)}(y)$	$H_{01}^{(1)}(x)'H_{12}^{(1)}(y)$	$H_{11}^{(1)}(x)'H_{12}^{(1)}(y)$
0	0	0	0	0	0	0	0	$H_{01}^{(1)}(x)H_{02}^{(1)}(y)'$	$H_{11}^{(1)}(x)H_{02}^{(1)}(y)'$	$H_{01}^{(1)}(x)H_{12}^{(1)}(y)'$	$H_{11}^{(1)}(x)H_{12}^{(1)}(y)'$

Table A.7 Portion of the [2x48] Matrix [G] Represented by the [2x12] Matrix $[G_{22}]$

0	0	0	0	0	0	0	0	$H_{02}^{(1)}(x)\cdot H_{02}^{(1)}(y)$	$H_{12}^{(1)}(x)\cdot H_{02}^{(1)}(y)$	$H_{02}^{(1)}(x)\cdot H_{12}^{(1)}(y)$	$H_{12}^{(1)}(x)\cdot H_{12}^{(1)}(y)$
0	0	0	0	0	0	0	0	$H_{02}^{(1)}(x)H_{02}^{(1)}(y)'$	$H_{12}^{(1)}(x)H_{02}^{(1)}(y)'$	$H_{02}^{(1)}(x)H_{12}^{(1)}(y)'$	$H_{12}^{(1)}(x)H_{12}^{(1)}(y)'$

Table A.8 Portion of the [2x48] Matrix [G] Represented by the [2x12] Matrix $[G_{21}]$

0	0	0	0	0	0	0	0	$H_{02}^{(1)}(x)\cdot H_{01}^{(1)}(y)$	$H_{12}^{(1)}(x)\cdot H_{01}^{(1)}(y)$	$H_{02}^{(1)}(x)\cdot H_{11}^{(1)}(y)$	$H_{12}^{(1)}(x)\cdot H_{11}^{(1)}(y)$
0	0	0	0	0	0	0	0	$H_{02}^{(1)}(x)H_{01}^{(1)}(y)'$	$H_{12}^{(1)}(x)H_{01}^{(1)}(y)'$	$H_{02}^{(1)}(x)H_{11}^{(1)}(y)'$	$H_{12}^{(1)}(x)H_{11}^{(1)}(y)'$

Table A.9 Portion of the [6x48] Matrix $[B_L]$ Represented by the [6x12] Matrix $[B_{L11}]$ and Associated Nodal Displacement Parameters

0	0	0	0	0	0	0	0	$(\partial w/\partial x)$ $H_{01}^{(1)}(x)'H_{01}^{(1)}(y)$	$(\partial w/\partial x)$ $H_{11}^{(1)}(x)'H_{01}^{(1)}(y)$	$(\partial w/\partial x)$ $H_{01}^{(1)}(x)'H_{11}^{(1)}(y)$	$(\partial w/\partial x)$ $H_{11}^{(1)}(x)'H_{11}^{(1)}(y)$
0	0	0	0	0	0	0	0	$(\partial w/\partial y)$ $H_{01}^{(1)}(x)H_{01}^{(1)}(y)'$	$(\partial w/\partial y)$ $H_{11}^{(1)}(x)H_{01}^{(1)}(y)'$	$(\partial w/\partial y)$ $H_{01}^{(1)}(x)H_{11}^{(1)}(y)'$	$(\partial w/\partial y)$ $H_{11}^{(1)}(x)H_{11}^{(1)}(y)'$
0	0	0	0	0	0	0	0	$(\partial w/\partial y)$ $H_{01}^{(1)}(x)'H_{01}^{(1)}(y)$ + $(\partial w/\partial x)$ $H_{01}^{(1)}(x)H_{01}^{(1)}(y)'$	$(\partial w/\partial y)$ $H_{11}^{(1)}(x)'H_{01}^{(1)}(y)$ + $(\partial w/\partial x)$ $H_{11}^{(1)}(x)H_{01}^{(1)}(y)'$	$(\partial w/\partial y)$ $H_{01}^{(1)}(x)'H_{11}^{(1)}(y)$ + $(\partial w/\partial x)$ $H_{01}^{(1)}(x)H_{11}^{(1)}(y)'$	$(\partial w/\partial y)$ $H_{11}^{(1)}(x)'H_{11}^{(1)}(y)$ + $(\partial w/\partial x)$ $H_{11}^{(1)}(x)H_{11}^{(1)}(y)'$
0	0	0	0	0	0	0	0	0	0	0	0
0	0	0	0	0	0	0	0	0	0	0	0
0	0	0	0	0	0	0	0	0	0	0	0

u_{11}	u_{x11}	u_{y11}	u_{xy11}	v_{11}	v_{x11}	v_{y11}	v_{xy11}	w_{11}	w_{x11}	w_{y11}	w_{xy11}

Table A.10 Portion of the [6x48] Matrix $[B_L]$ Represented by the [6x12] Matrix $[B_{L12}]$ and Associated Nodal Displacement Parameters

0	0	0	0	0	0	0	0	$(\partial w/\partial x)$ $H_{01}^{(1)}(x)'H_{02}^{(1)}(y)$	$(\partial w/\partial x)$ $H_{11}^{(1)}(x)'H_{02}^{(1)}(y)$	$(\partial w/\partial x)$ $H_{01}^{(1)}(x)'H_{12}^{(1)}(y)$	$(\partial w/\partial x)$ $H_{11}^{(1)}(x)'H_{12}^{(1)}(y)$
0	0	0	0	0	0	0	0	$(\partial w/\partial y)$ $H_{01}^{(1)}(x)H_{02}^{(1)}(y)'$	$(\partial w/\partial y)$ $H_{11}^{(1)}(x)H_{02}^{(1)}(y)'$	$(\partial w/\partial y)$ $H_{01}^{(1)}(x)H_{12}^{(1)}(y)'$	$(\partial w/\partial y)$ $H_{11}^{(1)}(x)H_{12}^{(1)}(y)'$
0	0	0	0	0	0	0	0	$(\partial w/\partial y)$ $H_{01}^{(1)}(x)'H_{02}^{(1)}(y)$ + $(\partial w/\partial x)$ $H_{01}^{(1)}(x)H_{02}^{(1)}(y)'$	$(\partial w/\partial y)$ $H_{11}^{(1)}(x)'H_{02}^{(1)}(y)$ + $(\partial w/\partial x)$ $H_{11}^{(1)}(x)H_{02}^{(1)}(y)'$	$(\partial w/\partial y)$ $H_{01}^{(1)}(x)'H_{12}^{(1)}(y)$ + $(\partial w/\partial x)$ $H_{01}^{(1)}(x)H_{12}^{(1)}(y)'$	$(\partial w/\partial y)$ $H_{11}^{(1)}(x)'H_{12}^{(1)}(y)$ + $(\partial w/\partial x)$ $H_{11}^{(1)}(x)H_{12}^{(1)}(y)'$
0	0	0	0	0	0	0	0	0	0	0	0
0	0	0	0	0	0	0	0	0	0	0	0
0	0	0	0	0	0	0	0	0	0	0	0

u_{12}	u_{x12}	u_{y12}	u_{xy12}	v_{12}	v_{x12}	v_{y12}	v_{xy12}	w_{12}	w_{x12}	w_{y12}	w_{xy12}

Table A.11 Portion of the [6x48] Matrix $[B_L]$ Represented by the [6x12] Matrix $[B_{L22}]$ and Associated Nodal Displacement Parameters

0	0	0	0	0	0	0	0	$(\partial w/\partial x)$ $H_{02}^{(1)}(x)'H_{02}^{(1)}(y)$	$(\partial w/\partial x)$ $H_{12}^{(1)}(x)'H_{02}^{(1)}(y)$	$(\partial w/\partial x)$ $H_{02}^{(1)}(x)'H_{12}^{(1)}(y)$	$(\partial w/\partial x)$ $H_{12}^{(1)}(x)'H_{12}^{(1)}(y)$
0	0	0	0	0	0	0	0	$(\partial w/\partial y)$ $H_{02}^{(1)}(x)H_{02}^{(1)}(y)'$	$(\partial w/\partial y)$ $H_{12}^{(1)}(x)H_{02}^{(1)}(y)'$	$(\partial w/\partial y)$ $H_{02}^{(1)}(x)H_{12}^{(1)}(y)'$	$(\partial w/\partial y)$ $H_{12}^{(1)}(x)H_{12}^{(1)}(y)'$
0	0	0	0	0	0	0	0	$(\partial w/\partial y)$ $H_{02}^{(1)}(x)'H_{02}^{(1)}(y)$ + $(\partial w/\partial x)$ $H_{02}^{(1)}(x)H_{02}^{(1)}(y)'$	$(\partial w/\partial y)$ $H_{12}^{(1)}(x)'H_{02}^{(1)}(y)$ + $(\partial w/\partial x)$ $H_{12}^{(1)}(x)H_{02}^{(1)}(y)'$	$(\partial w/\partial y)$ $H_{02}^{(1)}(x)'H_{12}^{(1)}(y)$ + $(\partial w/\partial x)$ $H_{02}^{(1)}(x)H_{12}^{(1)}(y)'$	$(\partial w/\partial y)$ $H_{12}^{(1)}(x)'H_{12}^{(1)}(y)$ + $(\partial w/\partial x)$ $H_{12}^{(1)}(x)H_{12}^{(1)}(y)'$
0	0	0	0	0	0	0	0	0	0	0	0
0	0	0	0	0	0	0	0	0	0	0	0
0	0	0	0	0	0	0	0	0	0	0	0

u_{22}	u_{x22}	u_{y22}	u_{xy22}	v_{22}	v_{x22}	v_{y22}	v_{xy22}	w_{22}	w_{x22}	w_{y22}	w_{xy22}

Table A.12 Portion of the [6x48] Matrix $[B_L]$ Represented by the [6x12] Matrix $[B_{L21}]$ and Associated Nodal Displacement Parameters

0	0	0	0	0	0	0	0	$(\partial w/\partial x)$ $H_{02}^{(1)}(x)'H_{01}^{(1)}(y)$	$(\partial w/\partial x)$ $H_{12}^{(1)}(x)'H_{01}^{(1)}(y)$	$(\partial w/\partial x)$ $H_{02}^{(1)}(x)'H_{11}^{(1)}(y)$	$(\partial w/\partial x)$ $H_{12}^{(1)}(x)'H_{11}^{(1)}(y)$
0	0	0	0	0	0	0	0	$(\partial w/\partial y)$ $H_{02}^{(1)}(x)H_{01}^{(1)}(y)'$	$(\partial w/\partial y)$ $H_{12}^{(1)}(x)H_{01}^{(1)}(y)'$	$(\partial w/\partial y)$ $H_{02}^{(1)}(x)H_{11}^{(1)}(y)'$	$(\partial w/\partial y)$ $H_{12}^{(1)}(x)H_{11}^{(1)}(y)'$
0	0	0	0	0	0	0	0	$(\partial w/\partial y)$ $H_{02}^{(1)}(x)'H_{01}^{(1)}(y)$ + $(\partial w/\partial x)$ $H_{02}^{(1)}(x)H_{01}^{(1)}(y)'$	$(\partial w/\partial y)$ $H_{12}^{(1)}(x)'H_{01}^{(1)}(y)$ + $(\partial w/\partial x)$ $H_{12}^{(1)}(x)H_{01}^{(1)}(y)'$	$(\partial w/\partial y)$ $H_{02}^{(1)}(x)'H_{11}^{(1)}(y)$ + $(\partial w/\partial x)$ $H_{02}^{(1)}(x)H_{11}^{(1)}(y)'$	$(\partial w/\partial y)$ $H_{12}^{(1)}(x)'H_{11}^{(1)}(y)$ + $(\partial w/\partial x)$ $H_{12}^{(1)}(x)H_{11}^{(1)}(y)'$
0	0	0	0	0	0	0	0	0	0	0	0
0	0	0	0	0	0	0	0	0	0	0	0
0	0	0	0	0	0	0	0	0	0	0	0

u_{21}	u_{x21}	u_{y21}	u_{xy21}	v_{21}	v_{x21}	v_{y21}	v_{xy21}	w_{21}	w_{x21}	w_{y21}	w_{xy21}

Appendix B. The $[K_0]$ and $[K_L]$ Stiffness Matrices

APPENDIX B

THE $[K_0]$ AND $[K_L]$ STIFFNESS MATRICES

B.1 Formulation of the $[[K_0] + [K_L]]$ Stiffness Matrices for the Computer Program

The first term on the right side of Eq. (3-22) in Chapter 3 defines the sum of the matrices $[K_0]$ and $[K_L]$ as

$$[K_0] + [K_L] = \int_V [\bar{B}]^T [D^*] [\bar{B}] \, dV \tag{B-1}$$

Following the nodal numbering scheme adopted in Appendix A, Eq. (B-1) can be written as

$$[K_0] + [K_L] = \int_V \begin{bmatrix} [\bar{B}_{11}]^T \\ \vdots \\ [\bar{B}_{12}]^T \\ \vdots \\ [\bar{B}_{22}]^T \\ \vdots \\ [\bar{B}_{21}]^T \end{bmatrix} \times [D^*] \times \left[[\bar{B}_{11}] \vdots [\bar{B}_{12}] \vdots [\bar{B}_{22}] \vdots [\bar{B}_{21}] \right] dV \tag{B-2}$$

The right side of Eq. (B-2) yields a [48x48] matrix which is partitioned into 16 [12x12] submatrices; for example, the first submatrix is

$$\int_V [\bar{B}_{11}]^T [D^*] [\bar{B}_{11}] \, dV \tag{B-3}$$

where $[\bar{B}_{11}]$ is a [6x12] matrix which is the sum of $[B_{011}]$ and $[B_{L11}]$.

For clarity, separate expressions for the elements of portions of the stiffness matrices $[K_0]$ and $[K_L]$ as defined by Eq. (B-3) are shown in sections B.2 and B.3, respectively.

B.2 Expressions for the Elements of Portion of the Stiffness Matrix $[K_0]$

The following are expressions for the elements of portion of the stiffness matrix $[K_0]$. It should be noted that the numbers in parenthesis indicate the position of that element in the stiffness matrix; for example, $K_0(01,01)$ is the first stiffness element in the first row and first column of the stiffness matrix $[K_0]$.

$$K_0(01,01) = \frac{Et}{1-\nu^2} \int_A [(H_{01}^{(1)}(x)' H_{01}^{(1)}(y))^2 + \frac{1-\nu}{2}(H_{01}^{(1)}(x) H_{01}^{(1)}(y)')^2] \, dA$$

$$K_0(01,02) = \frac{Et}{1-\nu^2} \int_A [(H_{01}^{(1)}(x)' H_{11}^{(1)}(x)' (H_{01}^{(1)}(y))^2 + \frac{1-\nu}{2} H_{01}^{(1)}(x) H_{11}^{(1)}(x) (H_{01}^{(1)}(y)')^2] \, dA$$

$$K_0(01,03) = \frac{Et}{1-\nu^2} \int_A [(H_{01}^{(1)}(x)')^2 H_{01}^{(1)}(y) H_{11}^{(1)}(y) + \frac{1-\nu}{2}(H_{01}^{(1)}(x))^2 H_{01}^{(1)}(y)' H_{11}^{(1)}(y)'] \, dA$$

$$K_0(01,04) = \frac{Et}{1-\nu^2} \int_A [H_{01}^{(1)}(x)' H_{01}^{(1)}(y) H_{11}^{(1)}(x)' H_{11}^{(1)}(y) + \frac{1-\nu}{2} H_{01}^{(1)}(x) H_{01}^{(1)}(y)' H_{11}^{(1)}(x) H_{11}^{(1)}(y)'] \, dA$$

$$K_0(01,05) = \frac{Et}{2(1+\nu)} \int_A [H_{01}^{(1)}(x)' H_{01}^{(1)}(y) H_{01}^{(1)}(x) H_{01}^{(1)}(y)'] \, dA$$

$$K_0(01,06) = \frac{Et}{1-\nu^2}\int_A [\nu\, H_{01}^{(1)}(x)' H_{01}^{(1)}(y) H_{11}^{(1)}(x) H_{01}^{(1)}(y)' + \frac{1-\nu}{2} H_{01}^{(1)}(x) H_{01}^{(1)}(y)' H_{11}^{(1)}(x)' H_{01}^{(1)}(y)]\, dA$$

$$K_0(01,07) = \frac{Et}{1-\nu^2}\int_A [\nu\, H_{01}^{(1)}(x)' H_{01}^{(1)}(y) H_{01}^{(1)}(x) H_{11}^{(1)}(y)' + \frac{1-\nu}{2} H_{01}^{(1)}(x)' H_{11}^{(1)}(y) H_{01}^{(1)}(x) H_{01}^{(1)}(y)']\, dA$$

$$K_0(01,08) = \frac{Et}{1-\nu^2}\int_A [\nu\, H_{01}^{(1)}(x)' H_{01}^{(1)}(y) H_{11}^{(1)}(x) H_{11}^{(1)}(y)' + \frac{1-\nu}{2} H_{01}^{(1)}(x) H_{01}^{(1)}(y)' H_{11}^{(1)}(x)' H_{11}^{(1)}(y)]\, dA$$

$$K_0(01,09) = K_0(01,10) = K_0(01,11) = K_0(01,12) = 0$$

$$K_0(02,01) = K_0(01,02)$$

$$K_0(02,02) = \frac{Et}{1-\nu^2}\int_A [(H_{11}^{(1)}(x)' H_{01}^{(1)}(y))^2 + \frac{1-\nu}{2}(H_{11}^{(1)}(x) H_{01}^{(1)}(y)')^2]\, dA$$

$$K_0(02,03) = \frac{Et}{1-\nu^2}\int_A [H_{11}^{(1)}(x)' H_{01}^{(1)}(y) H_{01}^{(1)}(x)' H_{11}^{(1)}(y) + \frac{1-\nu}{2} H_{11}^{(1)}(x) H_{01}^{(1)}(y)' H_{01}^{(1)}(x) H_{11}^{(1)}(y)']\, dA$$

$$K_0(02,04) = \frac{Et}{1-\nu^2}\int_A [(H_{11}^{(1)}(x)')^2 H_{01}^{(1)}(y) H_{11}^{(1)}(y) + \frac{1-\nu}{2}(H_{11}^{(1)}(x))^2 H_{01}^{(1)}(y)' H_{11}^{(1)}(y)']\, dA$$

$$K_0(02,05) = \frac{Et}{1-\nu^2}\int_A [\nu\, H_{11}^{(1)}(x)' H_{01}^{(1)}(y) H_{01}^{(1)}(x) H_{01}^{(1)}(y)' + \frac{1-\nu}{2} H_{11}^{(1)}(x) H_{01}^{(1)}(y)' H_{01}^{(1)}(x)' H_{01}^{(1)}(y)]\, dA$$

$$K_0(02,06) = \frac{Et}{2(1+\nu)}\int_A [H_{11}^{(1)}(x)' H_{01}^{(1)}(y) H_{11}^{(1)}(x) H_{01}^{(1)}(y)']\, dA$$

$$K_0(02,07) = \frac{Et}{1-\nu^2}\int_A [\nu\, H_{11}^{(1)}(x)' H_{01}^{(1)}(y) H_{01}^{(1)}(x) H_{11}^{(1)}(y)' + \frac{1-\nu}{2} H_{11}^{(1)}(x) H_{01}^{(1)}(y)' H_{01}^{(1)}(x)' H_{11}^{(1)}(y)]\, dA$$

$$K_0(02,08) = \frac{Et}{1-\nu^2}\int_A [\nu\, H_{11}^{(1)}(x)' H_{01}^{(1)}(y) H_{11}^{(1)}(x) H_{11}^{(1)}(y)' + \frac{1-\nu}{2} H_{11}^{(1)}(x) H_{01}^{(1)}(y)' H_{11}^{(1)}(x)' H_{11}^{(1)}(y)]\, dA$$

$$K_0(02,09) = K_0(02,10) = K_0(02,11) = K_0(02,12) = 0$$

$$K_0(03,01) = K_0(01,03),\ K_0(03,02) = K_0(02,03)$$

$$K_0(03,03) = \frac{Et}{1-\nu^2}\int_A [(H_{01}^{(1)}(x)' H_{11}^{(1)}(y))^2 + \frac{1-\nu}{2}(H_{01}^{(1)}(x) H_{11}^{(1)}(y)')^2]\, dA$$

$$K_0(03,04) = \frac{Et}{1-\nu^2}\int_A [H_{01}^{(1)}(x)' H_{11}^{(1)}(x)' (H_{11}^{(1)}(y))^2 + \frac{1-\nu}{2} H_{01}^{(1)}(x) H_{11}^{(1)}(x) (H_{11}^{(1)}(y)')^2]\, dA$$

$$K_0(03,05) = \frac{Et}{1-\nu^2}\int_A [\nu\, H_{01}^{(1)}(x)' H_{11}^{(1)}(y) H_{01}^{(1)}(x) H_{01}^{(1)}(y)' + \frac{1-\nu}{2} H_{01}^{(1)}(x)' H_{11}^{(1)}(y)' H_{01}^{(1)}(x)' H_{01}^{(1)}(y)]\, dA$$

$$K_0(03,06) = \frac{Et}{1-\nu^2}\int_A [\nu\, H_{01}^{(1)}(x)' H_{11}^{(1)}(y) H_{11}^{(1)}(x) H_{01}^{(1)}(y)' + \frac{1-\nu}{2} H_{01}^{(1)}(x) H_{11}^{(1)}(y)' H_{11}^{(1)}(x)' H_{01}^{(1)}(y)]\, dA$$

$$K_0(03,07) = \frac{Et}{2(1+\nu)}\int_A [H_{01}^{(1)}(x)' H_{11}^{(1)}(y) H_{01}^{(1)}(x) H_{11}^{(1)}(y)']\, dA$$

$$K_0(03,08) = \frac{Et}{1-\nu^2}\int_A [\nu\, H_{01}^{(1)}(x)' H_{11}^{(1)}(y) H_{11}^{(1)}(x) H_{11}^{(1)}(y)' + \frac{1-\nu}{2} H_{01}^{(1)}(x) H_{11}^{(1)}(y)' H_{11}^{(1)}(x)' H_{11}^{(1)}(y)]\, dA$$

$$K_0(03,09) = K_0(03,10) = K_0(03,11) = K_0(03,12) = 0$$

$$K_0(04,01) = K_0(01,04),\ K_0(04,02) = K_0(02,04),\ K_0(04,03) = K_0(03,04)$$

$$K_0(04,04) = \frac{Et}{1-\nu^2}\int_A [(H_{11}^{(1)}(x)' H_{11}^{(1)}(y))^2 + \frac{1-\nu}{2}(H_{11}^{(1)}(x) H_{11}^{(1)}(y)')^2]\, dA$$

$$K_0(04,05) = \frac{Et}{1-\nu^2}\int_A [\nu\, H_{11}^{(1)}(x)' H_{11}^{(1)}(y) H_{01}^{(1)}(x) H_{01}^{(1)}(y)' + \frac{1-\nu}{2} H_{11}^{(1)}(x) H_{11}^{(1)}(y)' H_{01}^{(1)}(x)' H_{01}^{(1)}(y)]\, dA$$

$$K_0(04,06) = \frac{Et}{1-\nu^2}\int_A [\nu\, H_{11}^{(1)}(x)' H_{11}^{(1)}(y) H_{11}^{(1)}(x) H_{01}^{(1)}(y)' + \frac{1-\nu}{2} H_{11}^{(1)}(x) H_{11}^{(1)}(y)' H_{11}^{(1)}(x)' H_{01}^{(1)}(y)]\, dA$$

$$K_0(04,07) = \frac{Et}{1-\nu^2}\int_A [\nu\, H_{11}^{(1)}(x)' H_{11}^{(1)}(y) H_{01}^{(1)}(x) H_{11}^{(1)}(y)' + \frac{1-\nu}{2} H_{11}^{(1)}(x) H_{11}^{(1)}(y)' H_{01}^{(1)}(x)' H_{11}^{(1)}(y)]\, dA$$

$$K_0(04,08) = \frac{Et}{2(1+\nu)} \int_A [H_{11}^{(1)}(x)' H_{11}^{(1)}(y) H_{11}^{(1)}(x) H_{11}^{(1)}(y)'] \, dA$$

$$K_0(04,09) = K_0(04,10) = K_0(04,11) = K_0(04,12) = 0$$

$$K_0(05,01) = K_0(01,05),\ K_0(05,02) = K_0(02,05),\ K_0(05,03) = K_0(03,05),$$

$$K_0(05,04) = K_0(04,05)$$

$$K_0(05,05) = \frac{Et}{1-\nu^2} \int_A [(H_{01}^{(1)}(x) H_{01}^{(1)}(y)')^2 + \frac{1-\nu}{2}(H_{01}^{(1)}(x)' H_{01}^{(1)}(y))^2] \, dA$$

$$K_0(05,06) = \frac{Et}{1-\nu^2} \int_A [H_{01}^{(1)}(x) H_{11}^{(1)}(x)(H_{01}^{(1)}(y)')^2 + \frac{1-\nu}{2} H_{01}^{(1)}(x)' H_{11}^{(1)}(x)' (H_{01}^{(1)}(y))^2] \, dA$$

$$K_0(05,07) = \frac{Et}{1-\nu^2} \int_A [(H_{01}^{(1)}(x))^2 H_{01}^{(1)}(y)' H_{11}^{(1)}(y)' + \frac{1-\nu}{2}(H_{01}^{(1)}(x)')^2 H_{01}^{(1)}(y) H_{11}^{(1)}(y)] \, dA$$

$$K_0(05,08) = \frac{Et}{1-\nu^2} \int_A [H_{01}^{(1)}(x) H_{01}^{(1)}(y)' H_{11}^{(1)}(x) H_{11}^{(1)}(y)' + \frac{1-\nu}{2} H_{01}^{(1)}(x)' H_{01}^{(1)}(y) H_{11}^{(1)}(x)' H_{11}^{(1)}(y)] \, dA$$

$$K_0(05,09) = K_0(05,10) = K_0(05,11) = K_0(05,12) = 0$$

$$K_0(06,01) = K_0(01,06),\ K_0(06,02) = K_0(02,06),\ K_0(06,03) = K_0(03,06)$$

$$K_0(06,04) = K_0(04,06),\ K_0(06,05) = K_0(05,06)$$

$$K_0(06,06) = \frac{Et}{1-\nu^2}\int_A [(H_{11}^{(1)}(x)H_{01}^{(1)}(y)')^2 + \frac{1-\nu}{2}(H_{11}^{(1)}(x)'H_{01}^{(1)}(y))^2]\,dA$$

$$K_0(06,07) = \frac{Et}{1-\nu^2}\int_A [H_{11}^{(1)}(x)H_{01}^{(1)}(y)'H_{01}^{(1)}(x)H_{11}^{(1)}(y)' + \frac{1-\nu}{2}H_{11}^{(1)}(x)' H_{01}^{(1)}(y)H_{01}^{(1)}(x)'H_{11}^{(1)}(y)]\,dA$$

$$K_0(06,08) = \frac{Et}{1-\nu^2}\int_A [(H_{11}^{(1)}(x))^2H_{01}^{(1)}(y)'H_{11}^{(1)}(y)' + \frac{1-\nu}{2}(H_{11}^{(1)}(x)')^2 H_{01}^{(1)}(y)H_{11}^{(1)}(y)]\,dA$$

$$K_0(06,09) = K_0(06,10) = K_0(06,11) = K_0(06,12) = 0$$

$$K_0(07,01) = K_0(01,07),\ K_0(07,02) = K_0(02,07),\ K_0(07,03) = K_0(03,07),$$

$$K_0(07,04) = K_0(04,07),\ K_0(07,05) = K_0(05,07),\ K_0(07,06) = K_0(06,07)$$

$$K_0(07,07) = \frac{Et}{1-\nu^2}\int_A [(H_{01}^{(1)}(x)H_{11}^{(1)}(y)')^2 + \frac{1-\nu}{2}(H_{01}^{(1)}(x)'H_{11}^{(1)}(y))^2]\,dA$$

$$K_0(07,08) = \frac{Et}{1-\nu^2}\int_A [H_{01}^{(1)}(x)H_{11}^{(1)}(x)(H_{11}^{(1)}(y)')^2 + \frac{1-\nu}{2}H_{01}^{(1)}(x)'H_{11}^{(1)}(x)' (H_{11}^{(1)}(y))^2]\,dA$$

$$K_0(07,09) = K_0(07,10) = K_0(07,11) = K_0(07,12) = 0$$

$$K_0(08,01) = K_0(01,08),\ K_0(08,02) = K_0(02,08),\ K_0(08,03) = K_0(03,08),$$

$$K_0(08,04) = K_0(04,08),\ K_0(08,05) = K_0(05,08),\ K_0(08,06) = K_0(06,08),$$

$$K_0(08,07) = K_0(07,08)$$

$$K_0(08,08) = \frac{Et}{1-\nu^2}\int_A [(H_{11}^{(1)}(x)H_{11}^{(1)}(y)')^2 + \frac{1-\nu}{2}(H_{11}^{(1)}(x)'H_{11}^{(1)}(y))^2]\ dA$$

$$K_0(08,09) = K_0(08,10) = K_0(08,11) = K_0(08,12) = 0$$

$$K_0(09,01) = K_0(01,09),\ K_0(09,02) = K_0(02,09),\ K_0(09,03) = K_0(03,09),$$

$$K_0(09,04) = K_0(04,09),\ K_0(09,05) = K_0(05,09),\ K_0(09,06) = K_0(06,09),$$

$$K_0(09,07) = K_0(07,09),\ K_0(09,08) = K_0(08,09)$$

$$K_0(09,09) = \frac{Et^4}{12(1-\nu^2)}\int_A [(H_{01}^{(1)}(x)''H_{01}^{(1)}(y))^2 + 2\nu\, H_{01}^{(1)}(x)''H_{01}^{(1)}(y)H_{01}^{(1)}(x) H_{01}^{(1)}(y)'' + (H_{01}^{(1)}(x)H_{01}^{(1)}(y)'')^2 + 2(1-\nu)(H_{01}^{(1)}(x)' H_{01}^{(1)}(y)')^2]\ dA$$

$$K_0(09,10) = \frac{Et^4}{12(1-\nu^2)}\int_A [H_{01}^{(1)}(x)''H_{11}^{(1)}(x)''(H_{01}^{(1)}(y))^2 + \nu\, H_{01}^{(1)}(x)''H_{01}^{(1)}(y) H_{11}^{(1)}(x)H_{01}^{(1)}(y)'' + \nu\, H_{01}^{(1)}(x)H_{01}^{(1)}(y)''H_{11}^{(1)}(x)'' H_{01}^{(1)}(y) + H_{01}^{(1)}(x)H_{11}^{(1)}(x)(H_{01}^{(1)}(y)'')^2 + 2(1-\nu) H_{01}^{(1)}(x)'H_{11}^{(1)}(x)'(H_{01}^{(1)}(y)')^2]\ dA$$

$$K_0(09,11) = \frac{Et^4}{12(1-\nu^2)}\int_A [(H_{01}^{(1)}(x)'')^2 H_{01}^{(1)}(y)H_{11}^{(1)}(y) + \nu\, H_{01}^{(1)}(x)''H_{01}^{(1)}(y)$$

$$H_{01}^{(1)}(x)H_{11}^{(1)}(y)'' + \nu H_{01}^{(1)}(x)H_{01}^{(1)}(y)''H_{01}^{(1)}(x)''$$
$$H_{11}^{(1)}(y) + (H_{01}^{(1)}(x))^2H_{01}^{(1)}(y)''H_{11}^{(1)}(y)'' + 2(1-\nu)$$
$$H_{01}^{(1)}(x)'H_{11}^{(1)}(x)'(H_{01}^{(1)}(y))^2]\,dA$$

$$K_0(09,12) = \frac{Et^4}{12(1-\nu^2)}\int_A [H_{01}^{(1)}(x)''H_{01}^{(1)}(y)H_{11}^{(1)}(x)''H_{11}^{(1)}(y) + \nu H_{01}^{(1)}(x)''$$
$$H_{01}^{(1)}(y)H_{11}^{(1)}(x)H_{11}^{(1)}(y)'' + \nu H_{01}^{(1)}(x)H_{01}^{(1)}(y)''$$
$$H_{11}^{(1)}(x)''H_{11}^{(1)}(y) + H_{01}^{(1)}(x)H_{01}^{(1)}(y)''H_{11}^{(1)}(x)H_{11}^{(1)}(y)''$$
$$+ 2(1-\nu)H_{01}^{(1)}(x)'H_{01}^{(1)}(y)'H_{11}^{(1)}(x)'H_{11}^{(1)}(y)']\,dA$$

$K_0(10,01) = K_0(01,10)$, $K_0(10,02) = K_0(02,10)$, $K_0(10,03) = K_0(03,10)$,

$K_0(10,04) = K_0(04,10)$, $K_0(10,05) = K_0(05,10)$, $K_0(10,06) = K_0(06,10)$,

$K_0(10,07) = K_0(07,10)$, $K_0(10,08) = K_0(08,10)$, $K_0(10,09) = K_0(09,10)$

$$K_0(10,10) = \frac{Et^4}{12(1-\nu^2)}\int_A [(H_{11}^{(1)}(x)''H_{01}^{(1)}(y))^2 + 2\nu H_{11}^{(1)}(x)''H_{01}^{(1)}(y)H_{11}^{(1)}(x)$$
$$H_{01}^{(1)}(y)'' + (H_{11}^{(1)}(x)H_{01}^{(1)}(y)'')^2 + 2(1-\nu)(H_{11}^{(1)}(x)'$$
$$H_{01}^{(1)}(y)')^2]\,dA$$

$$K_0(10,11) = \frac{Et^4}{12(1-\nu^2)}\int_A [H_{11}^{(1)}(x)''H_{01}^{(1)}(y)H_{01}^{(1)}(y)''H_{11}^{(1)}(y) + \nu H_{11}^{(1)}(x)''$$
$$H_{01}^{(1)}(y)H_{01}^{(1)}(x)H_{11}^{(1)}(y)'' + \nu H_{11}^{(1)}(x)H_{01}^{(1)}(y)''$$

$$H_{01}^{(1)}(x)''H_{11}^{(1)}(y) + H_{11}^{(1)}(x)H_{01}^{(1)}(y)''H_{01}^{(1)}(x)H_{11}^{(1)}(y)''$$
$$+ 2(1-\nu)H_{11}^{(1)}(x)'H_{01}^{(1)}(y)'H_{01}^{(1)}(y)'H_{11}^{(1)}(y)'] \, dA$$

$$K_0(10,12) = \frac{Et^4}{12(1-\nu^2)} \int_A [(H_{11}^{(1)}(x)'')^2 H_{01}^{(1)}(y)H_{11}^{(1)}(y) + \nu H_{11}^{(1)}(x)''H_{01}^{(1)}(y)$$
$$H_{11}^{(1)}(x)H_{11}^{(1)}(y)'' + \nu H_{11}^{(1)}(x)H_{01}^{(1)}(y)''H_{11}^{(1)}(x)''$$
$$H_{11}^{(1)}(y) + (H_{11}^{(1)}(x))^2 H_{01}^{(1)}(y)''H_{11}^{(1)}(y)'' + 2(1-\nu)$$
$$(H_{11}^{(1)}(x)')^2 H_{01}^{(1)}(y)'H_{11}^{(1)}(y)'] \, dA$$

$K_0(11,01) = K_0(01,11)$, $K_0(11,02) = K_0(02,11)$, $K_0(11,03) = K_0(03,11)$,

$K_0(11,04) = K_0(04,11)$, $K_0(11,05) = K_0(05,11)$, $K_0(11,06) = K_0(06,11)$,

$K_0(11,07) = K_0(07,11)$, $K_0(11,08) = K_0(08,11)$, $K_0(11,09) = K_0(09,11)$,

$K_0(11,10) = K_0(10,11)$

$$K_0(11,11) = \frac{Et^4}{12(1-\nu^2)} \int_A [(H_{01}^{(1)}(x)''H_{11}^{(1)}(y))^2 + 2\nu H_{01}^{(1)}(x)''H_{01}^{(1)}(y)H_{01}^{(1)}(x)$$
$$H_{11}^{(1)}(y)'' + (H_{01}^{(1)}(x)H_{11}^{(1)}(y)'')^2 + 2(1-\nu)(H_{01}^{(1)}(x)'$$
$$H_{11}^{(1)}(y)')^2] \, dA$$

$$K_0(11,12) = \frac{Et^4}{12(1-\nu^2)} \int_A [H_{01}^{(1)}(x)''H_{11}^{(1)}(x)''(H_{11}^{(1)}(y))^2 + \nu H_{01}^{(1)}(x)''H_{11}^{(1)}(y)$$
$$H_{11}^{(1)}(x)H_{11}^{(1)}(y)'' + \nu H_{01}^{(1)}(x)H_{11}^{(1)}(y)''H_{11}^{(1)}(x)''$$

$$H_{11}^{(1)}(y) + H_{01}^{(1)}(x)H_{11}^{(1)}(x)(H_{11}^{(1)}(y)'')^2 + 2(1-\nu)$$
$$H_{01}^{(1)}(x)'H_{11}^{(1)}(x)'(H_{11}^{(1)}(y)')^2] \, dA$$

$K_0(12,01) = K_0(01,12)$, $K_0(12,02) = K_0(02,12)$, $K_0(12,03) = K_0(03,12)$,

$K_0(12,04) = K_0(04,12)$, $K_0(12,05) = K_0(05,12)$, $K_0(12,06) = K_0(06,12)$,

$K_0(12,07) = K_0(07,12)$, $K_0(12,08) = K_0(08,12)$, $K_0(12,09) = K_0(09,12)$,

$K_0(12,10) = K_0(10,12)$, $K_0(12,11) = K_0(11,12)$

$$K_0(12,12) = \frac{Et^4}{12(1-\nu^2)} \int_A [(H_{11}^{(1)}(x)'' H_{11}^{(1)}(y))^2 + 2\nu \, H_{11}^{(1)}(x)'' H_{11}^{(1)}(y) H_{11}^{(1)}(x)$$
$$H_{11}^{(1)}(y)'' + (H_{11}^{(1)}(x)H_{11}^{(1)}(y)'')^2 + 2(1-\nu)(H_{11}^{(1)}(x)'$$
$$H_{11}^{(1)}(y)')^2] \, dA$$

B.3 Expressions for the Elements of Portion of the Stiffness Matrix $[K_L]$

The following are expressions for the elements of portion of the stiffness matrix $[K_L]$.

$K_L(01,01) = K_L(01,02) = K_L(01,03) = K_L(01,04) = 0$

$K_L(01,05) = K_L(01,06) = K_L(01,07) = K_L(01,08) = 0$

$$K_L(01,09) = \frac{Et}{1-\nu^2}\int_A [\ \frac{\partial w}{\partial x}(H_{01}^{(1)}(x)'H_{01}^{(1)}(y))^2 + (\frac{1-\nu}{2})\ \frac{\partial w}{\partial y}H_{01}^{(1)}(x)H_{01}^{(1)}(y)'$$
$$H_{01}^{(1)}(x)'H_{01}^{(1)}(y) + (\frac{1-\nu}{2})\ \frac{\partial w}{\partial x}(H_{01}^{(1)}(x)H_{01}^{(1)}(y)')^2]\ dA$$

$$K_L(01,10) = \frac{Et}{1-\nu^2}\int_A [\ \frac{\partial w}{\partial x}H_{01}^{(1)}(x)'H_{11}^{(1)}(x)'(H_{01}^{(1)}(y))^2 + \nu\ \frac{\partial w}{\partial y}H_{01}^{(1)}(x)'$$
$$H_{01}^{(1)}(y)H_{11}^{(1)}(x)H_{01}^{(1)}(y)' + (\frac{1-\nu}{2})(\frac{\partial w}{\partial y}H_{01}^{(1)}(x)H_{01}^{(1)}(y)'$$
$$H_{11}^{(1)}(x)'H_{01}^{(1)}(y) + \frac{\partial w}{\partial x}H_{01}^{(1)}(x)H_{11}^{(1)}(x)(H_{01}^{(1)}(y)')^2)]\ dA$$

$$K_L(01,11) = \frac{Et}{1-\nu^2}\int_A [\ \frac{\partial w}{\partial x}(H_{01}^{(1)}(x)')^2H_{01}^{(1)}(y)H_{11}^{(1)}(y) + \nu\ \frac{\partial w}{\partial y}H_{01}^{(1)}(x)'H_{01}^{(1)}(y)$$
$$H_{01}^{(1)}(x)H_{11}^{(1)}(y)' + (\frac{1-\nu}{2})(\frac{\partial w}{\partial y}H_{01}^{(1)}(x)H_{01}^{(1)}(y)'H_{01}^{(1)}(x)'$$
$$H_{11}^{(1)}(y) + \frac{\partial w}{\partial x}(H_{01}^{(1)}(x))^2H_{01}^{(1)}(y)'H_{11}^{(1)}(y)')]\ dA$$

$$K_L(01,12) = \frac{Et}{1-\nu^2}\int_A [\ \frac{\partial w}{\partial x}H_{01}^{(1)}(x)'H_{01}^{(1)}(y)H_{11}^{(1)}(x)'H_{11}^{(1)}(y) + \nu\ \frac{\partial w}{\partial y}H_{01}^{(1)}(x)'$$
$$H_{01}^{(1)}(y)H_{11}^{(1)}(x)H_{11}^{(1)}(y)' + (\frac{1-\nu}{2})(\frac{\partial w}{\partial y}H_{01}^{(1)}(x)H_{01}^{(1)}(y)'$$
$$H_{11}^{(1)}(x)'H_{11}^{(1)}(y) + \frac{\partial w}{\partial x}H_{01}^{(1)}(x)H_{01}^{(1)}(y)'H_{11}^{(1)}(x)$$
$$H_{11}^{(1)}(y)')]\ dA$$

$$K_L(02,01) = K_L(02,02) = K_L(02,03) = K_L(02,04) = 0$$

$$K_L(02,05) = K_L(02,06) = K_L(02,07) = K_L(02,08) = 0$$

$$K_L(02,09) = \frac{Et}{1-\nu^2}\int_A [\ \frac{\partial w}{\partial x}H_{11}^{(1)}(x)'H_{01}^{(1)}(x)'(H_{01}^{(1)}(y))^2 + \nu\ \frac{\partial w}{\partial y}H_{11}^{(1)}(x)'$$

$$H_{01}^{(1)}(y)H_{01}^{(1)}(x)H_{01}^{(1)}(y)' + (\frac{1-\nu}{2})(\frac{\partial w}{\partial y}H_{11}^{(1)}(x)H_{01}^{(1)}(y)'$$

$$H_{01}^{(1)}(x)'H_{01}^{(1)}(y) + \frac{\partial w}{\partial x}H_{11}^{(1)}(x)H_{01}^{(1)}(x)(H_{01}^{(1)}(y)')^2)]\ dA$$

$$K_L(02,10) = \frac{Et}{1-\nu^2}\int_A [\frac{\partial w}{\partial x}(H_{11}^{(1)}(x)'H_{01}^{(1)}(y))^2 + (\frac{1+\nu}{2})\frac{\partial w}{\partial y}H_{11}^{(1)}(x)'H_{01}^{(1)}(y)$$

$$H_{11}^{(1)}(x)H_{01}^{(1)}(y)' + (\frac{1-\nu}{2})(H_{11}^{(1)}(x)H_{01}^{(1)}(y)')^2\frac{\partial w}{\partial x}]\ dA$$

$$K_L(02,11) = \frac{Et}{1-\nu^2}\int_A [\frac{\partial w}{\partial x}H_{11}^{(1)}(x)'H_{01}^{(1)}(y)H_{01}^{(1)}(x)'H_{11}^{(1)}(y) + \nu\frac{\partial w}{\partial y}H_{11}^{(1)}(x)'$$

$$H_{01}^{(1)}(y)H_{01}^{(1)}(x)H_{11}^{(1)}(y)' + (\frac{1-\nu}{2})(\frac{\partial w}{\partial y}H_{11}^{(1)}(x)H_{01}^{(1)}(y)'$$

$$H_{01}^{(1)}(x)'H_{11}^{(1)}(y) + \frac{\partial w}{\partial x}H_{11}^{(1)}(x)H_{01}^{(1)}(y)'H_{01}^{(1)}(x)$$

$$H_{11}^{(1)}(y)')]\ dA$$

$$K_L(02,12) = \frac{Et}{1-\nu^2}\int_A [\frac{\partial w}{\partial x}(H_{11}^{(1)}(x)')^2H_{01}^{(1)}(y)H_{11}^{(1)}(y) + \nu\frac{\partial w}{\partial y}H_{11}^{(1)}(x)'H_{01}^{(1)}(y)$$

$$H_{11}^{(1)}(x)H_{11}^{(1)}(y)' + (\frac{1-\nu}{2})(\frac{\partial w}{\partial y}H_{11}^{(1)}(x)H_{01}^{(1)}(y)'H_{11}^{(1)}(x)'$$

$$H_{11}^{(1)}(y) + \frac{\partial w}{\partial x}(H_{11}^{(1)}(x))^2H_{01}^{(1)}(y)'H_{11}^{(1)}(y)')]\ dA$$

$$K_L(03,01) = K_L(03,02) = K_L(03,03) = K_L(03,04) = 0$$

$$K_L(03,05) = K_L(03,06) = K_L(03,07) = K_L(03,08) = 0$$

$$K_L(03,09) = \frac{Et}{1-\nu^2}\int_A [\frac{\partial w}{\partial x}(H_{01}^{(1)}(x)')^2H_{11}^{(1)}(y)H_{01}^{(1)}(y) + \nu\frac{\partial w}{\partial y}H_{01}^{(1)}(x)'H_{11}^{(1)}(y)$$

$$H_{01}^{(1)}(x)H_{01}^{(1)}(y)' + (\frac{1-\nu}{2})(\frac{\partial w}{\partial y}H_{01}^{(1)}(x)H_{11}^{(1)}(y)'H_{01}^{(1)}(x)'$$

$$H_{01}^{(1)}(y) + \frac{\partial w}{\partial x}(H_{01}^{(1)}(x))^2 H_{11}^{(1)}(y)' H_{01}^{(1)}(y)')] \, dA$$

$$K_L(03,10) = \frac{Et}{1-\nu^2} \int_A [\frac{\partial w}{\partial x} H_{01}^{(1)}(x)' H_{11}^{(1)}(y) H_{11}^{(1)}(x)' H_{01}^{(1)}(y) + \nu \frac{\partial w}{\partial y} H_{01}^{(1)}(x)' H_{11}^{(1)}(y) H_{11}^{(1)}(x) H_{01}^{(1)}(y)' + (\frac{1-\nu}{2})(\frac{\partial w}{\partial y} H_{01}^{(1)}(x) H_{11}^{(1)}(y)' H_{11}^{(1)}(x)' H_{01}^{(1)}(y) + \frac{\partial w}{\partial x} H_{01}^{(1)}(x) H_{11}^{(1)}(y)' H_{11}^{(1)}(x) H_{01}^{(1)}(y)')] \, dA$$

$$K_L(03,11) = \frac{Et}{1-\nu^2} \int_A [\frac{\partial w}{\partial x}(H_{01}^{(1)}(x)' H_{11}^{(1)}(y))^2 + (\frac{1+\nu}{2}) \frac{\partial w}{\partial y} H_{01}^{(1)}(x)' H_{11}^{(1)}(y) H_{01}^{(1)}(x) H_{11}^{(1)}(y)' + (\frac{1-\nu}{2}) \frac{\partial w}{\partial x} (H_{01}^{(1)}(x) H_{11}^{(1)}(y)')^2] \, dA$$

$$K_L(03,12) = \frac{Et}{1-\nu^2} \int_A [\frac{\partial w}{\partial x} H_{01}^{(1)}(x)' H_{11}^{(1)}(x)' (H_{11}^{(1)}(y))^2 + \nu \frac{\partial w}{\partial y} H_{01}^{(1)}(x)' H_{11}^{(1)}(y) H_{11}^{(1)}(x) H_{11}^{(1)}(y)' + (\frac{1-\nu}{2})(\frac{\partial w}{\partial y} H_{01}^{(1)}(x) H_{11}^{(1)}(y)' H_{11}^{(1)}(x)' H_{11}^{(1)}(y) + \frac{\partial w}{\partial x} H_{01}^{(1)}(x) H_{11}^{(1)}(x) (H_{11}^{(1)}(y)')^2)] \, dA$$

$$K_L(04,01) = K_L(04,02) = K_L(04,03) = K_L(04,04) = 0$$

$$K_L(04,05) = K_L(04,06) = K_L(04,07) = K_L(04,08) = 0$$

$$K_L(04,09) = \frac{Et}{1-\nu^2} \int_A [\frac{\partial w}{\partial x} H_{11}^{(1)}(x)' H_{11}^{(1)}(y) H_{01}^{(1)}(x)' H_{01}^{(1)}(y) + \nu \frac{\partial w}{\partial y} H_{11}^{(1)}(x)' H_{11}^{(1)}(y) H_{01}^{(1)}(x) H_{01}^{(1)}(y)' + (\frac{1-\nu}{2})(\frac{\partial w}{\partial y} H_{11}^{(1)}(x) H_{11}^{(1)}(y)' H_{01}^{(1)}(x)' H_{01}^{(1)}(y) + \frac{\partial w}{\partial x} H_{11}^{(1)}(x) H_{11}^{(1)}(y)' H_{01}^{(1)}(x)$$

$$H_{01}^{(1)}(y)')]\,dA$$

$$K_L(04,10) = \frac{Et}{1-\nu^2}\int_A [\frac{\partial w}{\partial x}(H_{11}^{(1)}(x)')^2 H_{11}^{(1)}(y)H_{01}^{(1)}(y) + \nu\frac{\partial w}{\partial y}H_{11}^{(1)}(x)'H_{11}^{(1)}(y)$$
$$H_{11}^{(1)}(x)H_{01}^{(1)}(y)' + (\frac{1-\nu}{2})(\frac{\partial w}{\partial y}H_{11}^{(1)}(x)H_{11}^{(1)}(y)'H_{11}^{(1)}(x)'$$
$$H_{01}^{(1)}(y) + \frac{\partial w}{\partial x}(H_{11}^{(1)}(x))^2 H_{11}^{(1)}(y)'H_{01}^{(1)}(y)')]\,dA$$

$$K_L(04,11) = \frac{Et}{1-\nu^2}\int_A [\frac{\partial w}{\partial y}H_{11}^{(1)}(x)'H_{01}^{(1)}(x)'(H_{11}^{(1)}(y))^2 + \nu\frac{\partial w}{\partial y}H_{11}^{(1)}(x)'$$
$$H_{11}^{(1)}(y)H_{01}^{(1)}(x)H_{11}^{(1)}(y)' + (\frac{1-\nu}{2})(\frac{\partial w}{\partial y}H_{11}^{(1)}(x)H_{11}^{(1)}(y)'$$
$$H_{01}^{(1)}(x)'H_{11}^{(1)}(y) + \frac{\partial w}{\partial x}H_{11}^{(1)}(x)H_{01}^{(1)}(x)(H_{11}^{(1)}(y)')^2)]\,dA$$

$$K_L(04,12) = \frac{Et}{1-\nu^2}\int_A [\frac{\partial w}{\partial x}(H_{11}^{(1)}(x)'H_{11}^{(1)}(y))^2 + (\frac{1+\nu}{2})\frac{\partial w}{\partial y}H_{11}^{(1)}(x)'H_{11}^{(1)}(y)$$
$$H_{11}^{(1)}(x)H_{11}^{(1)}(y)' + (\frac{1-\nu}{2})\frac{\partial w}{\partial x}(H_{11}^{(1)}(x)H_{11}^{(1)}(y)')^2]\,dA$$

$$K_L(05,01) = K_L(05,02) = K_L(05,03) = K_L(05,04) = 0$$

$$K_L(05,05) = K_L(05,06) = K_L(05,07) = K_L(05,08) = 0$$

$$K_L(05,09) = \frac{Et}{1-\nu^2}\int_A [\frac{\partial w}{\partial x}(\frac{1+\nu}{2})H_{01}^{(1)}(x)H_{01}^{(1)}(y)'H_{01}^{(1)}(x)'H_{01}^{(1)}(y) + \frac{\partial w}{\partial y}($$
$$H_{01}^{(1)}(x)H_{01}^{(1)}(y)')^2 + (\frac{1-\nu}{2})\frac{\partial w}{\partial y}(H_{01}^{(1)}(x)'H_{01}^{(1)}(y))^2]\,dA$$

$$K_L(05,10) = \frac{Et}{1-\nu^2}\int_A [\nu\frac{\partial w}{\partial x}H_{01}^{(1)}(x)H_{01}^{(1)}(y)'H_{11}^{(1)}(x)'H_{01}^{(1)}(y) + \frac{\partial w}{\partial y}(H_{01}^{(1)}(y))^2$$

$$H_{01}^{(1)}(x)H_{11}^{(1)}(x) + (\frac{1-\nu}{2})(\frac{\partial w}{\partial y} H_{01}^{(1)}(x)' H_{11}^{(1)}(x)' (H_{01}^{(1)}(y))^2 + \frac{\partial w}{\partial x} H_{01}^{(1)}(x)' H_{01}^{(1)}(y) H_{11}^{(1)}(x) H_{01}^{(1)}(y)')] \, dA$$

$$K_L(05,11) = \frac{Et}{1-\nu^2} \int_A [\nu \frac{\partial w}{\partial x} H_{01}^{(1)}(x)H_{01}^{(1)}(y)' H_{01}^{(1)}(x)' H_{11}^{(1)}(y) + \frac{\partial w}{\partial y}(H_{01}^{(1)}(x))^2 H_{01}^{(1)}(y)' H_{11}^{(1)}(y)' + (\frac{1-\nu}{2})(\frac{\partial w}{\partial y}(H_{01}^{(1)}(x)')^2 H_{01}^{(1)}(y) H_{11}^{(1)}(y) + \frac{\partial w}{\partial x} H_{01}^{(1)}(x)' H_{01}^{(1)}(y) H_{01}^{(1)}(x) H_{11}^{(1)}(y)')] \, dA$$

$$K_L(05,12) = \frac{Et}{1-\nu^2} \int_A [\nu \frac{\partial w}{\partial x} H_{01}^{(1)}(x)H_{01}^{(1)}(y)' H_{11}^{(1)}(x)' H_{11}^{(1)}(y) + \frac{\partial w}{\partial y} H_{01}^{(1)}(x) H_{01}^{(1)}(y)' H_{11}^{(1)}(x) H_{11}^{(1)}(y) + (\frac{1-\nu}{2})(\frac{\partial w}{\partial y} H_{01}^{(1)}(x)' H_{01}^{(1)}(y) H_{11}^{(1)}(x)' H_{11}^{(1)}(y) + \frac{\partial w}{\partial x} H_{01}^{(1)}(x)' H_{01}^{(1)}(y) H_{11}^{(1)}(x) H_{11}^{(1)}(y)')] \, dA$$

$$K_L(06,01) = K_L(06,02) = K_L(06,03) = K_L(06,04) = 0$$

$$K_L(06,05) = K_L(06,06) = K_L(06,07) = K_L(06,08) = 0$$

$$K_L(06,09) = \frac{Et}{1-\nu^2} \int_A [\nu \frac{\partial w}{\partial x} H_{11}^{(1)}(x)H_{01}^{(1)}(y)' H_{01}^{(1)}(x)' H_{01}^{(1)}(y) + \frac{\partial w}{\partial y} H_{11}^{(1)}(x) H_{01}^{(1)}(x)(H_{01}^{(1)}(y)')^2 + (\frac{1-\nu}{2})(\frac{\partial w}{\partial y} H_{11}^{(1)}(x)' H_{01}^{(1)}(x)' (H_{01}^{(1)}(y))^2 + \frac{\partial w}{\partial x} H_{11}^{(1)}(x)' H_{01}^{(1)}(y) H_{01}^{(1)}(x) H_{01}^{(1)}(y)')] \, dA$$

$$K_L(06,10) = \frac{Et}{1-\nu^2} \int_A [\frac{\partial w}{\partial x}(\frac{1+\nu}{2}) H_{11}^{(1)}(x)H_{01}^{(1)}(y)' H_{11}^{(1)}(x)' H_{01}^{(1)}(y) + \frac{\partial w}{\partial y}(H_{11}^{(1)}(x$$

$$)H_{01}^{(1)}(y)')^2 + (\frac{1-\nu}{2})(\frac{\partial w}{\partial y}(H_{11}^{(1)}(x)'H_{01}^{(1)}(y))^2]\ dA$$

$$K_L(06,11) = \frac{Et}{1-\nu^2}\int_A [\nu \frac{\partial w}{\partial x} H_{11}^{(1)}(x)H_{01}^{(1)}(y)'H_{01}^{(1)}(x)'H_{11}^{(1)}(y) + \frac{\partial w}{\partial y} H_{11}^{(1)}(x)$$
$$H_{01}^{(1)}(y)'H_{01}^{(1)}(x)H_{11}^{(1)}(y)' + (\frac{1-\nu}{2})(\frac{\partial w}{\partial y} H_{11}^{(1)}(x)'H_{01}^{(1)}(y)$$
$$H_{01}^{(1)}(x)'H_{11}^{(1)}(y) + \frac{\partial w}{\partial x} H_{11}^{(1)}(x)'H_{01}^{(1)}(y)H_{01}^{(1)}(x)H_{11}^{(1)}(y$$
$$)')]\ dA$$

$$K_L(06,12) = \frac{Et}{1-\nu^2}\int_A [\nu \frac{\partial w}{\partial x} H_{11}^{(1)}(x)H_{01}^{(1)}(y)'H_{11}^{(1)}(x)'H_{11}^{(1)}(y) + \frac{\partial w}{\partial y}(H_{11}^{(1)}(x))^2$$
$$H_{01}^{(1)}(y)'H_{11}^{(1)}(y)' + (\frac{1-\nu}{2})(\frac{\partial w}{\partial y}(H_{11}^{(1)}(x)')^2 H_{01}^{(1)}(y)$$
$$H_{11}^{(1)}(y) + \frac{\partial w}{\partial x} H_{11}^{(1)}(x)'H_{01}^{(1)}(y)H_{11}^{(1)}(x)H_{11}^{(1)}(y)')]\ dA$$

$$K_L(07,01) = K_L(07,02) = K_L(07,03) = K_L(07,04) = 0$$

$$K_L(07,05) = K_L(07,06) = K_L(07,07) = K_L(07,08) = 0$$

$$K_L(07,09) = \frac{Et}{1-\nu^2}\int_A [\nu \frac{\partial w}{\partial x} H_{01}^{(1)}(x)H_{11}^{(1)}(y)'H_{01}^{(1)}(x)'H_{01}^{(1)}(y) + \frac{\partial w}{\partial y}(H_{01}^{(1)}(x))^2$$
$$H_{11}^{(1)}(y)'H_{01}^{(1)}(y)' + (\frac{1-\nu}{2})(\frac{\partial w}{\partial y}(H_{01}^{(1)}(x)')^2 H_{11}^{(1)}(y)$$
$$H_{01}^{(1)}(y) + \frac{\partial w}{\partial x} H_{01}^{(1)}(x)'H_{11}^{(1)}(y)H_{01}^{(1)}(x)H_{01}^{(1)}(y)')]\ dA$$

$$K_L(07,10) = \frac{Et}{1-\nu^2}\int_A [\nu \frac{\partial w}{\partial x} H_{01}^{(1)}(x)H_{11}^{(1)}(y)'H_{11}^{(1)}(x)'H_{01}^{(1)}(y) + \frac{\partial w}{\partial y} H_{01}^{(1)}(x)$$
$$H_{11}^{(1)}(y)'H_{11}^{(1)}(x)H_{01}^{(1)}(y)' + (\frac{1-\nu}{2})(\frac{\partial w}{\partial y} H_{01}^{(1)}(x)'H_{11}^{(1)}($$

$$y)H_{11}^{(1)}(x)'H_{01}^{(1)}(y) + \frac{\partial w}{\partial x} H_{01}^{(1)}(x)'H_{11}^{(1)}(y)H_{11}^{(1)}(x)H_{01}^{(1)}(y)')] \, dA$$

$$K_L(07,11) = \frac{Et}{1-\nu^2} \int_A [\frac{\partial w}{\partial x}(\frac{1-\nu}{2}) H_{01}^{(1)}(x)H_{11}^{(1)}(y)'H_{01}^{(1)}(x)'H_{11}^{(1)}(y) + \frac{\partial w}{\partial x}(H_{01}^{(1)}(x) H_{11}^{(1)}(y)')^2 + (\frac{1-\nu}{2}) \frac{\partial w}{\partial y}(H_{01}^{(1)}(x)'H_{11}^{(1)}(y))^2] \, dA$$

$$K_L(07,12) = \frac{Et}{1-\nu^2} \int_A [\nu \frac{\partial w}{\partial x} H_{01}^{(1)}(x)H_{11}^{(1)}(y)'H_{11}^{(1)}(x)'H_{11}^{(1)}(y) + \frac{\partial w}{\partial y} H_{01}^{(1)}(x) H_{11}^{(1)}(x)(H_{11}^{(1)}(y)')^2 + (\frac{1-\nu}{2})(\frac{\partial w}{\partial y} H_{01}^{(1)}(x)'H_{11}^{(1)}(y)' (H_{11}^{(1)}(y))^2 + \frac{\partial w}{\partial x} H_{01}^{(1)}(x)'H_{11}^{(1)}(y)H_{11}^{(1)}(x)H_{11}^{(1)}(y)')] \, dA$$

$$K_L(08,01) = K_L(08,02) = K_L(08,03) = K_L(08,04) = 0$$

$$K_L(08,05) = K_L(08,06) = K_L(08,07) = K_L(08,08) = 0$$

$$K_L(08,09) = \frac{Et}{1-\nu^2} \int_A [\nu \frac{\partial w}{\partial x} H_{11}^{(1)}(x)H_{11}^{(1)}(y)'H_{01}^{(1)}(x)'H_{01}^{(1)}(y) + \frac{\partial w}{\partial y} H_{11}^{(1)}(x) H_{11}^{(1)}(y)'H_{01}^{(1)}(x)H_{01}^{(1)}(y)' + (\frac{1-\nu}{2})(\frac{\partial w}{\partial y} H_{11}^{(1)}(x)'H_{11}^{(1)}(y) H_{01}^{(1)}(x)'H_{01}^{(1)}(y) + \frac{\partial w}{\partial x} H_{11}^{(1)}(x)'H_{11}^{(1)}(y)H_{01}^{(1)}(x)H_{01}^{(1)}(y)')] \, dA$$

$$K_L(08,10) = \frac{Et}{1-\nu^2} \int_A [\nu \frac{\partial w}{\partial x} H_{11}^{(1)}(x)H_{11}^{(1)}(y)'H_{11}^{(1)}(x)'H_{01}^{(1)}(y) + \frac{\partial w}{\partial y}(H_{11}^{(1)}(x))^2 H_{11}^{(1)}(y)'H_{01}^{(1)}(y)' + (\frac{1-\nu}{2})(\frac{\partial w}{\partial y}(H_{11}^{(1)}(x)')^2 H_{11}^{(1)}(y)$$

$$H_{01}^{(1)}(y) + \frac{\partial w}{\partial x} H_{11}^{(1)}(x)' H_{11}^{(1)}(y) H_{11}^{(1)}(x) H_{01}^{(1)}(y)')] \, dA$$

$$K_L(08,11) = \frac{Et}{1-\nu^2} \int_A [\nu \frac{\partial w}{\partial x} H_{11}^{(1)}(x) H_{11}^{(1)}(y)' H_{01}^{(1)}(x)' H_{11}^{(1)}(y) + \frac{\partial w}{\partial y} H_{11}^{(1)}(x) H_{01}^{(1)}(x) (H_{11}^{(1)}(y)')^2 + (\frac{1-\nu}{2})(\frac{\partial w}{\partial y} H_{11}^{(1)}(x)' H_{11}^{(1)}(y) H_{01}^{(1)}(x)' H_{11}^{(1)}(y) + \frac{\partial w}{\partial x} H_{11}^{(1)}(x)' H_{11}^{(1)}(y) H_{01}^{(1)}(x) H_{11}^{(1)}(y)')] \, dA$$

$$K_L(08,12) = \frac{Et}{1-\nu^2} \int_A [(\frac{1+\nu}{2}) \frac{\partial w}{\partial x} H_{11}^{(1)}(x) H_{11}^{(1)}(y)' H_{11}^{(1)}(x)' H_{11}^{(1)}(y) + \frac{\partial w}{\partial y}(H_{11}^{(1)}(x) H_{11}^{(1)}(y)')^2 + (\frac{1-\nu}{2}) \frac{\partial w}{\partial y}(H_{11}^{(1)}(x)' H_{11}^{(1)}(y))^2] \, dA$$

$$K_L(09,01) = K_L(01,09), \; K_L(09,02) = K_L(02,09), \; K_L(09,03) = K_L(03,09),$$

$$K_L(09,04) = K_L(04,09), \; K_L(09,05) = K_L(05,09), \; K_L(09,06) = K_L(06,09),$$

$$K_L(09,07) = K_L(07,09), \; K_L(09,08) = K_L(08,09)$$

$$K_L(09,09) = \frac{-Et}{1-\nu^2} \int_A [\frac{\partial w}{\partial x} H_{01}^{(1)}(x)'' H_{01}^{(1)}(x)' (H_{01}^{(1)}(y))^2 + \nu \frac{\partial w}{\partial y} H_{01}^{(1)}(x)'' H_{01}^{(1)}(y) H_{01}^{(1)}(x) H_{01}^{(1)}(y)' + \nu \frac{\partial w}{\partial x} H_{01}^{(1)}(x) H_{01}^{(1)}(y)'' H_{01}^{(1)}(x)' H_{01}^{(1)}(y) + \frac{\partial w}{\partial y}(H_{01}^{(1)}(x))^2 H_{01}^{(1)}(y)' H_{01}^{(1)}(y)'' - (1-\nu)(\frac{\partial w}{\partial y}(H_{01}^{(1)}(x)')^2 H_{01}^{(1)}(y)' H_{01}^{(1)}(y) + \frac{\partial w}{\partial x} H_{01}^{(1)}(x) H_{01}^{(1)}(x)' (H_{01}^{(1)}(y)')^2)] \, dA$$

$$K_L(09,10) = \frac{-Et}{1-\nu^2}\int_A [\frac{\partial w}{\partial x} H_{01}^{(1)}(x)'' H_{11}^{(1)}(x)' (H_{01}^{(1)}(y))^2 + \nu \frac{\partial w}{\partial y} H_{01}^{(1)}(x)''$$
$$H_{01}^{(1)}(y) H_{11}^{(1)}(x) H_{01}^{(1)}(y)' + \nu \frac{\partial w}{\partial x} H_{01}^{(1)}(x) H_{01}^{(1)}(y)''$$
$$H_{11}^{(1)}(x)' H_{01}^{(1)}(y) + \frac{\partial w}{\partial y} H_{01}^{(1)}(x) H_{01}^{(1)}(y)'' H_{11}^{(1)}(x) H_{01}^{(1)}(y)'$$
$$- (1-\nu)(\frac{\partial w}{\partial y} H_{01}^{(1)}(x)' H_{01}^{(1)}(y)' H_{11}^{(1)}(x)' H_{01}^{(1)}(y) + \frac{\partial w}{\partial x}$$
$$H_{01}^{(1)}(x)' H_{11}^{(1)}(x)(H_{01}^{(1)}(y)')^2)]\ dA$$

$$K_L(09,11) = \frac{-Et}{1-\nu^2}\int_A [\frac{\partial w}{\partial x} H_{01}^{(1)}(x)'' H_{01}^{(1)}(y) H_{01}^{(1)}(x)' H_{11}^{(1)}(y) + \nu \frac{\partial w}{\partial y} H_{01}^{(1)}(x)''$$
$$H_{01}^{(1)}(y) H_{01}^{(1)}(x) H_{11}^{(1)}(y)' + \nu \frac{\partial w}{\partial x} H_{01}^{(1)}(x) H_{01}^{(1)}(y)''$$
$$H_{01}^{(1)}(x)' H_{11}^{(1)}(y) + \frac{\partial w}{\partial y}(H_{01}^{(1)}(x))^2 H_{01}^{(1)}(y)'' H_{11}^{(1)}(y)' -$$
$$(1-\nu)(\frac{\partial w}{\partial y}(H_{01}^{(1)}(x)')^2 H_{01}^{(1)}(y)' H_{11}^{(1)}(y) + \frac{\partial w}{\partial x} H_{01}^{(1)}(x)'$$
$$H_{01}^{(1)}(y) H_{01}^{(1)}(x) H_{11}^{(1)}(y)')]\ dA$$

$$K_L(09,12) = \frac{-Et}{1-\nu^2}\int_A [\frac{\partial w}{\partial x} H_{01}^{(1)}(x)'' H_{01}^{(1)}(y) H_{11}^{(1)}(x)' H_{11}^{(1)}(y) + \nu \frac{\partial w}{\partial y} H_{01}^{(1)}(x)''$$
$$H_{01}^{(1)}(y) H_{11}^{(1)}(x) H_{11}^{(1)}(y)' + \nu \frac{\partial w}{\partial x} H_{01}^{(1)}(x) H_{01}^{(1)}(y)''$$
$$H_{11}^{(1)}(x)' H_{11}^{(1)}(y) + \frac{\partial w}{\partial y} H_{01}^{(1)}(x) H_{01}^{(1)}(y)'' H_{11}^{(1)}(x) H_{11}^{(1)}(y)'$$
$$- (1-\nu)(\frac{\partial w}{\partial y} H_{01}^{(1)}(x)' H_{01}^{(1)}(y)' H_{11}^{(1)}(x)' H_{11}^{(1)}(y) + \frac{\partial w}{\partial x}$$
$$H_{01}^{(1)}(x)' H_{01}^{(1)}(y)' H_{11}^{(1)}(x) H_{11}^{(1)}(y)')]\ dA$$

$K_L(10,01) = K_L(01,10)$, $K_L(10,02) = K_L(02,10)$, $K_L(10,03) = K_L(03,10)$,

$$K_L(10,04) = K_L(04,10),\ K_L(10,05) = K_L(05,10),\ K_L(10,06) = K_L(06,10),$$

$$K_L(10,07) = K_L(07,10),\ K_L(10,08) = K_L(08,10),\ K_L(10,09) = K_L(09,10)$$

$$K_L(10,10) = \frac{-Et}{1-\nu^2}\int_A [\ \frac{\partial w}{\partial x} H_{11}^{(1)}(x)'' H_{11}^{(1)}(x)' (H_{01}^{(1)}(y))^2 + \nu \frac{\partial w}{\partial y} H_{11}^{(1)}(x)'' H_{01}^{(1)}(y) H_{11}^{(1)}(x) H_{01}^{(1)}(y)' + \nu \frac{\partial w}{\partial x} H_{11}^{(1)}(x) H_{01}^{(1)}(y)'' H_{11}^{(1)}(x)' H_{01}^{(1)}(y) + \frac{\partial w}{\partial y}(H_{11}^{(1)}(x))^2 H_{01}^{(1)}(y)'' H_{01}^{(1)}(y)' - (1-\nu)(\ \frac{\partial w}{\partial y} (H_{11}^{(1)}(x)')^2 H_{01}^{(1)}(y)' H_{01}^{(1)}(y) + \frac{\partial w}{\partial x} H_{11}^{(1)}(x)' H_{11}^{(1)}(x) (H_{01}^{(1)}(y)')^2)]\ dA$$

$$K_L(10,11) = \frac{-Et}{1-\nu^2}\int_A [\ \frac{\partial w}{\partial x} H_{11}^{(1)}(x)'' H_{01}^{(1)}(y) H_{01}^{(1)}(x)' H_{11}^{(1)}(y) + \nu \frac{\partial w}{\partial y} H_{11}^{(1)}(x)'' H_{01}^{(1)}(y) H_{01}^{(1)}(x) H_{11}^{(1)}(y)' + \nu \frac{\partial w}{\partial x} H_{11}^{(1)}(x) H_{01}^{(1)}(x)'' H_{01}^{(1)}(x)' H_{11}^{(1)}(y) + \frac{\partial w}{\partial y} H_{11}^{(1)}(x) H_{01}^{(1)}(y)'' H_{01}^{(1)}(x) H_{11}^{(1)}(y)' - (1-\nu)(\ \frac{\partial w}{\partial y} H_{11}^{(1)}(x)' H_{01}^{(1)}(y)' H_{01}^{(1)}(x)' H_{11}^{(1)}(y) + \frac{\partial w}{\partial x} H_{11}^{(1)}(x)' H_{01}^{(1)}(y)' H_{01}^{(1)}(x) H_{11}^{(1)}(y)')]\ dA$$

$$K_L(10,12) = \frac{-Et}{1-\nu^2}\int_A [\ \frac{\partial w}{\partial x} H_{11}^{(1)}(x)'' H_{01}^{(1)}(y) H_{11}^{(1)}(x)' H_{11}^{(1)}(y) + \nu \frac{\partial w}{\partial y} H_{11}^{(1)}(x)'' H_{01}^{(1)}(y) H_{11}^{(1)}(x) H_{11}^{(1)}(y)' + \nu \frac{\partial w}{\partial x} H_{11}^{(1)}(x) H_{01}^{(1)}(x)'' H_{11}^{(1)}(x)' H_{11}^{(1)}(y) + \frac{\partial w}{\partial y}(H_{11}^{(1)}(x))^2 H_{01}^{(1)}(y)'' H_{11}^{(1)}(y)' - (1-\nu)(\ \frac{\partial w}{\partial y}(H_{11}^{(1)}(x)')^2 H_{01}^{(1)}(y)' H_{11}^{(1)}(y) + \frac{\partial w}{\partial y} H_{11}^{(1)}(x)'$$

$$H_{01}^{(1)}(y)'H_{11}^{(1)}(x)H_{11}^{(1)}(y)')]\ dA$$

$K_L(11,01) = K_L(01,11)$, $K_L(11,02) = K_L(02,11)$, $K_L(11,03) = K_L(03,11)$,

$K_L(11,04) = K_L(04,11)$, $K_L(11,05) = K_L(05,11)$, $K_L(11,06) = K_L(06,11)$,

$K_L(11,07) = K_L(07,11)$, $K_L(11,08) = K_L(08,11)$, $K_L(11,09) = K_L(09,11)$,

$K_L(11,10) = K_L(10,11)$

$$K_L(11,11) = \frac{-Et}{1-\nu^2}\int_A [\frac{\partial w}{\partial x}H_{01}^{(1)}(x)''H_{01}^{(1)}(x)'(H_{11}^{(1)}(y))^2 + \nu\frac{\partial w}{\partial y}H_{01}^{(1)}(x)''H_{11}^{(1)}(y)H_{01}^{(1)}(x)H_{11}^{(1)}(y)' + \nu\frac{\partial w}{\partial x}H_{01}^{(1)}(x)H_{11}^{(1)}(y)''H_{01}^{(1)}(x)'H_{11}^{(1)}(y) + \frac{\partial w}{\partial y}(H_{01}^{(1)}(x))^2H_{11}^{(1)}(y)''H_{11}^{(1)}(y)' - (1-\nu)(\frac{\partial w}{\partial y}(H_{01}^{(1)}(x)')^2H_{11}^{(1)}(y)'H_{11}^{(1)}(y) + \frac{\partial w}{\partial x}H_{01}^{(1)}(x)'H_{01}^{(1)}(x)(H_{11}^{(1)}(y)')^2)]\ dA$$

$$K_L(11,12) = \frac{-Et}{1-\nu^2}\int_A [\frac{\partial w}{\partial x}H_{01}^{(1)}(x)''H_{11}^{(1)}(x)'(H_{11}^{(1)}(y))^2 + \nu\frac{\partial w}{\partial y}H_{01}^{(1)}(x)''H_{11}^{(1)}(y)H_{11}^{(1)}(x)H_{11}^{(1)}(y)' + \nu\frac{\partial w}{\partial x}H_{01}^{(1)}(x)H_{11}^{(1)}(y)''H_{11}^{(1)}(x)'H_{11}^{(1)}(y) + \frac{\partial w}{\partial y}H_{01}^{(1)}(x)H_{11}^{(1)}(y)''H_{11}^{(1)}(x)H_{11}^{(1)}(y)' - (1-\nu)(\frac{\partial w}{\partial y}H_{01}^{(1)}(x)'H_{11}^{(1)}(y)'H_{11}^{(1)}(x)'H_{11}^{(1)}(y) + \frac{\partial w}{\partial x}H_{01}^{(1)}(x)'H_{11}^{(1)}(x)(H_{11}^{(1)}(y)')^2)]\ dA$$

$$K_L(12,01) = K_L(01,12),\ K_L(12,02) = K_L(02,12),\ K_L(12,03) = K_L(03,12),$$

$$K_L(12,04) = K_L(04,12),\ K_L(12,05) = K_L(05,12),\ K_L(12,06) = K_L(06,12),$$

$$K_L(12,07) = K_L(07,12),\ K_L(12,08) = K_L(08,12),\ K_L(12,09) = K_L(09,12),$$

$$K_L(12,10) = K_L(10,12),\ K_L(12,11) = K_L(11,12)$$

$$K_L(12,12) = \frac{-Et}{1-\nu^2} \int_A [\ \frac{\partial w}{\partial x} H_{11}^{(1)}(x)'' H_{11}^{(1)}(x)' (H_{11}^{(1)}(y))^2 + \nu \frac{\partial w}{\partial y} H_{11}^{(1)}(x)'' H_{11}^{(1)}(y) H_{11}^{(1)}(x) H_{11}^{(1)}(y)' + \nu \frac{\partial w}{\partial x} H_{11}^{(1)}(x) H_{11}^{(1)}(y)'' H_{11}^{(1)}(x)' H_{11}^{(1)}(y) + \frac{\partial w}{\partial y} (H_{11}^{(1)}(x))^2 H_{11}^{(1)}(y)'' H_{11}^{(1)}(y)' - (1-\nu)(\frac{\partial w}{\partial y} (H_{11}^{(1)}(x)')^2 H_{11}^{(1)}(y)' H_{11}^{(1)}(y) + \frac{\partial w}{\partial x} H_{11}^{(1)}(x)' H_{11}^{(1)}(x) (H_{11}^{(1)}(y)')^2)]\ dA$$

Appendix C. The $[K_\sigma]$ Stiffness Matrix

APPENDIX C

THE $[K_\sigma]$ STIFFNESS MATRIX

C.1 Formulation of the $[K_\sigma]$ Stiffness Matrix for the Computer Program

Following the nodal numbering scheme adopted in Appendices A and B, Eq. (3-43) of Chapter 3 can be written as

$$|K_\sigma|\{\delta\alpha\} = t \int_A \left[[\delta B_{L11}]^T \vdots [\delta B_{L12}]^T \vdots [\delta B_{L22}]^T \vdots [\delta B_{L21}]^T \right] \begin{Bmatrix} \{\sigma_{11}\} \\ \{\sigma_{12}\} \\ \{\sigma_{22}\} \\ \{\sigma_{21}\} \end{Bmatrix} dA \qquad (C\text{-}1)$$

where $\{\sigma_{11}\}$, $\{\sigma_{12}\}$, $\{\sigma_{22}\}$, and $\{\sigma_{21}\}$ are vector matrices expressing the membrane stress resultants as defined by Eq. (3-45). The subscripts on these vectors refer to the respective nodal numbers. When the matrix manipulation in the right side of Eq. (C-1) is carried out according to the mathematical principal illustrated in section 3-4.C, it can be shown that Eq. (C-1) yields the stiffness matrix due to initial stresses and that the "initial stress" stiffness matrix of a finite element has the form

$$[K_\sigma] = \begin{bmatrix} [0] & [0] \\ [0] & [K_\sigma^b] \end{bmatrix} \qquad (C\text{-}2)$$

where

$$[K_\sigma^b] = t \int_A [G_{11}]^T \begin{bmatrix} N_x & N_{xy} \\ N_{xy} & N_y \end{bmatrix} [G_{11}] \, dA \qquad \text{(C-3)}$$

C.2 Expressions for the Elements of Portion of the Stiffness Matrix $[K_\sigma]$

The following are expressions for the elements of portion of the "initial stress" stiffness matrix $[K_\sigma]$.

$$K_\sigma(01,01) = K_\sigma(01,02) = K_\sigma(01,03) = K_\sigma(01,04) = K_\sigma(01,05) = K_\sigma(01,06) = 0$$

$$K_\sigma(01,07) = K_\sigma(01,08) = K_\sigma(01,09) = K_\sigma(01,10) = K_\sigma(01,11) = K_\sigma(01,12) = 0$$

$$K_\sigma(02,01) = K_\sigma(02,02) = K_\sigma(02,03) = K_\sigma(02,04) = K_\sigma(02,05) = K_\sigma(02,06) = 0$$

$$K_\sigma(02,07) = K_\sigma(02,08) = K_\sigma(02,09) = K_\sigma(02,10) = K_\sigma(02,11) = K_\sigma(02,12) = 0$$

$$K_\sigma(03,01) = K_\sigma(03,02) = K_\sigma(03,03) = K_\sigma(03,04) = K_\sigma(03,05) = K_\sigma(03,06) = 0$$

$$K_\sigma(03,07) = K_\sigma(03,08) = K_\sigma(03,09) = K_\sigma(03,10) = K_\sigma(03,11) = K_\sigma(03,12) = 0$$

$$K_\sigma(04,01) = K_\sigma(04,02) = K_\sigma(04,03) = K_\sigma(04,04) = K_\sigma(04,05) = K_\sigma(04,06) = 0$$

$$K_\sigma(04,07) = K_\sigma(04,08) = K_\sigma(04,09) = K_\sigma(04,10) = K_\sigma(04,11) = K_\sigma(04,12) = 0$$

$$K_\sigma(05,01) = K_\sigma(05,02) = K_\sigma(05,03) = K_\sigma(05,04) = K_\sigma(05,05) = K_\sigma(05,06) = 0$$

$$K_\sigma(05,07) = K_\sigma(05,08) = K_\sigma(05,09) = K_\sigma(05,10) = K_\sigma(05,11) = K_\sigma(05,12) = 0$$

$$K_\sigma(06,01) = K_\sigma(06,02) = K_\sigma(06,03) = K_\sigma(06,04) = K_\sigma(06,05) = K_\sigma(06,06) = 0$$

$$K_\sigma(06,07) = K_\sigma(06,08) = K_\sigma(06,09) = K_\sigma(06,10) = K_\sigma(06,11) = K_\sigma(06,12) = 0$$

$$K_\sigma(07,01) = K_\sigma(07,02) = K_\sigma(07,03) = K_\sigma(07,04) = K_\sigma(07,05) = K_\sigma(07,06) = 0$$

$$K_\sigma(07,07) = K_\sigma(07,08) = K_\sigma(07,09) = K_\sigma(07,10) = K_\sigma(07,11) = K_\sigma(07,12) = 0$$

$$K_\sigma(08,01) = K_\sigma(08,02) = K_\sigma(08,03) = K_\sigma(08,04) = K_\sigma(08,05) = K_\sigma(08,06) = 0$$

$$K_\sigma(08,07) = K_\sigma(08,08) = K_\sigma(08,09) = K_\sigma(08,10) = K_\sigma(08,11) = K_\sigma(08,12) = 0$$

$$K_\sigma(09,01) = K_\sigma(09,02) = K_\sigma(09,03) = K_\sigma(09,04) = K_\sigma(09,05) = K_\sigma(09,06) = 0$$

$$K_\sigma(09,07) = K_\sigma(09,08) = 0$$

$$K_\sigma(09,09) = t \int_A \Big[N_x \big(H_{01}^{(1)}(x)' H_{01}^{(1)}(y)\big)^2 + 2N_{xy} H_{01}^{(1)}(x)' H_{01}^{(1)}(y) H_{01}^{(1)}(x) H_{01}^{(1)}(y)' + N_y \big(H_{01}^{(1)}(x) H_{01}^{(1)}(y)'\big)^2 \Big] \, dA$$

$$K_\sigma(09,10) = t \int_A \Big[N_x H_{01}^{(1)}(x)' H_{11}^{(1)}(x)' \big(H_{01}^{(1)}(y)\big)^2 + N_{xy} H_{01}^{(1)}(x)' H_{01}^{(1)}(y)$$

$$H_{11}^{(1)}(x)H_{01}^{(1)}(y)' + N_{xy}H_{01}^{(1)}(x)H_{01}^{(1)}(y)'H_{11}^{(1)}(x)'H_{01}^{(1)}(y)$$
$$+ N_y H_{01}^{(1)}(x)H_{11}^{(1)}(x)(H_{01}^{(1)}(y)')^2 \Big] \, dA$$

$$K_\sigma(09,11) = t\int_A \Big[N_x(H_{01}^{(1)}(x)')^2 H_{01}^{(1)}(y)H_{11}^{(1)}(y) + N_{xy}H_{01}^{(1)}(x)'H_{01}^{(1)}(y)$$
$$H_{01}^{(1)}(x)H_{11}^{(1)}(y)' + N_{xy}H_{01}^{(1)}(x)H_{01}^{(1)}(y)'H_{01}^{(1)}(x)'H_{11}^{(1)}(y)$$
$$+ N_y(H_{01}^{(1)}(x))^2 H_{01}^{(1)}(y)'H_{11}^{(1)}(y)' \Big] \, dA$$

$$K_\sigma(09,12) = t\int_A \Big[N_x H_{01}^{(1)}(x)'H_{01}^{(1)}(y)H_{11}^{(1)}(x)'H_{11}^{(1)}(y) + N_{xy}H_{01}^{(1)}(x)'H_{01}^{(1)}(y)$$
$$H_{11}^{(1)}(x)H_{11}^{(1)}(y)' + N_{xy}H_{01}^{(1)}(x)H_{01}^{(1)}(y)'H_{11}^{(1)}(x)'H_{11}^{(1)}(y)$$
$$+ N_y H_{01}^{(1)}(x)H_{01}^{(1)}(y)'H_{11}^{(1)}(x)H_{11}^{(1)}(y)' \Big] \, dA$$

$$K_\sigma(10,01) = K_\sigma(10,02) = K_\sigma(10,03) = K_\sigma(10,04) = K_\sigma(10,05) = K_\sigma(10,06) = 0$$

$$K_\sigma(10,07) = K_\sigma(10,08) = 0, \quad K_\sigma(10,09) = K_\sigma(09,10)$$

$$K_\sigma(10,10) = t\int_A \Big[N_x(H_{11}^{(1)}(x)'H_{01}^{(1)}(y))^2 + 2N_{xy}H_{11}^{(1)}(x)'H_{01}^{(1)}(y)H_{11}^{(1)}(x)$$
$$H_{01}^{(1)}(y)' + N_y(H_{11}^{(1)}(x)H_{01}^{(1)}(y)')^2 \Big] \, dA$$

$$K_\sigma(10,11) = t\int_A \Big[N_x H_{11}^{(1)}(x)'H_{01}^{(1)}(y)H_{01}^{(1)}(x)'H_{11}^{(1)}(y) + N_{xy}H_{11}^{(1)}(x)'H_{01}^{(1)}(y)$$
$$H_{01}^{(1)}(x)H_{11}^{(1)}(y)' + N_{xy}H_{11}^{(1)}(x)H_{01}^{(1)}(y)'H_{01}^{(1)}(x)'H_{11}^{(1)}(y)$$
$$+ N_y H_{11}^{(1)}(x)H_{01}^{(1)}(y)'H_{01}^{(1)}(x)H_{11}^{(1)}(y)' \Big] \, dA$$

$$K_\sigma(10,12) = t \int_A [\, N_x (H_{11}^{(1)}(x)')^2 H_{01}^{(1)}(y) H_{11}^{(1)}(y) + N_{xy} H_{11}^{(1)}(x)' H_{01}^{(1)}(y) H_{11}^{(1)}(x) H_{11}^{(1)}(y)' + N_{xy} H_{11}^{(1)}(x) H_{01}^{(1)}(y)' H_{11}^{(1)}(x)' H_{11}^{(1)}(y) + N_y (H_{11}^{(1)}(x))^2 H_{01}^{(1)}(y)' H_{11}^{(1)}(y)' \,] \, dA$$

$$K_\sigma(11,01) = K_\sigma(11,02) = K_\sigma(11,03) = K_\sigma(11,04) = K_\sigma(11,05) = K_\sigma(11,06) = 0$$

$$K_\sigma(11,07) = K_\sigma(11,08) = 0$$

$$K_\sigma(11,09) = K_\sigma(09,11), \; K_\sigma(11,10) = K_\sigma(10,11)$$

$$K_\sigma(11,11) = t \int_A [\, N_x (H_{01}^{(1)}(x)' H_{11}^{(1)}(y))^2 + 2N_{xy} H_{01}^{(1)}(x)' H_{11}^{(1)}(y) H_{01}^{(1)}(x) H_{11}^{(1)}(y)' + N_y (H_{01}^{(1)}(x) H_{11}^{(1)}(y)')^2 \,] \, dA$$

$$K_\sigma(11,12) = t \int_A [\, N_x H_{01}^{(1)}(x)' H_{11}^{(1)}(x)' (H_{11}^{(1)}(y))^2 + N_{xy} H_{01}^{(1)}(x)' H_{11}^{(1)}(y) H_{11}^{(1)}(x) H_{11}^{(1)}(y)' + N_{xy} H_{01}^{(1)}(x) H_{11}^{(1)}(y)' H_{11}^{(1)}(x)' H_{11}^{(1)}(y) + N_y H_{01}^{(1)}(x) H_{11}^{(1)}(x) (H_{11}^{(1)}(y))^2 \,] \, dA$$

$$K_\sigma(12,01) = K_\sigma(12,02) = K_\sigma(12,03) = K_\sigma(12,04) = K_\sigma(12,05) = K_\sigma(12,06) = 0$$

$$K_\sigma(12,07) = K_\sigma(12,08) = 0$$

$$K_\sigma(12,09) = K_\sigma(09,12), \; K_\sigma(12,10) = K_\sigma(10,12), \; K_\sigma(12,11) = K_\sigma(11,12)$$

$$K_\sigma(12,12) = t \int_A [\, N_x (H_{11}^{(1)}(x)' H_{11}^{(1)}(y))^2 + 2N_{xy} H_{11}^{(1)}(x)' H_{11}^{(1)}(y) H_{11}^{(1)}(x) H_{11}^{(1)}(y)' + N_y (H_{11}^{(1)}(x) H_{11}^{(1)}(y)')^2 \,]\, dA$$